# LIQUID PHASE SINTERING OF BaTiO$_3$

By

K. RAMESH CHOWDARY
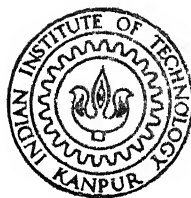
**DEPARTMENT OF METALLURGICAL ENGINEERING**

## INDIAN INSTITUTE OF TECHNOLOGY, KANPUR

AUGUST, 1981

# LIQUID PHASE SINTERING OF BaTiO$_3$

A Thesis Submitted
in Partial Fulfilment of the Requirements
for the Degree of
**MASTER OF TECHNOLOGY**

By

K. RAMESH CHOWDARY

to the
**DEPARTMENT OF METALLURGICAL ENGINEERING**
**INDIAN INSTITUTE OF TECHNOLOGY, KANPUR**
AUGUST, 1981
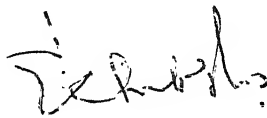
ME - 1981 - M - CHO - LIQ

# C E R T I F I C A T E

Certified that this work on ' Liquid phase sintering of $BaTiO_3'$ by K. Ramesh Chowdary has been carried out under my supervision and the same has not been submitted elsewhere for a degree.

E. C. Subbarao
Professor
Department of Metallurgical Engineering
Indian Institute of Technology Kanpur
K A N P U R

# ACKNOWLEDGEMENTS

I am deeply indebted to Prof. E.C. Subbarao
for the excellent guidance throughout the work. I
immensely enjoyed the numerous lively discussions I had
with him on the present work. Needless to say, this work
would not have been possible without his encouragement
and guidance.

I am grateful to Messrs. E.M.T. Velu, B.N. Rao,
V. Bhaskar, S. Bhattacharjee, S. Pandian and S. Laha for
their Co-operation and suggestions at various stages of
the work.

I sincerely acknowledge the help of Mrs. Padma-
vati Shankar, for doing the chemical analysis, Mr. V. P.
Srivastava for setting up various instruments and Mr.
Mukherjee and Mr. Prasad in metallography work.

I am thankful to Messrs. Umesh Kumar, Swami-
nathan, Gopichand, Shaw and Arunachalam for their help
during the final stages of the work. I am thankful to
Mr. Vishwanath Singh, Mr. Bajpai, Mr. R.N. Misra and

Mr. Bhardwaj for their prompt and timely help in getting the thesis in the printed form.

Finally I wish to thank my friends Apparao, Bose, Hemadri, Sharma, Verma, and Murty whose company was most enjoyable and helpful.

K. RAMESH CHOWDARY.

CONTENTS

# LIST OF TABLES

LIST OF FIGURES

# A B S T R A C T

Ba Ti $O_3$ ceramics are conventionally sintered at 1300 - 1400°C. Lower sintering temperatures result in energy savings as well as enable the use of cheaper electrode materials than expensive Pd and Pt electrodes in multilayer capacitors. Lead germanate glass has been used to lower the sintering temperature of Ba Ti $O_3$ ceramics. In the present work, bismuth borate glass (upto 40 wt percent) is admixed with Ba Ti $O_3$ and sintering experiments carried out at temperatures between 800 to 1200°C for a period of 10min to 3hrs. Density, microstructure, phase identification by X.ray diffraction, dielectric constant and loss have been studied as a function of glass content and sintering conditions. Reasonably dense bodies ( greater than 85% theoretical density) are obtained with 10 to 20% glass additions by sintering at 1000-1050°C, which can be used with 70 Ag-30Pd alloy electrodes. There is no shift of the x-ray diffraction lines or the Curie temperature of Ba Ti $O_3$, indicating no solid solutions are formed with Ba Ti $O_3$ by the glass constituents. X-ray studies revealed the formation of $Bi_4Ti_3O_{12}$ and Ba $Bi_4$ $Ti_4$ $O_{15}$, the latter being the prominent and its amount depending upon the amount of glass and sintering conditions. Microstructure shows the glass

present as a coating over the grains. Densification
mechanisms during liquid phase sintering are discussed.
Dielectric properties are measured with respect to
temperature, voltage and frequency. These measurements
show that the dielectric properties are not affected
markedly with glass addition upto 20% and exhibit
better temperature characteristics than pure $Ba Ti O_3$.

# I. INTRODUCTION

Majority of the capacitors produced today are made of ceramic materials. More than 95 percent of these ceramic materials are ferroelectric in nature. Ferroelectric materials have a high dielectric constant which makes them ideal for capacitor industry.

A ceramic capacitor consists of a ceramic dielectric material sandwiched between two parallel metal plates, which serve as the electrodes. The usual electrode material is silver. Before world war II, Titanium dioxide with a dielectric constant of around 100, was the favoured dielectric material. During the world war II, it was discovered that barium titanate has a high dielectric constant (1500-2000). Thus barium titanate became the basic dielectric material for ceramic capacitors for the last 35 years. This enabled the size (volume) of the capacitor to be decreased correspondingly. The capacitance of a normal parallel plate capacitor can also be increased either by reducing the thickness or by increasing the electrode area. Due to the brittle nature of the ceramic materials the capacitors with a large area and small thickness are very fragile and cannot be used without any mechanical support. The drive towards miniaturization led to the development of i) Multilayer capacitors and ii) Internal boundary layer capacitors.

## I.1 Multilayer Capacitors:

Schematic representation of a multilayer capacitor is given in Figure I.1,. These are generally rectangular in shape with parallel electrodes brought out at the narrow ends of the rectangle. A margin of bare dielectric is allowed around the metal plate to prevent edge brakedown.. Such an arrangement being compact, has a high volumetric efficiency. The whole stacking consisting of alternate layers of dielectric ceramic and the electrode is sintered around $1350^{\circ}C$, which necessitates the use of high melting point metals like $Pt$ and $Pt$ as the electrodes,.

Today multilayer capacitors with 100 active layers of 20 micron thickness are not uncommon.. Capacitance values of the order of microfarads are easily obtained.

## I.2 Internal Boundary Layer (IBL) Capacitors:

Commercial capacitors are usually manufactured from titanate based materials of the perovskite $(ABX_3)$ family, which are made semiconducting (n-type) by aliovalent chemical substitution, gaseous reduction, or combination thereof.. Resistivity distributions are developed within the micro-structure by boundary counter diffusion, or by sintering in the presence of a liquid phase which solidifies on cooling into an insulator, Ideally, the former method is characterized by grain to grain contact, with interfacial compensation slates, and the latter by grain to grain separation, with an insulating intergranular phase. Anomalously high apparent dielectric

Solderlands

Electrodes

End terminal

Ceramic material
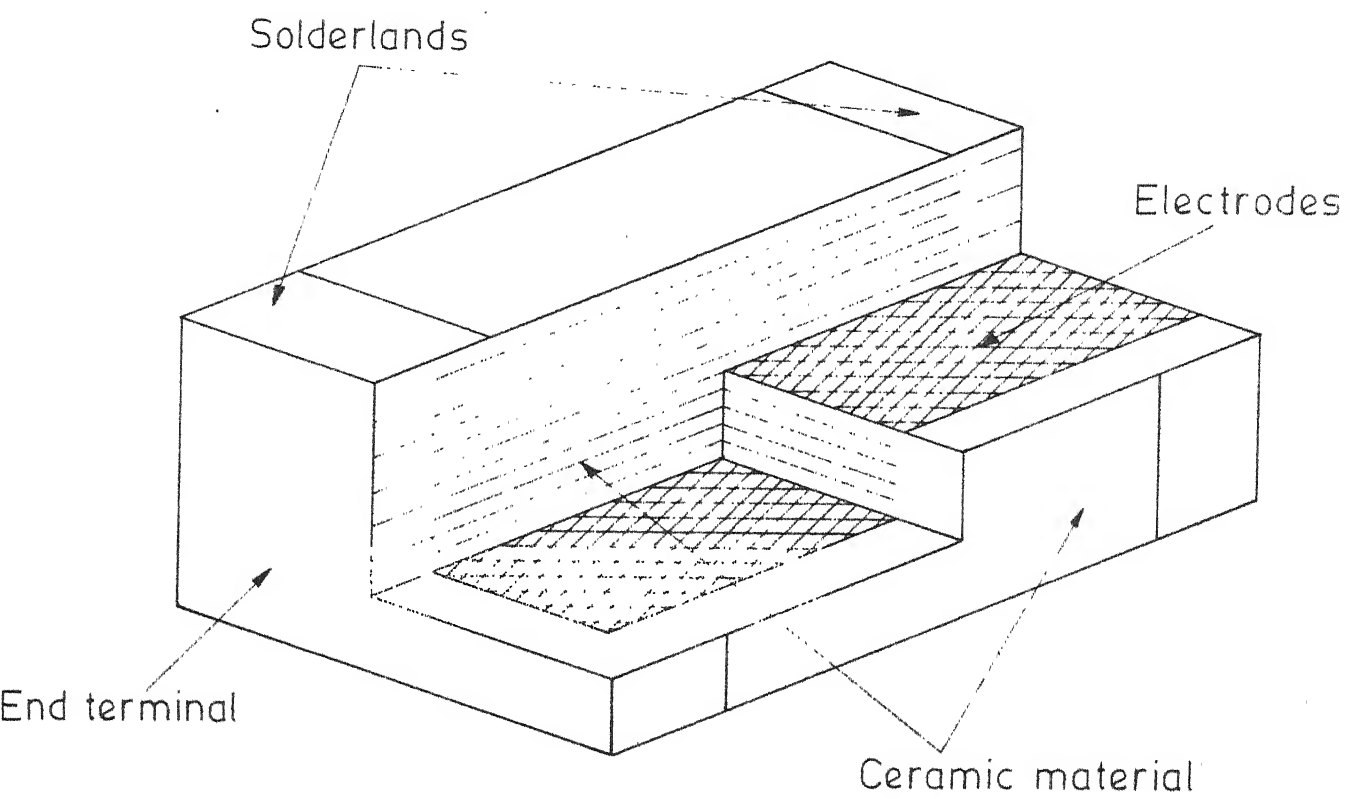
Fig I .1. Schematic representation of a multilayer capacitor.

constants (over 20,000) calculated for IBL capacitors are
generally attributed to enhanced space charge polarization
processes taking place between semiconducting grains and resistive
boundaries.

There are certain problems to be tackled in the
development of these capacitors (1).

I.3  Electrode Problems:

All multilayer capacitors discussed previously
require Pt, Au or Pd electrodes, which add substantially to
their cost.  Today's noble metal prices and other reasons
make it imperative to search for techniques to replace them.
But silver, even though a noble metal, does not belong to Au,
Pt or Pd group because it is much cheaper.  It is an ideal
electrode material, used exclusively in discs and on the
outside of the multilayer capacitors.  For this reason it
could and should be used to replace the other noble metals
wherever possible.

The usability of a metal or an electrode material
in monolithics is determined by two properties; its melting
point should be higher than the sintering temperature of the
ceramic and its metal/metal oxide equilibrium oxygen vapour
pressure should be higher than that of the oxygen partial
pressure during firing.  Since the firing temperature of most
ceramics is in the 1300-1400°C range, and the firing atmosphere
is air, the only suitable candidates seem to be Pt (MP 1769°C)
and Pd (MP 1552°C) which are indeed the two most frequently
used metals.  Gold (MP 1063°C) sometimes is also used, but

usually as a Pd alloy, which brings its melting point above the 1300-1400°C range. Silver has too low a melting point (961°C) and some of the transition metals (Ni, Co, Fe) which would be suitable because of their high melting temperatures are unsuitable because of their low oxygen equilibrium pressures.

So now for the replacement of Pt, Pd and Au electrodes, either we have to develop ceramics which can be fired in an atmosphere with an oxygen partial pressure lower than the equilibrium pressure of one of the transition metals at this temperature, or to lower the firing temperature of the ceramic below the melting temperature of Ag or one of the low melting Ag - Pd alloys. From the Ag-Pd phase diagram (2) given in Fig. I.2 one can see that a 70 Pd 30 Ag alloy is needed for a sintering temperature of 1300°C, where as 30 Pd 70 Ag alloy can be used if the sintering temperature is reduced to 1000-1050°C.

Another major advantage of lowering the sintering temperature is to bring about energy savings during sintering. For example, if the sintering temperature can be reduced to 1000°C or below we can use nichrome furnaces instead of the expensive globar furnaces or other high temperature
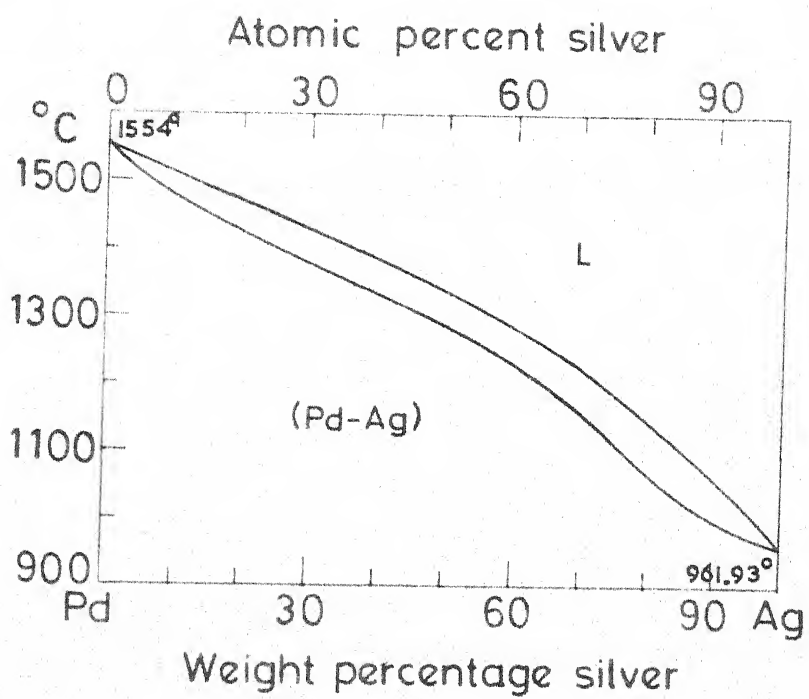
Fig. 12. Ag-Pd Phase diagram.

furnaces, and also the power consumption of these temperatures
will be nearly one third of that needed for the conventional
firing around $1350^\circ C$.

So the two possible solutions for the electrode
problems are using (i) base metal electrodes or (ii) liquid phase
sintering.

## I.3.1  Base metal electrodes:

A base metal, such as nickel, has a melting point
higher than the sintering temperatures employed in capacitor
manufacture and is much cheaper than Pd or even Ag.  However,
at the sintering temperatures, Ni oxidizes to NiO and in the
process reduces $BaTiO_3$ by converting a corresponding number of
$Ti^{4+}$ ions to the $Ti^{3+}$ state.  The presence of Ti in two valence
states on crystallographically equivalent sites leads to large
electronic conductivity and the ceramic is no longer useful
as a dielectric.  The reduction of $BaTiO_3$ can be prevented by
doping it with Mn (3 - 6).  The disadvantage with these base
metal electrodes is that they have higher resistivity values
compared to noble metals, thus increasing the series resistance
and in turn dissipation factor of the capacitor.

## I.3.2  Liquid phase sintering:

The use of the noble metals like Pt and Pd can
also be avoided by reducing the sintering temperature of the
ceramic dielectric from the usual $1300-1400^\circ C$ to below the
melting temperature of Ag or one of the low melting Ag-Pd alloys.

The sintering temperature is lowered by the use of a transient liquid phase. The liquid phase should possess the following characteristics (7)

i) it should melt at or below 800-900°C

ii) it should not react with the dielectric composition

iii) the crystalline phase, formed on cooling, should preferably have a relatively high dielectric constant, so that the dielectric constant of the composite is not too greatly . . . . . reduced.

iv) the viscosity of the liquid should be low at the sintering temperature so that the amount of liquid phase is kept to a minimum.

Lead germanate is one such additive which can meet the above requirements using this. Park (8) has developed dielectric ceramics which can sinter at 800-900°C. The fact that crystalline lead germanate ($Pb_5 Ge_3 O_{11}$) is ferroelectric is a distinct advantage in retaining fairly high dielectric constant of the composite.

Recently Mukherjee and Ravishankar reported the liquid phase sintering of $BaTiO_3$ using lead germanate (9). They observed that for liquid phase sintering of $BaTiO_3$ with 0.6 to 1 mole percent glass addition a minimum of 1150-1200°C sintering temperature is needed. They also observed that above 1200°C there is no glass present and PbO and $GeO_2$ have diffused into the $BaTiO_3$ grains. The disadvantage with this glass addition is that during sintering lead substitutes for Ba in $BaTiO_3$ lattice and thereby reduces the room temperature dielectric constant.

The toxic nature of lead and the high cost of germanium are other deterrent factors in the use of $Pb_5Ge_3O_{11}$ as a sintering aid.

Using CuO additive, Hennings studied the liquid phase sintering of $BaTiO_3$(10). With the addition of 0.5 to 1 mole percent of CuO he was able to reduce the sintering temperature to about $1200^oC$. The problem with the CuO addition is that if it is in excess the sample becomes conductive and thus useless, and also the sintering temperature is not too greatly reduced.

## II. STATEMENT OF THE PROBLEM

Liquid phase sintering of Barium Titanate has been tried to solve the electrode problems in multilayer capacitors (8 - 10). None of these studies are completely successful in reducing the cost of these capacitors by replacing the noble metal electrodes (Pt and Pd) with Ag or low melting Ag-Pd alloys without sacrificing the dielectric properties of $BaTiO_3$. So an alternative additive has been sought.

In the present work, a glass from the $Bi_2O_3$ - $B_2O_3$ system (11) was used as an additive. The dielectric properties of some of the glasses in this system are given in Table II.1. From there, 74 percent $Bi_2O_3$, 26 percent $B_2O_3$ glass which has the highest dielectric constant and a low melting temperature ($700-750^oC$) was chosen as the additive. Some of the properties of this glass were compared with lead germanate in Table II.2. From this one can see that the melting temperature and densities

Table II.1 : Dielectric properties of $Bi_2O_3$ - $B_2O_3$ glasses
( Dielectric constant at room temperature and
resistivity ($\Omega$- cm) at 130°C and 230°C)

| Glass No. | Composition mol pct. | | Dielectric constant | | | | 100 tan $\delta$ | | $\rho_{130}$ | $\rho_{230}$ |
|---|---|---|---|---|---|---|---|---|---|---|
| | $Bi_2O_3$ | $B_2O_3$ | $10^3$ c/s | $10^5$ c/s | $10^7$ c/s | $9.6 \times 10^9$ c/s | $10^3$ c/s | $9.6 \times 10^9$ c/s | (x$10^{14}$) $\Omega$-cm | (x $10^{11}$) $\Omega$-cm |
| 19 | 26 | 74 | 14.1 | 13.9 | 13.6 | 10.3 | 0.13 | 0.84 | 34 | 340 |
| 25 | 32 | 68 | 21.8 | 21.8 | 21.4 | 16.1 | 0.15 | 1.24 | 6.4 | 10 |
| 26 | 40 | 60 | 28.0 | 28.0 | 26.6 | 19.1 | 0.14 | 2.88 | 1.3 | 5.9 |
| 27 | 46 | 54 | 31.0 | 31.1 | 29.8 | 22.1 | 0.18 | 3.29 | 0.55 | 0.70 |
| 22 | 54 | 46 | 31.1 | 31.1 | 29.9 | 21.5 | 0.32 | 2.41 | 0.16 | 0.25 |
| 60 | 60 | 40 | 37.6 | 37.1 | 36.2 | 24.3 | 0.22 | 1.72 | 0.023 | 0.042 |
| 28 | 66 | 34 | 38.8 | 38.7 | 36.5 | 26.6 | 0.22 | 1.98 | 0.013 | 0.022 |
| 29 | 74 | 26 | 42.5 | 42.5 | 41.2 | 31.1 | 0.21 | 1.90 | 0.0017 | 0.0058 |

Table II.2 : Properties of Lead Germanate Crystals (13)
and Bismuth Borate Glass.

| Property | $Pb_5Ge_3O_{11}$ single crystal | 74 pct $Bi_2O_3$ 26 pct $B_2O_3$ glass |
|---|---|---|
| Melting point ($^{\circ}$C) | $738^{\circ}$ | $700 - 750^{\circ}$ |
| Density (g/cc) | 7.38 | 7.74 |
| Linear thermal expansion coefficient | - | $115 \times 10^{-7}/^{\circ}$C |
| Dielectric constant at 1 KHz | $\varepsilon_{11RT} - 22$ $\varepsilon_{33RT} - 36$ $\varepsilon_{33Max} - 2300$ | $\varepsilon_{RT} - 42.5$ |
| Curie point $^{\circ}$C | $178^{\circ}$ | - |

of both are comparable, and the dielectric constant at room temperature for Bismuth Borate glass is higher than that of lead germanate crystal in both crystallographic directions.

The aim of the present work is to study the usability of this glass as an additive for liquid phase sintering of $BaTiO_3$ and to sinter $BaTiO_3$ at temperatures where we can use 70 Ag 30 Pd alloy or even lower melting alloys of this system as an electrode, without sacrificing the dielectric properties significantly.

More specifically, the aims of the present work are:

i) to investigate the effect of glass addition on sintering temperature (upto 40 wt pct of glass was used)

ii) to study the effect of amount of glass addition, sintering temperature and sintering time on densification

iii) to attempt an explanation on the mechanism of sintering in the presence of liquid phase

iv) to relate the dielectric properties to structural and micro-structural changes during sintering.

The sintered pellets are investigated using

i) weight loss measurements during sintering

ii) DTA

iii) chemical analysis

iv) x-ray diffraction

v) density

vi) volume shrinkage

vii) microstructure observation, and

viii) variation of dielectric constant and dissipation factor

with

        a) temperature

        b) dc bias, and

        c) frequency

## III. EXPERIMENTAL TECHNIQUES

III.1 :   Sample Preparation

III.1.1:   Raw materials:

Raw materials used were (all of them are AR Grade, more than 99.5 percent purity) barium carbonate (Sarabhai Chemicals, India), boric acid (Sarabhai Chemicals, India), titanium Dioxide (Bake  Analysed Reagent, USA), bismuth oxide (Mayfair and Raydon, England).

III.1.2 : Preparation of Barium Titanate:

$BaTiO_3$ was prepared by calcining equimolar amounts of $BaCO_3$ and $TiO_2$ (14).  These powders were mixed thoroughly in an alumina ball mill using alumina balls and acetone. The mixes were then compacted at 40,000 psi pressure using a hydraulic press to improve reaction during calcination. Calcination was done in an alumina cricible at $1250^\circ C$ for 4 to 6 hrs.  After calcination the material was crushed and ground into a fine powder. X-ray analysis of the calcined powder showed the presence of $Ba_2TiO_4$ phase in addition to $BaTiO_3$ (15). The calcined powder was then boiled in hot water, filtered and washed with hot water repeatedly till the filtrate shows a pH of 7.  These washings were done to remove any traces of $Ba(OH)_2$ present since $Ba(OH)_2$ will be formed when any $Ba_2TiO_4$ present reacts with water.

$$Ba_2TiO_4 + H_2O \longrightarrow BaTiO_3 + Ba(OH)_2 \qquad (14)$$
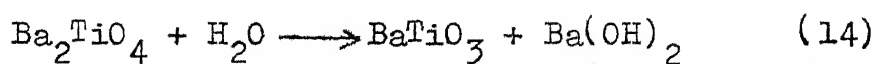
III.1.2.a : Determination of the amount of recovery:

Gravimetric analysis was done on the calcined powder to determine the amount of recovery. A weighed amount of calcined powder was taken into a baker and boiled in distilled water, filtered and washed with distilled water repeatedly till the filtrate shows a pH of 7. The filtered solution was then evaporated and weighed to determine the amount of $Ba_2TiO_4$ dissolved. The amount of the undissolved $BaTiO_3$ left in the filter paper was weighed after burning the filter paper. These results are given below:

wt. of calcined powder boiled in water $= 9. \quad 4$ gm

wt. of $BaTiO_3$ recovered as undissolved material $= 8.53\ 7$ gm

wt. loss of calcined material $= 1.1279$ gm

$\therefore$ percentage weight loss $= 11.\ 4$

or recovery $= 88.4$ pct.

wt. of filtrate as $BaCO_3$ after evaporating the water $= 1.3975$ gm

or wt. of BaO $= 1.0858$ gm

III.1.2.b  Grinding :

Two types of grinding was used.

1) Dry grinding: Barium titanate powder was ground in a Fritsch pulverisette using corundum ball and mortar. The sample was ground for 6 hours and then the particle size was measured using a Fisher subsieve sizer.

2) Wet grinding : Here the powder was ground in two grinding media

a) Grinding in an alumina jar using alumina balls and distilled water. Samples were taken intermittently and

analyzed for particle size using Fisher subsieve sizer.
The results are given in Table III.1.

b) Grinding in an agate jar using agate balls
and distilled water in a Fritsch pulverisette. Here also
samples were taken intermittently and analyzed for particle
size. The results are given in Table III.1

III.1.3 : Preparation of Glass:

Two batches   i) 50 gm   ii) 25 gm of glass were
prepared. The amount of raw materials needed to prepare
50 gm batch of glass   74 pct. $Bi_2O_3$, 2 6 pct. $B_2O_3$   are:

$Bi_2O_3$   99 pct pure       = 47.51 gm
$H_3BO_3$   AR grade          = 4.43 gm

The raw materials were mixed thoroughly in an agate mortar
using acetone. The batch was then taken into an alumina
crucible for melting in a muffle furnace. The furnace was
kept around $750^oC$ and the melts were occasionally mixed by
swirling the liquid. The 25 gm batch of molten glass was
cast into discs for measuring the properties of glass. During
casting the glass has crystallized many times, even though
it was cast using chilled water bath. Finally the glass pieces
which are clear were taken for experimentation. These results are
given T.III2 Another batch of molten glass was quenched by
pouring the melt into a tray containing distilled water.
The glass pieces were then collected, dried and then ground
in a ball mill for 12-16 hours. The particle size of the
ground powder measured by Fisher subsieve sizer was 1 6- 18 μm.

Table III.1 : Size reduction during grinding

| Grinding in an alumina jar | | Grinding in an agate jar | |
|---|---|---|---|
| Grinding time | The particle size in microns | Grinding time | The particle size in micron |
| Starting material | 18 – 20 | Starting Material | 18 – 20 |
| 1 h | 13 – 15 | 6 h | 5 – 6 |
| 10 h | 8 – 10 | 12 h | 3 – 4 |
| 24 h | 5 – 6 | 24 h | 2 – 25 |
| 48 h | 2 – 3 | | |

This powder was used in the initial sintering experiments. This glass powder was further ground in a Fritsch pulverisette for 2 hours and 10 hours to get a particle size of 4 - 5 $\mu$m and 2-3 $\mu$m respectively.

III.1.3.a : Chemical Analysis of the glass:

Chemical analysis of the glass was done using the procedure given in appendix A. Actual analysis was done for bismuth and alumina and boron was determined by difference. Analysis was done for the two batches of glass prepared and the results are as shown below:

| | wt.pct. | $Bi_2O_3$ | $B_2O_3$[x] | $Al_2O_3$ |
|---|---|---|---|---|
| Batch 1 which was ground for 12 hrs with a particle size of 16-18 $\mu$m | | 94.31 | 5.2 | 0.43 |
| Batch 2 which was cast into discs | | 92.35 | 7.44 | 0.21 |
| Actual amounts taken | | 95.01 | 4.99 | - |

[x]calculated as the difference

Traces of alumina were present in both the cases and it might be due to the melting of glass in an alumina cricible. Alumina content was more in the ground sample, probaly due to grinding in an alumina jar. The difference in $Bi_2O_3$ content from the intended value may be due to the evaporation of some $Bi_2O_3$ during melting. The difference in $Bi_2O_3$ amounts in the two batches may be due to the crystallization of part of the glass during casting.

III.1.4 : Preparation of samples for liquid phase sintering:

Initial experiments were carried out over a wide range of compositions and sintering temperature. Six different 10 gm batches of $BaTiO_3$, each containing 0.4, 2, 10, 20, 30 and 40 wt. pct. of glass were prepared. Particle size of the powders used were, 13 - 14 μm $BaTiO_3$ and 16 -18 μm glass. The raw materials were mixed thoroughly for at least 1 hr in an agate mortar using acetone. It was then made into pellets each weighing approximately 1 gm, using a $\frac{1}{2}$" dia die at 40,000 psi pressure for further experimentation. Five different batches were prepared with 20, 10, 2 and 0.4 wt pct. of glass. These batches along with their heating schedules are given in Table III. 3.

Raw materials were mixed in the same way as described above. Here the powder was made into pellets in a 3/8" dia die, each weighing approximately 0.5 gm using PVA binder. Pressing was done in a double acting automatic hydraulic press at 100000psi pressure. Green densities were measured for all these pellets from geometry and weight, before firing.

III.1.5 : Liquid phase sintering:

Initial sintering experiments were done in a globar muffle furnace to which a programmable controller Honeywell) was attached. Sixdifferent batches each containing 0.4, 2, 10, 20, 30 and 40 wt pct. of glass were fired at five different temperatures, 800, 900, 1000, 1100 and 1200°C for 2 hours. Each time five pellets were taken in a platinum crucible and were stacked one over the other keeping some loose

Table III.3   Different batches prepared for liquid phase
sintering and their heating schedule.

| Batch No. | Wt% glass | Particle size (μm) of BaTiO$_3$ | Particle size (μm) of Glass | Sintering temperature °C. | Sintering times (h) |
|-----------|-----------|-------------------|-------|------------------------|---------------------|
| 1 | 20 | 13 | 17 | 1000 | 1/2, 1, 3 |
|   |    |    |    | 1100 | 1/6, 1/2, 1 |
| 2 | 10 | 13 | 17 | 1000 | 1/6,1/2,1,2 |
|   |    |    |    | 1100 | 1/6,1/2,1,2 |
| 3 | 10 | 5  | 4  | 1000 | 1/6,1/2,1,2 |
|   |    |    |    | 1050 | 1/6,1/2,1,2 |
|   |    |    |    | 1100 | 1/6,1/2,1,2 |
|   |    |    |    | 1150 | 1/6,1/2,1,2 |
| 4 | 2  | 2  | 2.5 | 1100 | 1/6,1/2,1,2 |
|   |    |    |    | 1150 | 1/6,1/2,1,2 |
|   |    |    |    | 1200 | 1/6,1/2,1,2 |
| 5 | 0.4 | 2 | 2.5 | 1100 | 1/6,1/2,1,2 |
|   |    |    |    | 1150 | 1/6,1/2,1,2 |
|   |    |    |    | 1200 | 1/6,1/2,1,2 |

BaTiO$_3$ powder in between these pellets. Sintering of the five different batches mentioned previously was done in a globar horizontal tube furnace to which a proportional controller ( L and N Electromax) was attached. The temperature profile of the furnace is shown in Fig. III.1. Each time five pellets were taken in an alumina boat and were charged from one end of the furnace and pulled through the other end by a stainless steel rod which passes through a brass flange attached to the end of the tube. Two boats were connected to each other by a nichrome wire and the first boat was hooked to the stainless steel rod such that by pulling the rod from one end, the two boats will travel along the length of the furnace. The time schedule was made in such a manner that by pulling the boat through the length of the furnace it will pass through heating, soaking and cooling zones. Since two boats were connected to each other, as one boat is in the soaking zone the other will be in the heating zone, and as the first boat moves through the cooling zone the second boat will reach the soaking zone. In each case the time taken to reach the soaking zone was kept constant as 2 hours 40 minutes and soaking time was varied from 10 minutes to 2 hours and finally the time through the cooling zone was maintained constant as 2 hours.

The sintering temperatures and times followed for the five different batches mentioned previously are given in Table III.3. On batch 3 few more sintering experiments were done with longer heating cycle. Here the time taken to reach the soaking zone was made double and triple than that of the standard one, to investigate its effect on density. In these experiments the time through cooling zone
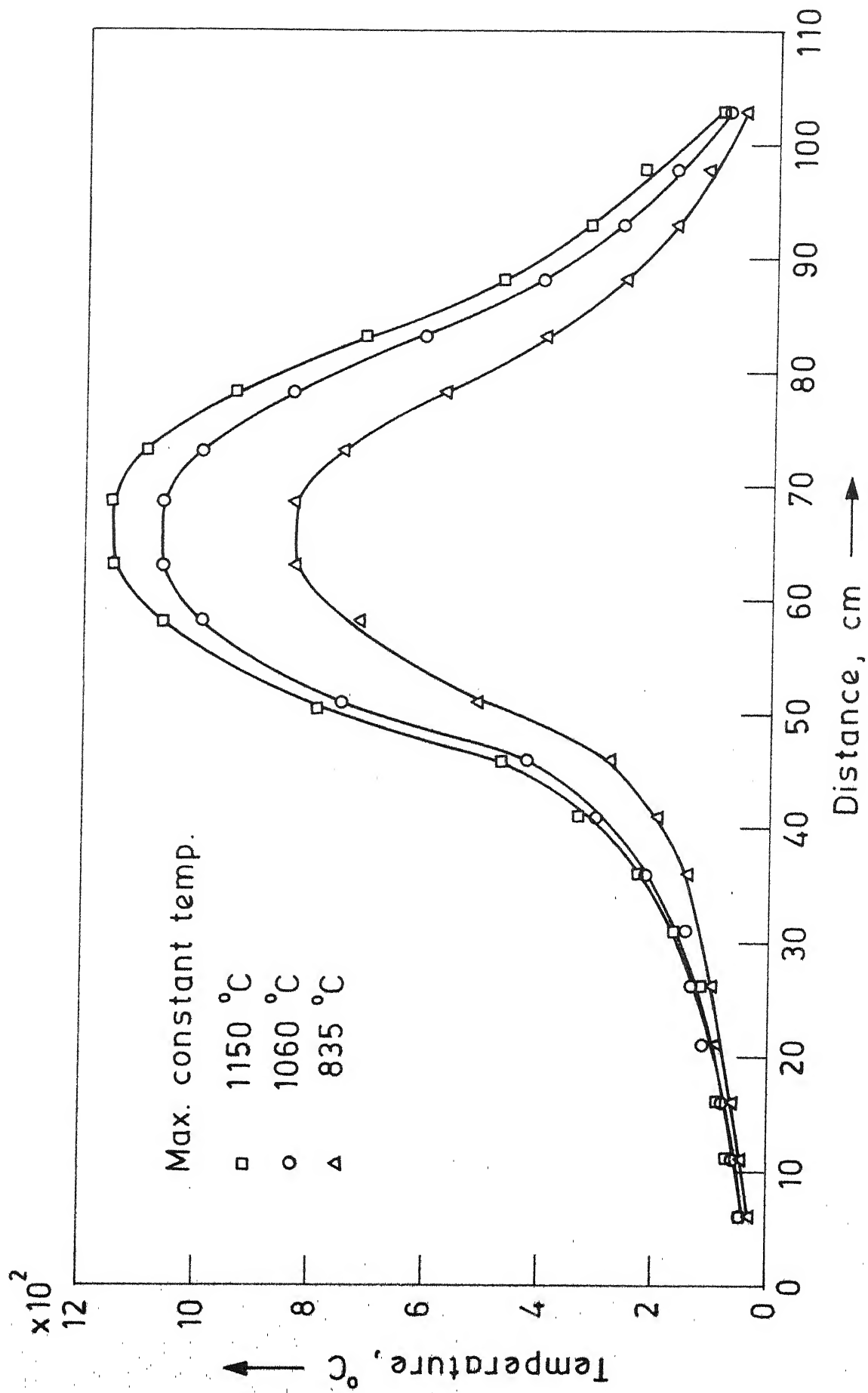
Fig. III-1 - Temperature profile of the tube furnace used in the sintering experiments.

## III.2 Characterisation:

### III.2.1 Weight loss measurements during sintering:

Weight loss was determined for each pellet after sintering using a Mettler single pan, electric balance    accuracy 0.0001 gm).

### III.2.2 Thermal Analysis:

The simultaneous DTA, DTG and TGA studies of the mixture of $BaTiO_3$ + 20 pct. glass sample was done on MOM Derivatograph.   The instrument parameters are given in Table III.4.

### III.2.3 Density Measurements:

Two types of densities were reported.

1) Geometrical density:  Geometrical densities were measured on each sintered pellet.  The pellets were weighed ( w) in a Mettler single pan, electric balance and volume ( v) of the pellet was measured using a screw guage. Density was calculated as ( w/v).

2) Bulk density:  Bulk density was calculated on one pellet from each sintering experiment.  Here density was measured by water displacement method.  The dried pellets were weighed ( D) in a mettler single pan, electric balance. The pellets were boiled in distilled water fnr 5 − 6 hours and soaked for 24 hours.  The water suspended wt. ( s) and water saturated wt. ( w) were determined.  The bulk density was evaluated using the expression $\left(\dfrac{D}{w-s}\right)$.

Table III.4 : Instrument parameters of Derivatograph:

1.  Heating rate                           $5^{\circ}/min$

2.  Reference sample                        Alumina

3.  Sensitivity of DTA                      1/5
                 DTG                        1/20

4.  Maximum temperature
    upto which it was run                   $1000^{\circ}C$

5.  Amount of the sample                    2.019 gm.

III.2.4  Microstructural observation:

For microstructural study, the samples were mounted in a thermosetting plastic so that one face of the disc was exposed. The sample was then ground on a silicon carbide powder over a glass plate using liquid paraffin. Grinding was done successively on 200, 400, 600 and 800 mesh size SiC powders. After grinding over 800 mesh powder, the sample was polished on a rotating cloth using diamond paste. Polishing was done at least for one day. After polishing the sample was etched approximately for 30 sec with a solution containing 5 pct. Hcl and 0.5 pct. HF (16). The etched sample was then observed under the NU 20 microscope using reflected light.

III.2.5  X-ray diffraction studies:

X-ray diffraction patterns of the calcined powder and the liquid phase sintered pellets were taken with a General Electric XRD-6 and Philips Automatic x-ray diffracto-meter (Type PW 1730/10) fixing the instrument parameters given in Table III.5. For diffraction studies on the pellets, the samples were mounted in a perspex sample holder with two tefflon screws, taking care that the sample surface was flat and in line with the sample holder. All these samples were scanned from $2\theta = 20^{\circ}$ to $60^{\circ}$.

Table III.5 : Instrument parameters for x-ray diffraction
studies.

| Parameters | GE XRD- 6 | Philips XRD Type 1730/10) |
|---|---|---|
| Radiation | CuK$_\alpha$ with Ni filter) | CuK$_\alpha$ with Ni filter) |
| Excitation voltage | 35 KV | 35 KV |
| X-ray current | 15 mA | 20 mA |
| Divergent slit | $3^\circ$ | $4^\circ$ |
| Sollar slit for incident beam | MR | MR |
| Sollar slit for diffracted beam | MR and HR | MR and HR |
| Detector slit | $0.1^\circ$ and $0.02^\circ$ | $0.20$ and $1^\circ$ |
| Scanning speed | $2^\circ$/min and $0.2^\circ$/min | $2^\circ$/min and $1^\circ$/ |
| Chart speed | 1" /min | 2 cm/min |
| Time constant | 2 - 4 sec | 2 - 4 sec |

III.2.6.a  Temperature Dependence of Dielectric Properties:

Dielectric properties, capacitance and dissipation factor were measured using GR - 1620 A capacitance bridge assembly. The measuring frequency was 1 KHz at 0.5V. Before measuring, the sample was made flat on both ends and its diameter and thickness were measured accurately. It was then electroded with air dry silver paint on both the flat surfaces.

A high temperature sample holder with an access to three samples used for the temperature dependence of the dielectric properties is shown in Fig. III.2. The essential parts are the two electrodes, for the sake of simplicity, with associated connections and insulations built in an all metal unit. The low potential electrode in 1/8" thick steel plate of diameter 1.6" common to all the three samples. The steel plate is held rigidly by a support rod which is welded into the base plate at one end and the other end passes through the central hole in the top brass lid and is clamped by means of ar ldite. The high potential leads are made up of stainless steel wires insulated from outside in a glass tube over which a grounded metal sheath is wound. This lead assembly is again insulated in a bigger glass tube. A spring loaded arrangement presses these leads on the base plate which can be raised a bit to keep the specimens in position. The lower end of the wire is made into a bead to give proper contact on the electrode while the other end soldered to a positional plug of a three position switch.
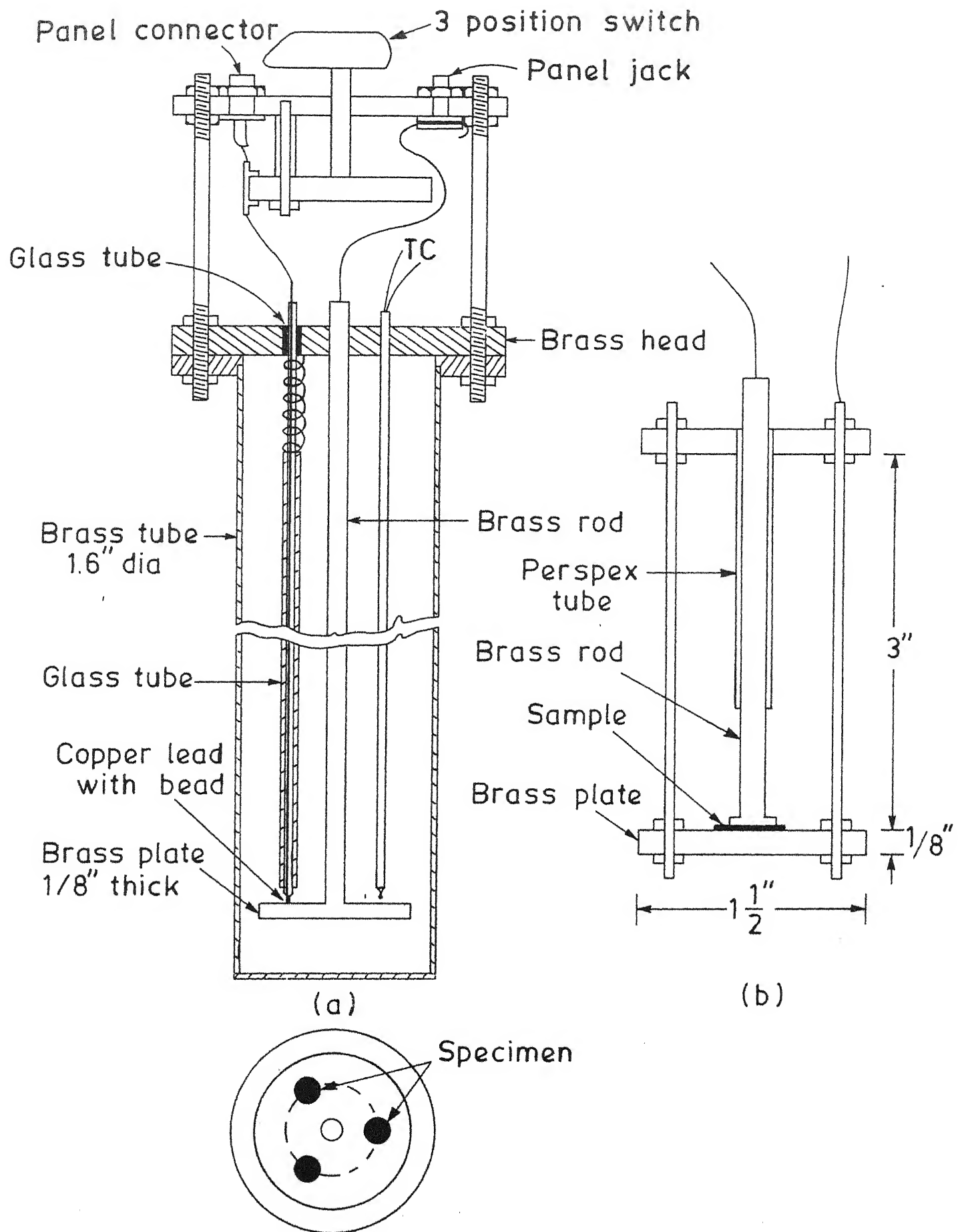
Fig. III.2 Sample holder for (a) high temperature dielectric measurements (b) DC bias studies.

The above assembly is inserted in a thin walled stainless steel tube, 2" in diameter and 18" in length. The panel carrying the connector, the jack and the switch is firmly attached to the top lid. The sample holder could be inserted into a small kanthal furnace. The heating rate ($1^o$/min) was regulated manually by a variable autotransformer. The temperature was measured by a chromel-alumel thermocouple (located near the samples) with a Honeywell potentiometer. These measurements were done from room temperature to $180^o$C for most of the samples and upto $410^o$C for few samples, at an interval of $10^o$C from room temperature to $10^o$C below the Curie point and afterwards measurements were made every $2^o$ till it crosses the Curie point.

### III.2.6.b  D.C. bias effect on dielectric properties:

A different sample holder, small in size with both the high and low potential terminals free, was fabricated to study the d.c. bias effects and hysteresis loop character-istics. A sketch of the sample holder is shown in Figure III.2. The bottom electrode was a 1/8" thick circular brass plate capable of transferring the majority of the heat generated within the sample to the immersant. Threaded ends of two brass rods (1/8" dia) passed through the base plate on either ends and clamped by means of a nut. The upper ends are threaded into a circular perspex disc on either ends. The upper electrode consists of an insulated brass rod threaded into the same perspex disc at the centre. The capacitor and the holder were kept immersed in dry silicone oil at room

temperature to provide protection against corona at the electrode edges and to facilitate in maintaining the sample temperature.

A high voltage d.c. supply 0.10 KV, PS 900, (Electronic Upkaran Vikas Co. Kanpur) were used to study the d.c. bias behaviour. The capacitance bridge was protected from the d.c. bias by a 100 M $\Omega$ resistor and 1 $\mu$F blocking capacitor in series in a circuit similar to employed by Biggers et al (17) (Figure III.3). The value of the resistance was chosen to be two to three orders of magnitude higher than the reactance of the sample at 1 KHz. The capacitance value of the blocking capacitor was again chosen to be two to three orders of magnitude higher than the capacitance of the specimen.

The capacitance and dissipation factor ( tan $\delta$ ) were measured at room temperature upto a bias field of 110-120 volts/mil. The behaviour was studied during both increasing and decreasing bias field. These measurements were made from 0 to 2400 V at an interval of 200 V.

III.2.6.c Frequency dependence of dielectric properties:

Type GR 1620 A capacitance bridge assembly to which a 1210 CRC oscillator unit was attached, was used to measure the frequency dependence of dielectric properties. The capacitance and dissipation factor were measured from 100 C to 100 KC frequency at 0.45 V, using the same sample holder described in section III.2.6.a.

100 M Ω   1 μF

0 - 3 KV
DC power
supply

Sample XXXXX

Capacitance
bridge

NE 51
over volta
protection
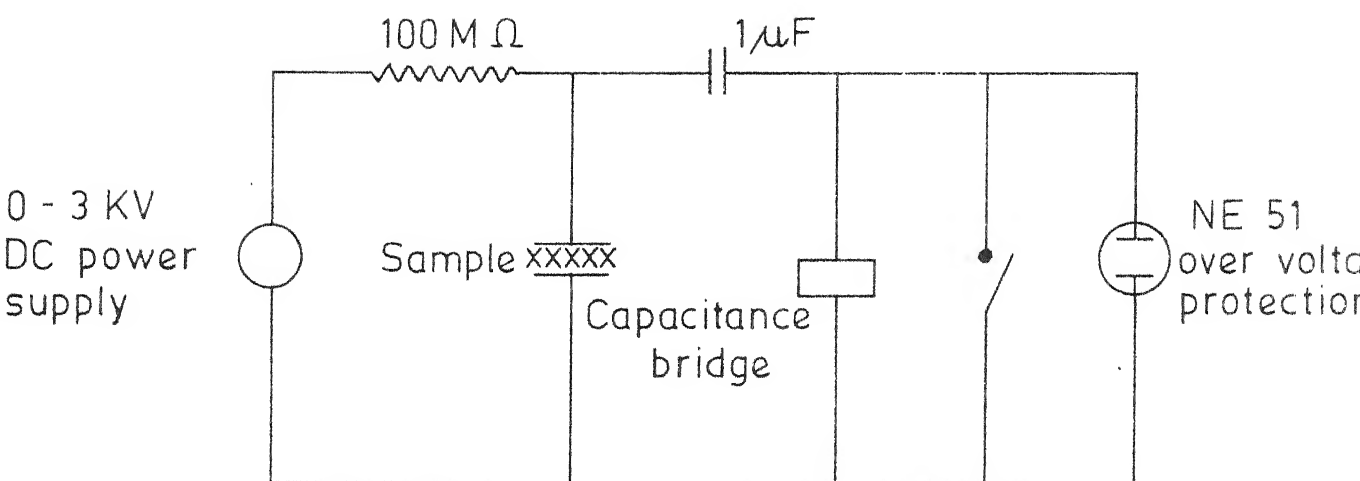
Fig. III-3 Circuit used for DC bias studies .

# IV.  RESULTS AND DISCUSSION

IV.1  Weight loss during sintering:

Weight loss measurements were made on all the sintered pellets.  These results are shown in Tables IV.1 and IV.2.

Table IV.1 gives the weight loss measurements during the critical sintering experiments.  It shows that the weight loss was almost constant at $\leq$ 1 pct. till $1100^{o}C$. This loss increases substantially from 1 to $\geq$ 2 pct. at higher temperatures and larger glass additions.  For example, this change becomes prominent with 20 pct. glass addition at $1200^{o}C$ with 30 pct. glass addition at $1100^{o}C$ and with 40 pct. glass addition at $1000^{o}C$.  Considering the whole weight loss was only due to the evaporation of the glass, a 20 pct. glass sample sintered at $1200^{o}C$ with a weight loss of 2.3 pct. indicates that over 10 pct. of the glass added is evaporating after sintering.  It indicates that most of the glass is still remaining in the sintered body.

Thermal analysis of the sample with 20 pct. glass addition (Fig. IV.1) heated upto $1000^{o}C$ showed a total weight loss of 1.1 pct., which is comparable with the values given in Table IV.1.

Since the weight loss was not significant at temperatures below $1100^{o}C$ for the next set of sintering experiments there data were given (Table IV.2) only for those samples which are sintered above $1100^{o}C$.  These results also shows that the weight loss increases with increasing sintering

Table IV.1 : Sintered density (g/cc) and pct. wt. loss of liquid phase sintered BaTiO$_3$

| S.No. | Wt.pct. glass additive | Green density g/cc | Sintering Temperature | | | | | | | | | |
| | | | 800°C | | 900°C | | 1000°C | | 1100°C | | 1200°C | |
| | | | Density | pct. wt. loss | Density | pct. wt. loss | Density | pct. wt. loss | Density | pct. wt. loss | Density | pct. wt. loss |
| 1 | 0.4 | 3.85 | 3.81 | 1.2 | 3.85 | 1.13 | 3.89 | 1.09 | 3.95 | 1.4 | 4.33 | 1.15 |
| 2 | 2.0 | 3.83 | 3.84 | 0.79 | 3.86 | 1.02 | 3.93 | 1.15 | 4.16 | 1.09 | 4.62 | 1.13 |
| 3 | 10.0 | 3.88 | 3.88 | 1.03 | 4.04 | 0.90 | 4.59 | 0.77 | 5.16 (86 pct td.) | 1.06 | 5.49 (91.2 pct td.) | — |
| 4 | 20.0 | 4.16 | 4.15 | 1.1 | 4.21 | 1.04 | 5.22 (86.8 pct. td.) | 0.91 | 5.94 (98.7 pct. td.) | 1.15 | 4.62 | 2.33 |
| 5 | 30.0 | 4.41 | 4.49 | 1.05 | 4.52 | 0.9 | 5.24 (87.1 pct. td.) | 0.98 | 5.70 (94.7 pct. td.) | 1.57 | 4.74 | 2.03 |
| 6 | 40.0 | 4.35 | 4.59 | 1.53 | 4.85 | 1.15 | 4.65 | 1.82 | — | — | — | — |

Table IV.2 : Weight loss data of liquid phase sintered $BaTiO_3$

| pot. glass addition | pct. wt. loss for sintering time, hr. | | | |
|---|---|---|---|---|
| | 1/6 | $\frac{1}{2}$ | 1 | 2 |
| Sintering Temperature $1150^{\circ}C$ | | | | |
| 10 | 1.87 | 2.33 | 2.46 | 2.27 |
| 2 | 0.73 | 1.02 | 2.39 | 2.4 |
| 0.4 | 0.65 | 0.97 | 1.78 | 1.85 |
| Sintering Temperature $1200^{\circ}C$ | | | | |
| 2 | 2.43 | 2.50 | 2.20 | 2.35 |
| 0.4 | 1.78 | 1.77 | 1.69 | 1.64 |

temperature and also with increasing glass addition.

IV.2   Thermal Analysis:

Results of the simultaneous DTA, DTG and TGA studies of the mixture of $BaTiO_3$ and 20 pct. glass powders sample are shown in Figure IV.1. The total weight of the sample was 2.019 gm.

The DTA curve shows two transformations, one at 350°C and another at 830°C.   The transformation at 350°C may be due to the crystallization point of the glass. This glass has a melting point around 700-750°C (Table II.2), which is not clearly resolved in the DTA plot. The second transformation at 830°C appears to be due to the reaction of the glass with $BaTiO_3$, as discussed below.

TGA plot shows that there is a gradual weight loss ( ∼ 0.85 pct.) till 350°C,  which may be due to the evaporation of the moisture and binder.  The weight change was constant till 750°C.  This weight loss (∼ 0.85 pct.) may be compared with the loss ( ∼ 1 pct.) observed in the sintering experiments upto 1000°C.  Around 900°C there is a sudden additional weight loss ( ∼ 0.45 pct.).

To confirm these results two experiments were carried out.  In one experiment X-ray diffraction studies were carried out with samples of $BaTiO_3$ and 20 pct. glass mixture which were heated to 725, 800, 900, 1000 and 1100°C for 15 min.   For 725°C samples alone,  15min.  and

Weight loss (mg)

DTA

830°C

350°C

TGA

0

10

20

30
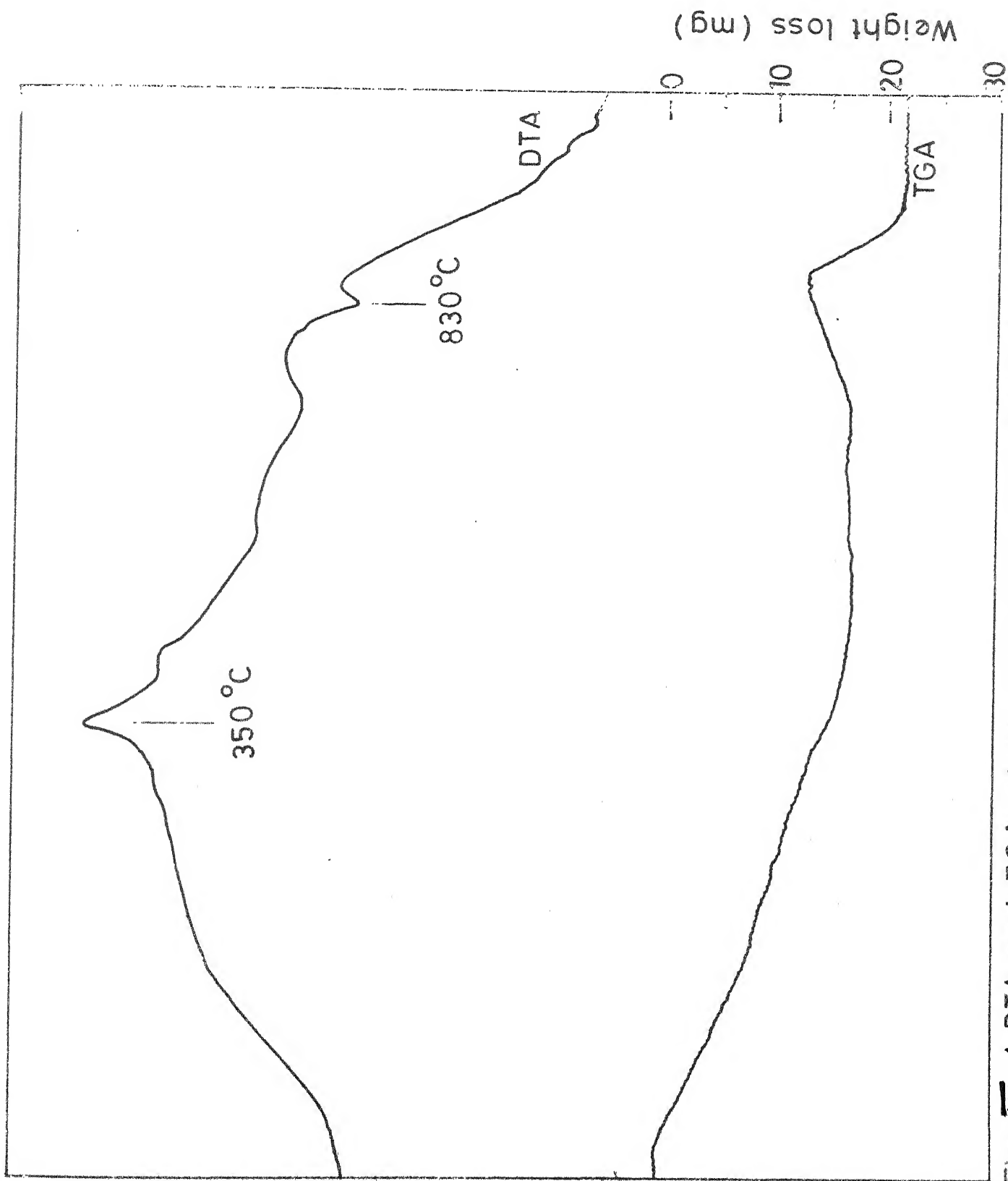
Fig. IV-1 DTA and TGA plots of BaTiO$_3$ and 20% glass mixture.

2h heating time were provided. These results are discussed in detail in section IV.5. The diffraction pattern of the sample heated upto 725°C for 15min showed the presence of crystallized glass in the form of $12Bi_2O_3 \cdot B_2O_3$ alongwith $BaTiO_3$. Where as at 2h the glass started reacting with $BaTiO_3$ and the diffraction pattern showed the presence of $BaBi_4Ti_4O_{15}$ and crystallized glass along with $BaTiO_3$. The sample heated upto 800°C showed the presence of $BaBi_4Ti_4O_{15}$ phase along with $BaTiO_3$, but no crystallized glass phase was observed. It indicates that the glass is reacting with $BaTiO_3$ forming $BaBi_4Ti_4O_{15}$ around 800°C. The diffraction patterns at 900°C, 1000 and 1100°C show that the formation of $BaBi_4Ti_4O_{15}$ reaches a maximum at 900°C and its amount decreases with increasing temperature.

In another experiment a $Bi_2O_3 \cdot B_2O_3$ (74:26) glass piece was heated in the furnace at 525°C for 8h. After cooling the sample was crystallized in $12Bi_2O_3 \cdot B_2O_3$ and $2 Bi_2O_3 \cdot B_2O_3$ form ( discussed in section IV.5). So from this experiment it can be concluded that the peak at 350°C in DTA plot may be due to the crystallization of glass.

From the DTA, TGA and X-ray diffraction studies it can therefore be concluded that the glass reacts with $BaTiO_3$ forming $Ba Bi_4Ti_4O_{15}$ at about 725°C and its amount reaches a maximum at 900°C and $BaBi_4Ti_4O_{15}$ appears to be decomposing with increasing temperature beyond 900°C.

## IV. 3  Density:

Sintered samples were investigated using density measurements to study the effect of various parameters on sintering.

## IV.3.1   Effect of Glass Addition:

Effect of glass addition on density was studied using density measurements on samples with 0.4, 2,10,20,30 and 40 Wt. pct glass, sintered at 800, 900, 1000, 1100 and 1200°C for 2h. Particle size of sintered powders were 13/um Ba Ti $O_3$ and 17 /um glass. These results are given in Table IV.1 and shown in Figs. IV.2 and 3. All the densities measured in this case were geometrical densities except in those cases where it was not possible due to the sticking of the pellets to each other. Fig. IV.2 shows density vs glass addition for the samples sintered at different temperatures. Fig. IV.3 shows density vs sintering temperatures for the samples with different glass addition. From these figures,it can be seen that to get densities greater than 85% theoretical density of Ba Ti $O_3$ ( 6.02 g/cc) at 1000°C, a minimum of 20% glass is necessary and on the other hand with 10% glass addition,a minimum sintering temperature of 1100°C is necessary. The maximum density obtained was  5.22 g/cc (87% td) for the samples with 20% glass addition sintered at 1000°C for the particular sintering parameters employed. It can be observed
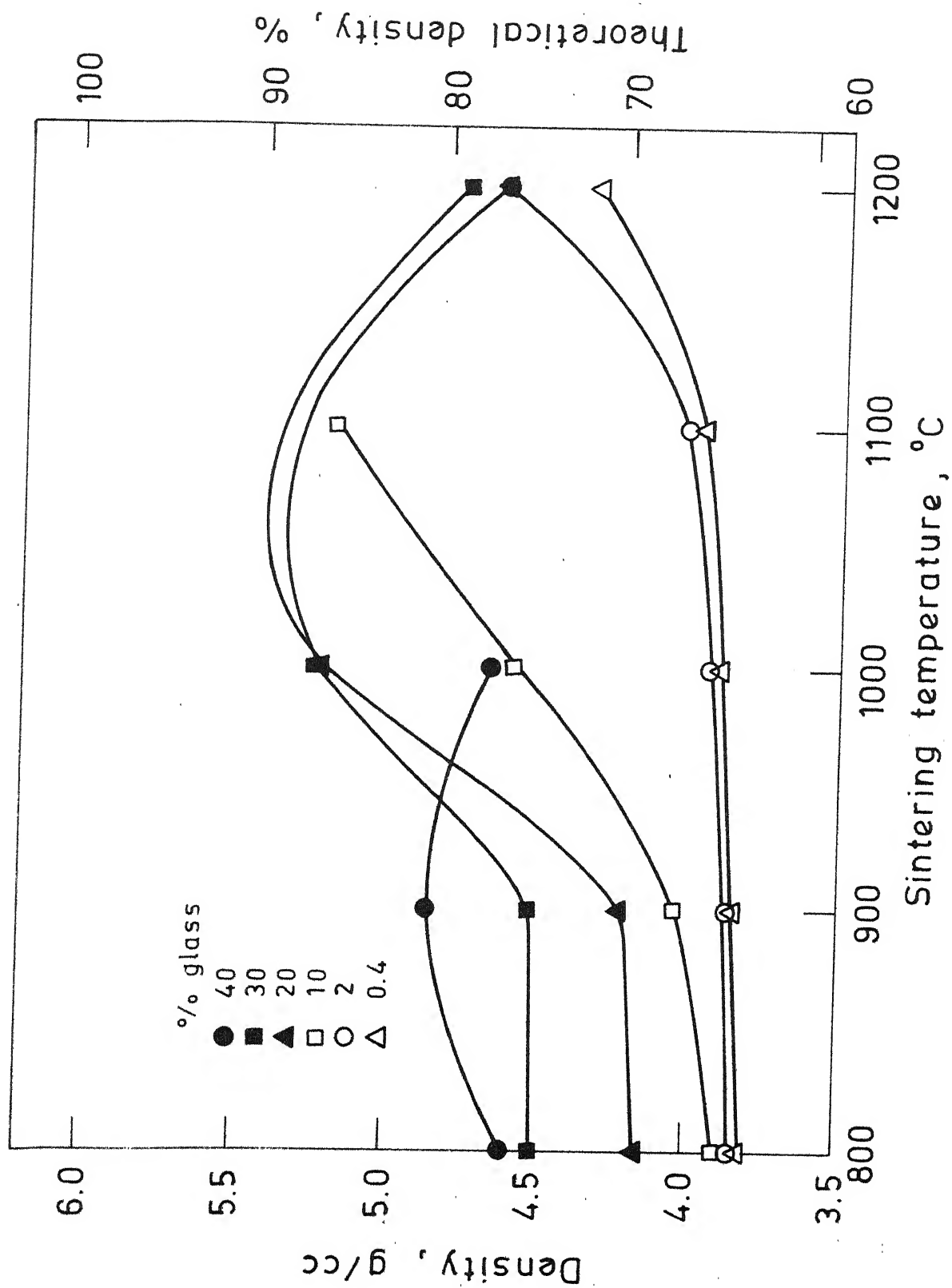
Fig. IV-2 Density vs sintering temperature of BaTiO$_3$ with different amounts of glass addition (sintering time : 2 hours)
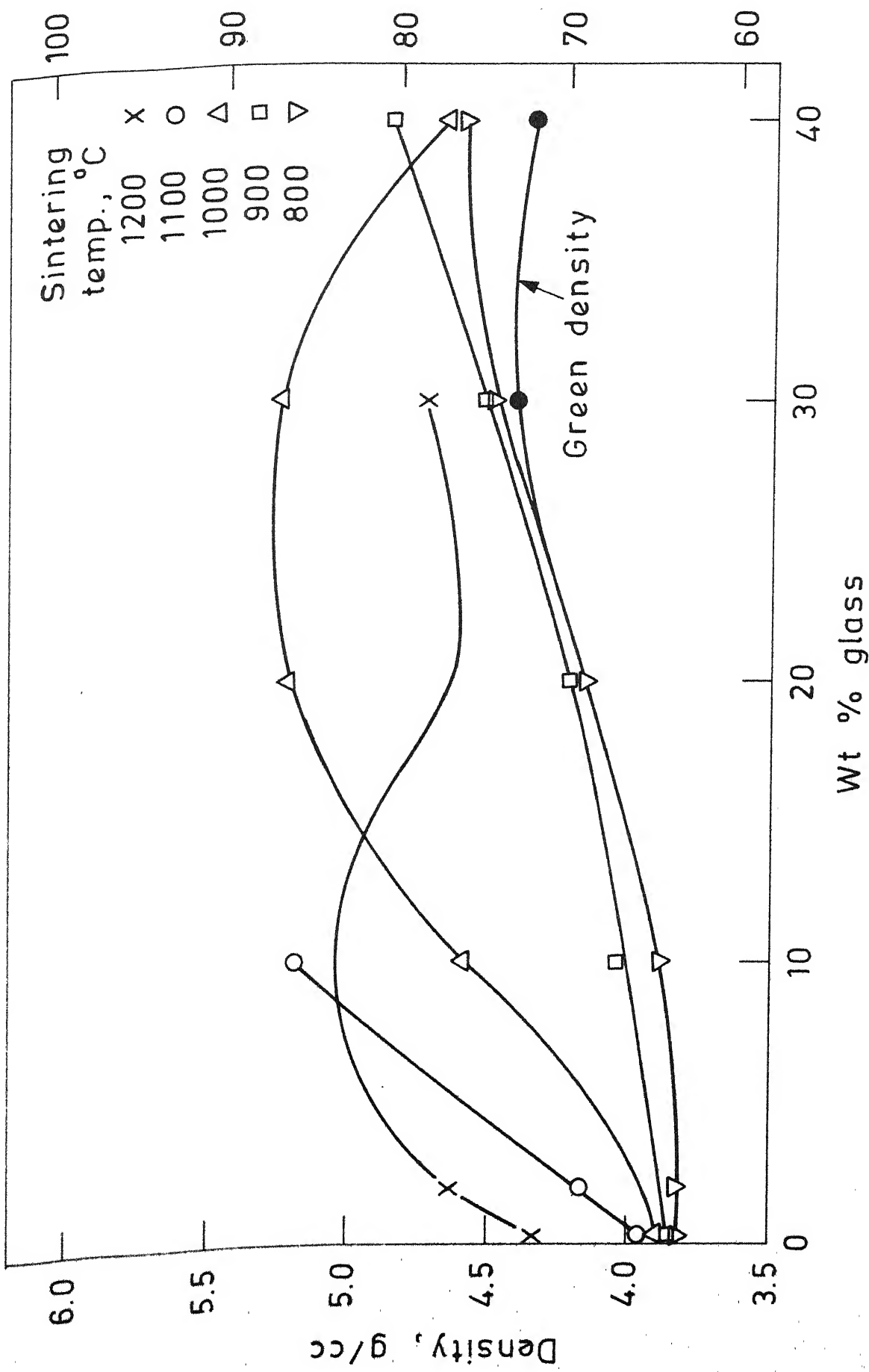
Fig. IV-3   Density vs wt % glass addition to BaTiO$_3$ at different sinteri temperatures (sintering time : 2 hours).

from these figures, that for the samples with 20% and higher glass additions, the densities were decreasing at higher sintering temperatures ( above 1100°C). Visual examination of these samples with 20% and 30% glass sintered at 1100°C and above showed that a layer of glass was collected on the bottom surface and the pellet was distorted in shape. This clearly shows that at 1100°C the viscosity of the glass is too low and it is flowing out of the pellet. From the weight loss data shown in Table IV.1 it can be observed that for 20 and 30% samples the weight loss was less than 1% till 1000°C, but afterwards it is increasing significantly from 1 to 2% at 1200°C for 20% sample and at 1100°C for 30% sample. It indicates that the glass is evoporating at these temperatures. This evoporation and oozing out of the glass must be the reasons for decrease in densities of these samples at higher sintering temperatures. It can also be observed from this figure that with 0.4 and 2% glass additions a sintering temperature of more than 1200°C is necessary to get reasonable de densities.

So from these density results it can be concluded that for liquid phase sintering of $BaTiO_3$ at 1000-1100°C a minimum of 10 to 20% glass addition is necessary, and also it is not possible to decrease the sintering temperature by increasing the amount of glass above 20% using the same sintering

perameters employed here.

IV.3.2   Effect of sintering temperature and time:

To study the densification process more closely
sintering experiments were done on 20%, 10%, 2% amd 0.4% glass
samples with respect to temperature and time.  Sintering
temperatures, times and particle sizes of these different
batches are given in Table IV.3 along with the green
densities ( average of 5 pellets) geometrical densities (avg of 5 pellets) and the displacement
densities ( based on one sample).  The reason for considering
both the densities is, that in the case of geometrical
density it includes both open and closed porosity ( total
porosity), where as in the case of displacement densities
it will include only the closed porosity.  Table IV.4. gives
these porosity data for the samples with 10% glass sintered
at different temperatures and times.  Percent theoretical
density calculated by taking 6.02 g/cc as the theoretical
density of $Ba\ Ti\ O_3$, without considering the glass addition
is shown with-in brackets next to each density value.  These
density results are plotted in Figs. IV. 4-8.   Fig. IV.4
show the geometrical and the displacement densities for the
samples with 20% glass addition, sintered at 1000°C for 1/2,
1 and 3h. and at 1100°C for  1/6, 1/2 and 1h.  This figure
shows the displacement densities are more than geometrical

densities for all these samples as expected. It may be due
to the evaporation of some of the glass from the surface at
these temperatures causing more open porosity. It can also be
observed from this figure that at 1000°C the density is
increasing sharply between 1/2 and 1h. and afterwards it is
gradual till 3h. where-as at 1100°C most of the densification
is taking place with-in the first 10 min. and afterwards
there is very little increase in density with sintering time.
This may be because of the viscosity of the glass being
lower at 1100°C than 1000°C, facilitating easy densification
with in a short time at 1100°C. The reason for the decrease
in the displacement densities at 1100°C with increase in
sintering time may be due to the oozing out of the glass from
the pellet, which was observed by visual examination of the
pellet. Fig. IV.5 shows the geometrical and the displacement
densities for the samples with 10% glass addition sintered
at 1000 and 1100°C for 1/6, 1/2, 1 and 2h. Here the particle
sizes of Ba Ti $O_3$ and glass used are 13/u and 17/u respectively,
It can be observed from these figures that at 1000°C the
densities are increasing gradually with increasing sintering
time till 2h, where-as at 1100°C most of the densification
is taking place with-in the first 10 min and there is
gradual increase in density between 10 min and /2h, and
afterwords there is very little increase in density till 2h.
Here also it can be observed that the displacement densities

are more than geometrical densities for all the samples.
Table IV.4. shows that as the sintering temperature increases
from 1000-1100°C the open porosity is increasing while the
closed porosity decreases. It clearly indicates that the
glass is evaporating at 1100°C, causing more open porosity.
Figs. IV. 6 and 7 shows the geometrical and the displacement
densities for the samples with 10% glass, sintered at 1000,
1050, 1100 and 1150°C for 1/6, 1/2, 1 and 2h. Here the
initial particle sizes of Ba Ti $O_3$ and glass are 5 /um and
4 /um respectively. These figures also show. same trend as
in Fig. IV.5. At 1000°C the densities are increasing
gradually with increasing sintering time till 2h. At 1050 a.
and 1100°C densities are increasing sharply upto. 1h and
afterwards there is very little increase till 2h. Where-as
in the case of 1150°C it can be observed that most of the
densification is taking place with-in the first 10 min. and
afterwards there is very little increase in density. Fig. IV.6
shows that the geometrical densities are better for the
samples sintered at 1050°C than those samples sintered at
1000˙ , 1100 and 1150°C, but Fig. IV.7 shows that the
displacement densities are increasing with increasing
sintering temperature. This implies that while the closed
porosity decreases with increasing temperature, the open
porosity reaches a minimum at 1050°C and increases at 1100

and 1150°C presumably due to the oozing out or evaporation of glass.

Fig. IV. 8. shows the geometrical densities for the samples with 2% and 0.4% glass addition, sintered at 1100, 1150 and 1200°C for 1/6, 1/2, 1 and 2h. This figure shows that the densities are increasing gradually for all the samples with increasing sintering temperature and time. It can also be observed from this figure that the densities are slightly better for 0.4 % samples than for 2% samples. This may be due to the greater evaporation of the glass from the 2% glass sample at these high temperatures. Weight loss data given in Table IV.2. also shows the weight loss for 2% samples was more than for the 0.4% samples. From these density results if can be concluded that with 20% glass addition a sintering temperature of 1100°C may be high because of the problem of glass flowing out at 1000°C seems to be too low, so that the ideal temperature for these samples may be in between these two. In the case of 10% glass, samples sintered at 1050°C are showing better densities, and also a sintering time of 1h is sufficient at this temperature. With 0.4 and 2% glass addition, to get reasonable densities (~85% td) higher sintering temperatures e.g. 1200°C are necessary.

Table IV.3  <u>Density of Green and Sintered Pellets.</u>

| Batch No. | Sample | Sintering temp. °C | Sintering time | Green density g/cc | Sintered Density (g/cc) Geometrical | Displacement |
|---|---|---|---|---|---|---|
| 1. | BaTiO₃ with 20% glass using 13/um BaTiO₃ and 17/um glass | 1000 | 1/2h | 4.35(72.3) | 4.66(77.4) | 5.03 (83.6) |
| | | | 1 h | 4.33(71.9) | 5.02(83.4) | 5.18 (86.0) |
| | | | 3 h | 4.36(72.4) | 5.16(85.7) | 5.20 (86.4) |
| | | 1100 | 10min | 4.33(71.9) | 5.10(84.7) | 5.41 (89.9) |
| | | | 1/2 h | 4.35(72.3) | 5.15(85.5) | 5.34 (88.7) |
| | | | 1 h. | 4.35(72.3) | 5.18(86.0) | 5.25 (87.2) |
| 2. | BaTiO₃ with 10% glass using 13/um BaTiO₃ and 17/um glass | 1000 | 10min | 4.20(69.8) | 4.78(79.4) | 4.84 (80.4) |
| | | | 1/2 h | 4.21(69.9) | 4.87(80.9) | 4.94 (82.1) |
| | | | 1 h | 4.25(70.6) | 5.03(83.6) | 5.08 (84.4) |
| | | | 2 h | 4.22(70.1) | 5.26(87.4) | 5.39 (89.5) |
| | | 1100 | 10min | 4.28(71.1) | 5.06(84.1) | 5.25 (87.2) |
| | | | 1/2 h | 4.28(71.1) | 5.24(87.0) | 5.54 (92.0) |
| | | | 1 h | 4.23(70.3) | 5.25(87.2) | 5.56 (92.4) |
| | | | 2 h | 4.24(70.4) | 5.27(87.5) | 5.58 (92.7) |
| 3. | BaTiO₃ with 10% glass using 5/um BaTiO₃ and 4/um glass | 1000 | 10min | 4.42(73.4) | 4.68(77.7) | 4.41 (73.8) |
| | | | 1/2 h | 4.41(73.3) | 4.79(79.6) | 4.75 (78.9) |
| | | | 1 h | 4.43(73.6) | 4.86(80.7) | 4.81 (79.9) |
| | | | 2 h | 4.42(73.4) | 5.01(83.2) | 5.28 (87.7) |
| | | 1050 | 10min | 4.43(73.6) | 5.20(86.4) | 5.40 (89.7) |
| | | | 1/2 h | 4.43(73.6) | 5.32(88.4) | 5.48 (91.0) |
| | | | 1 h | 4.39(72.9) | 5.40(89.7) | 5.50 (91.4) |
| | | | 2 h | 4.39(72.9) | 5.37(89.2) | 5.54 (92.0) |
| | | 1100 | 10min | 4.45(73.9) | 5.10(84.7) | 5.43 (90.2) |
| | | | 1/2 h | 4.44(73.8) | 5.25(87.2) | 5.61 (93.2) |
| | | | 1 h | 4.42(73.4) | 5.30(88.0) | 5.78 (96.0) |
| | | | 2 h | 4.42(73.4) | 5.27(87.5) | 5.79 (96.2) |
| | | 1150 | 10min | 4.39(72.9) | 5.27(87.5) | 5.49 (91.2) |
| | | | 1/2 h | 4.40(73.1) | 5.35(88.9) | 5.63 (93.5) |
| | | | 1 h | 4.39(72.9) | 5.30(88.0) | 5.78 (96.0) |
| | | | 2 h | 4.41(73.3) | 5.31(88.2) | 5.91 (98.2) |

| Batch No. | Sample | Sintering temp. °C | Sintering time | Green dinsity g/cc | Sintered Density (g/cc) Geometrical | Displacement. |
|-----------|--------|-------------------|----------------|--------------------|-------------------|---------------|
| 4. | BaTiO$_3$ with 2% glass using 2 /um BaTiO$_3$ and 2.5 /um glass | 1100 | 10min | 3.95(65.6) | 4.55 | (75.6) |
| | | | 1/2 h | 3.96(65.8) | 4.56 | (75.7) |
| | | | 1 h | 3.93(65.3) | 4.66 | (77.4) |
| | | | 2 h | 3.94(65.4) | 4.70 | (78.1) |
| | | 1150 | 10min | 3.84(63.8) | 4.7 | (78.1) |
| | | | 1/2 h | 3.98(66.1) | 4.81 | (79.9) |
| | | | 1 h | 3.98(66.1) | 4.91 | (81.6) |
| | | | 2 h | 4.05(67.3) | 5.08 | (84.4) |
| | | 1200 | 10min | 3.98(66.1) | 5.01 | (83.2) |
| | | | 1/2 h | 4.00(66.5) | 5.04 | (83.7) |
| | | | 1 h | 4.02(66.8) | 5.10 | (84.7) |
| | | | 2 h | 4.02(66.8) | 5.20 | (86.4) |
| 5. | BaTiO$_3$ with 0.4% glass using 2 /um BaTiO$_3$ and 2.5 /um glass | 1100 | 10min | 4.07(67.6) | 4.55 | (75.6) |
| | | | 1/2 h | 3.97(65.9) | 4.65 | (77.2) |
| | | | 1 h | 3.99(66.3) | 4.52 | (75.1) |
| | | | 2 h | 4.18(69.4) | 4.88 | (81.1) |
| | | 1150 | 10min | 4.13(68.6) | 5.03 | (83.6) |
| | | | 1/2h | 4.12(68.4) | 5.08 | (84.4) |
| | | | 1 h | 4.13(68.6) | 5.10 | (84.7) |
| | | | 2 h | 4.11(68.3) | 5.22 | (86.7) |
| | | 1200 | 10min | 3.94(65.4) | 4.93 | (81.9) |
| | | | 1/2 h | 3.98(66.1) | 5.05 | (83.9) |
| | | | 1 h | 4.17(69.3) | 5.27 | (87.5) |
| | | | 2 h | 4.19(69.6) | 5.45 | (90.5) |

IV. 4  Porosity change with sintering temperature and time.

| Sample | Sintering temperature °C | Sintering Time (h) | Total porosity % | Closed porosity % | open porosity % |
|---|---|---|---|---|---|
| BaTiO$_3$ with 10% glass using 13 um BaTiO$_3$ and 17 um glass | 1000 | 1/6 | 20.6 | 19.6 | 0.99 |
| | | 1/2 | 19.1 | 17.9 | 1.16 |
| | | 1 | 16.4 | 15.6 | 0.83 |
| | | 2 | 12.6 | 10.5 | 2.1 |
| | 1100 | 1/6 | 15.9 | 12.3 | 3.16 |
| | | 1/2 | 12.9 | 7.9 | 5.0 |
| | | 1 | 12.8 | 7.6 | 5.15 |
| | | 2 | 12.5 | 7.3 | 5.15 |
| BaTiO$_3$ with 10% glass using 5 um BaTiO$_3$ 4 um glass | 1000 | 1/6 | 22.2 | 26.2 | - |
| | | 1/2 | 20.4 | 21.1 | - |
| | | 1 | 19.3 | 20.1 | - |
| | | 2 | 16.8 | 12.2 | 4.5 |
| | 1050 | 1/6 | 13.6 | 10.3 | 3.32 |
| | | 1/2 | 11.6 | 8.9 | 2.32 |
| | | 1 | 10.3 | 8.6 | 1.66 |
| | | 2 | 10.8 | 8.0 | 2.82 |
| | 1100 | 1/6 | 15.3 | 9.8 | 5.48 |
| | | 1/2 | 12.8 | 6.8 | 6.31 |
| | | 1 | 12.0 | 4.0 | 7.97 |
| | | 2 | 12.5 | 3.8 | 8.6 |
| | 1150 | 1/6 | 12.5 | 8.8 | 3.65 |
| | | 1/2 | 11.1 | 6.5 | 4.65 |
| | | 1 | 11.9 | 4.0 | 7.77 |
| | | 2 | 11.7 | 1.8 | 1.97 |
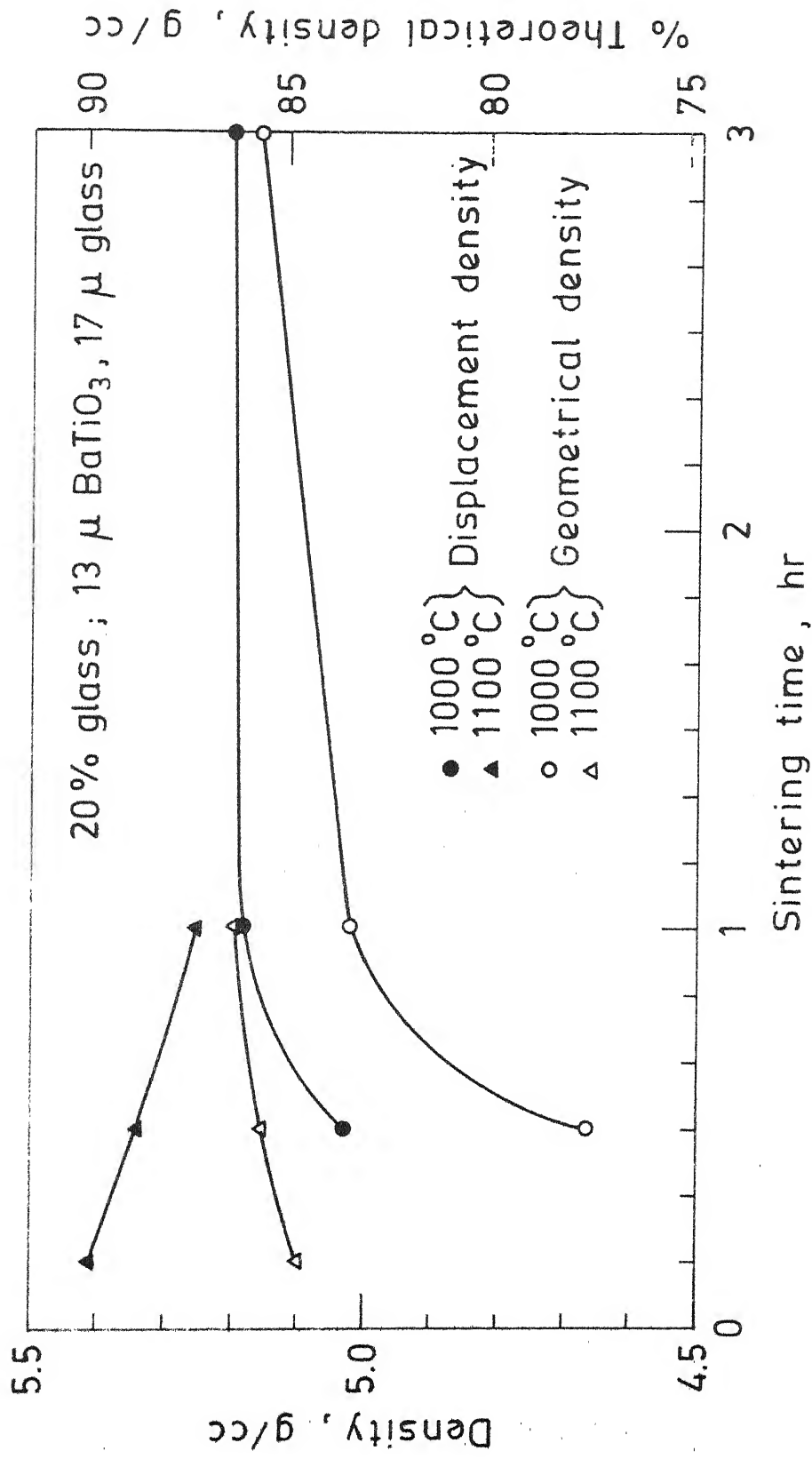
Fig. IV-4- Densification of BaTiO$_3$ as a function of sintering time with 20 % glass addition.
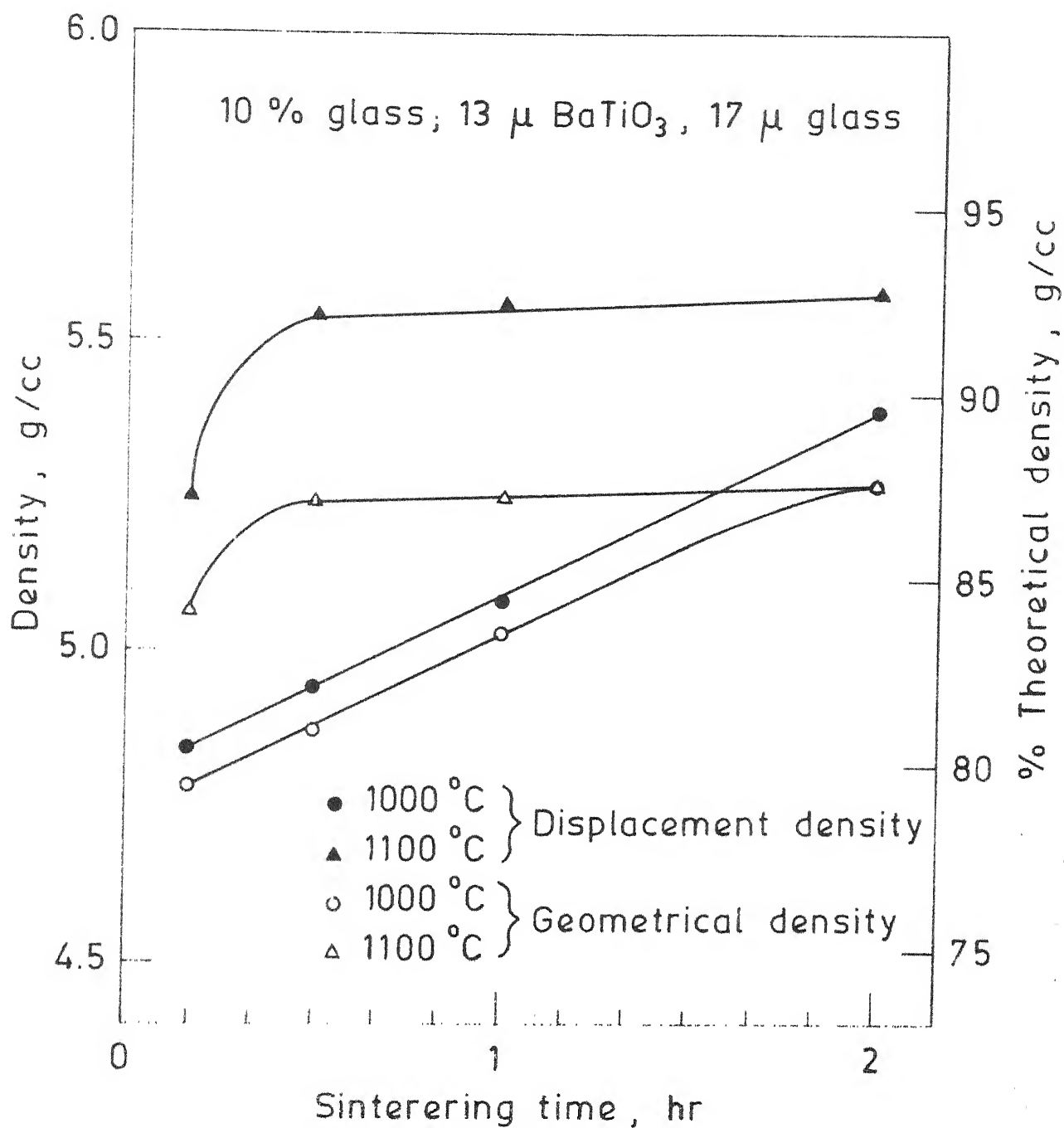
g. $\overline{IV}$-5 - Densification of BaTiO$_3$ as a function of sintering time with 10 % glass addition.
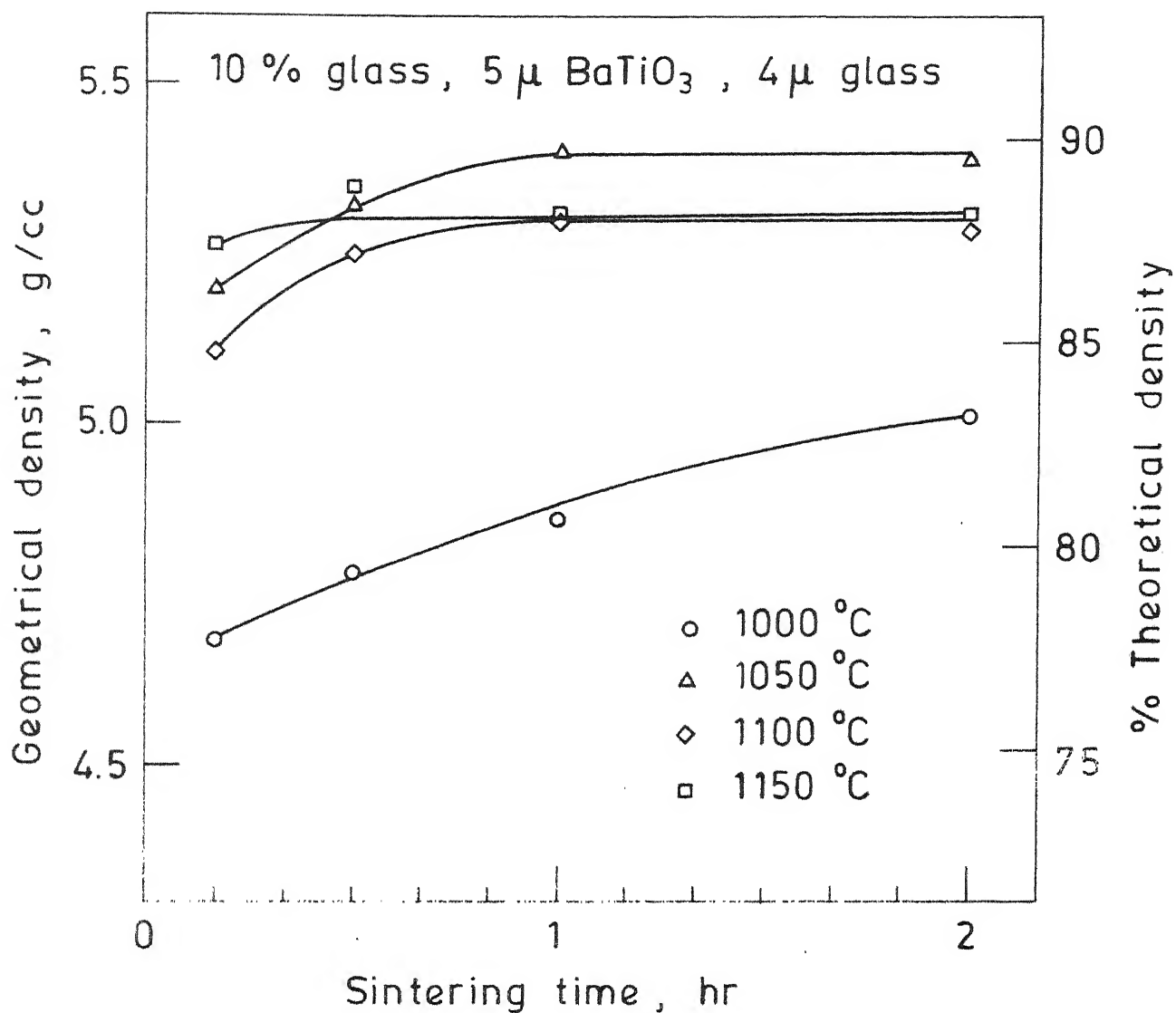
g. **IV** 6 - Geometrical density vs sintering time for BaTiO$_3$ with 10 % glass addition at different sintering temperatures.
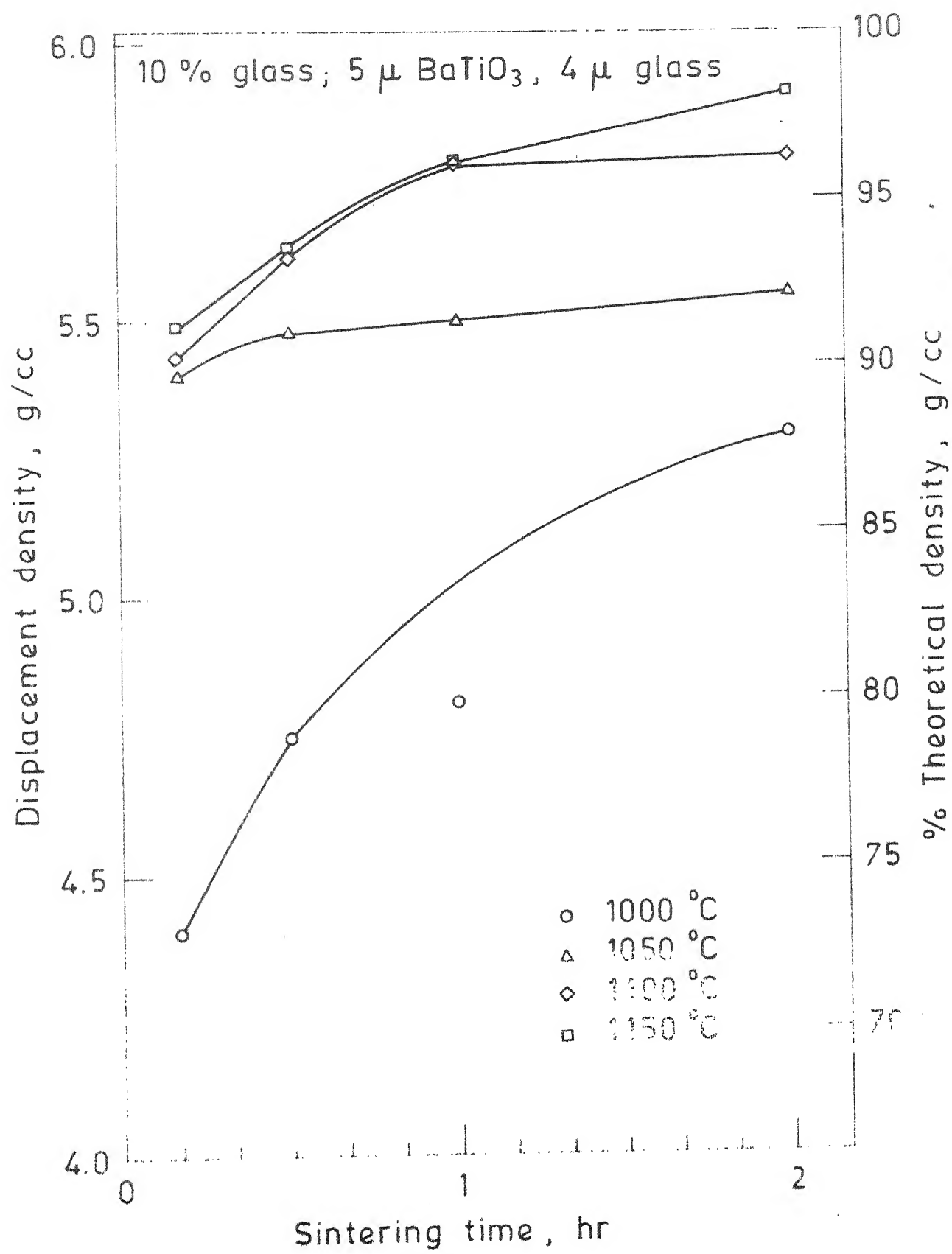
Fig. IV-7 - Displacement density vs sintering time for BaTiO₃ with 10 % glass addition at different sintering temperatures.
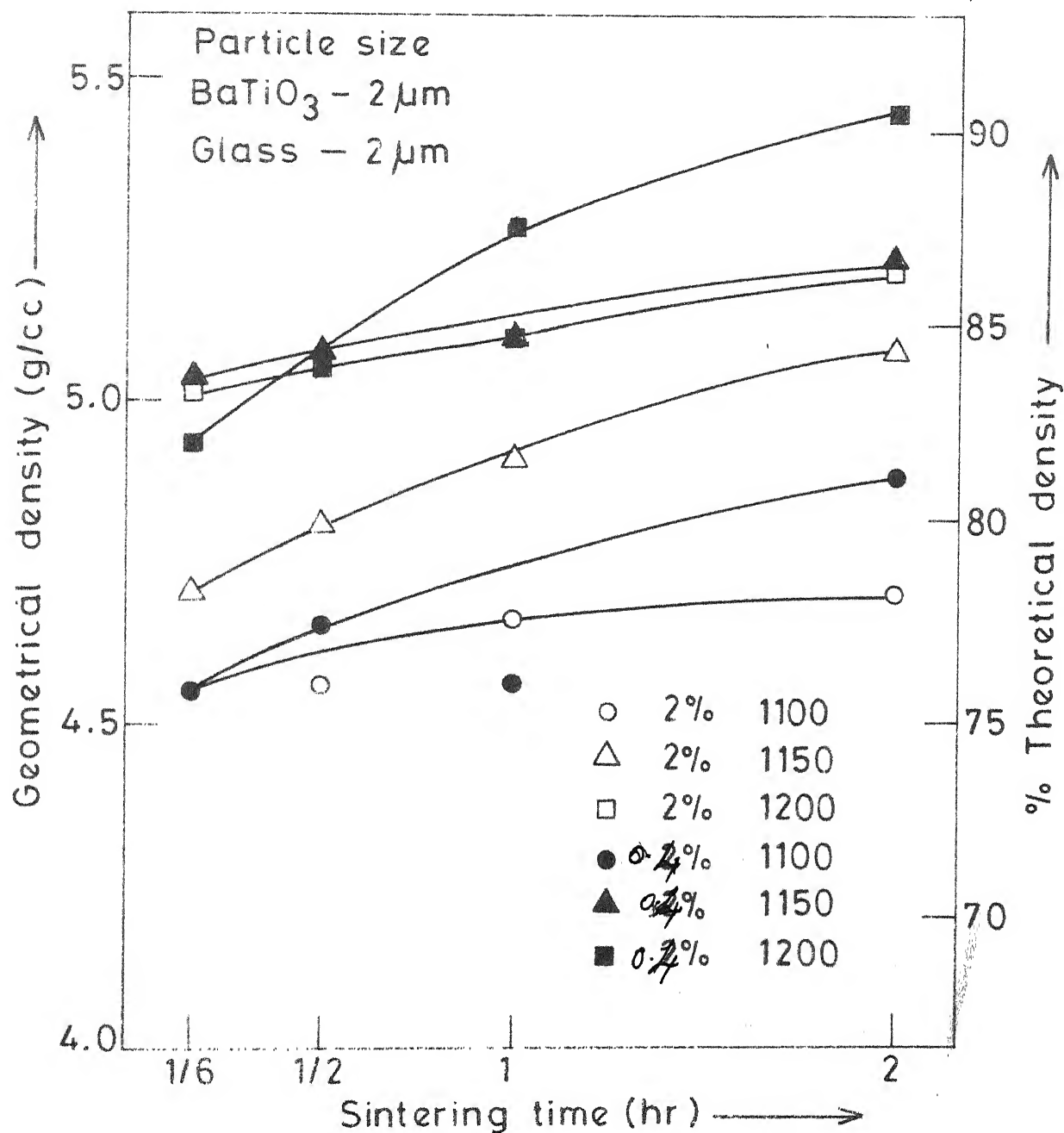
Fig. IV-8 Geometrical density vs. sintering time for BaTiO₃ with 0.4 and 2% glass addition at different temperatures.
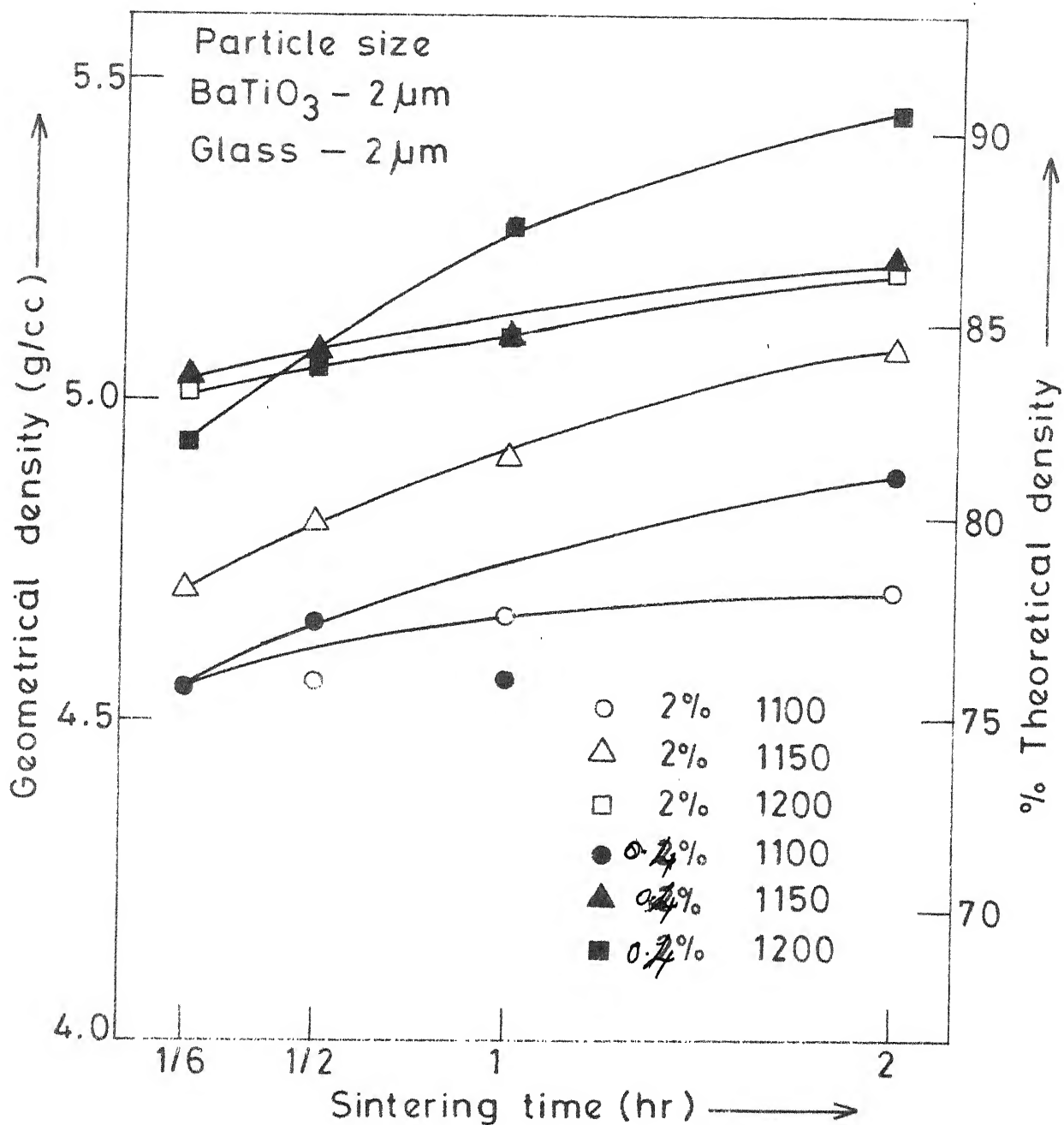
Fig. $\overline{IV}$-8 Geometrical density vs. sintering time for BaTiO$_3$ with 0.4 and 2% glass addition at different temperatures.

IV. 3.3   Effect of particle size:

Effect of particle size on densification was studied on 10% glass samples sintered at 1000 and 1100°C for 1/6, 1/2, 1 and 2h.  For this purpose two batches with different particle sizes of Ba Ti $O_3$ and glass ( 13 μum Ba Ti $O_3$ + 17 μum glass and 5 μum Ba Ti $O_3$ + 4 μum glass) were  used .  Fig. IV. 9 shows the geometrical densities of these samples as a function of sintering temperature and time.  It can be observed from this figure that there is no marked difference in densification in the particle size ranges used particularly at 1100°C.  Still lower particle size may have some effect.

IV. 3.4   Effect of rate of heating:

Effect of rae of heating on densification was studied on samples with 10% glass additions sintered at 1000, 1050 and 1100°C for 10 min and 2h with three different heatin; rates namely 2h 40min, 5h 20min, and 8h.  Particle size of  the powders used in this study were 5 μum Ba Ti $O_3$ and 4 μum glass.  These results are  given in Table IV.5.  These results show that for  8h heating schedule the densities are slightly better than at 2h 40min. But the increase in densities was not too large and there may not be much advantage in employing 8h heating schedule which is three times that of the usual 2h 40min. heating schedule used in all sintering experiments.

# TABLE IV.5

## Effect of rate of heating on densification

| % glass | Sintering temperature (°C) | Sintering Time (h) | Heating rate (time taken to reach sooking zone | Density (Geometrical) g/cc |
|---------|---------------------------|--------------------|-------------------------------------------------|----------------------------|
| 10% | 1000 | 1/6 | 2h 40 min. | 4.68 |
| | | | 5h 20min. | 4.64 |
| | | | 8h | 4.75 |
| | 1000 | 2 | 2h 40min. | 5.01 |
| | | | 5h 20min. | 5.02 |
| | | | 8h. | 5.26 |
| | 1050 | 1/6 | 2h 40min | 5.20 |
| | | | 5h 20min. | 5.18 |
| | | | 8h. | 5.20 |
| | 1050 | 2 | 2h 40min. | 5.37 |
| | | | 5h 20min. | 5.39 |
| | | | 8h. | 5.50 |
| | 1100 | 1/6 | 2h 40min. | 5.10 |
| | | | 5h 20min. | 5.36 |
| | | | 8h. | 5.38 |
| | 1100 | 2 | 2h 40min. | 5.27 |
| | | | 5h 20min. | 5.43 |
| | | | 8h. | 5.43 |

## IV. 4.  Microstructural Observation:

Samples were prepared for microstructural observation to study i) the effect of glass addition and ii) the effect of sintering temperature and time on microstructure, so as to understand the reaction Kinetics during liquid phase sintering of Ba Ti $O_3$ with bismuth borate glass.

Microstructures of the sintered samples containing 0.4, 2, 10, 20 and 30 wt pct glass are shown in Figs. IV 10-14 Sintering temperature was 1200°C for 0.4 and 2% samples and 1100°C for 10,20 and 30% samples. Sintering time was constant at 2 h for all these samples.

These figures show that a glassy phase is distributed uniformly around the grains as a coating over the grains. It can be observed that the amount of this glassy phase is increasing with increasing glass content for a fixed sintering temperature and time as expected.

Effect of sintering temperature and time on micro-structure was studied on the samples with 10% glass sintered at 1000 and 1100°C for 1/6, 1/2, 1 and 2 h. The average particle size of Ba Ti $O_3$ and glass used for making these samples were 13 and 17 /um respectively. Figs. IV 15-18 show the microstructures of the samples sintered at 1000°C for 10 min. to 2 h, while Figs. IV.19-22 show the microstructures of the samples sintered at 1100°C for 10 min to 2 h. Average grain size and boundary layer thickness were measured quantitatively under a microscope at 250 magnification for all these samples. Measurement ........
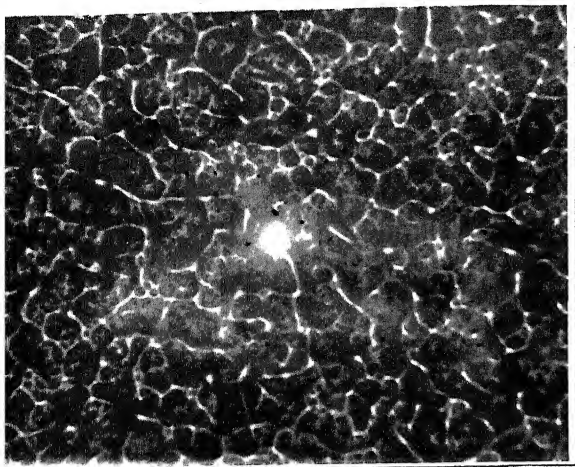
IV.10  0.4%/1200°C/3h
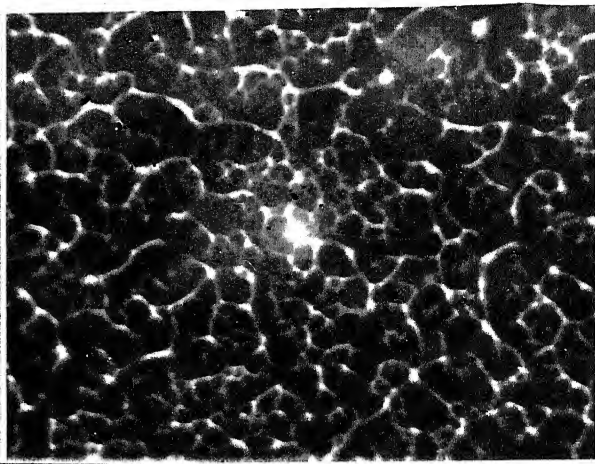


IV.11   2%/1200°C/2h.
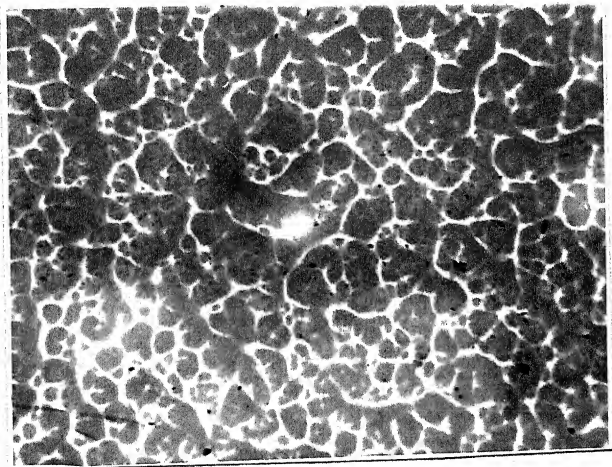


IV.12    10%/1100°C/2h.
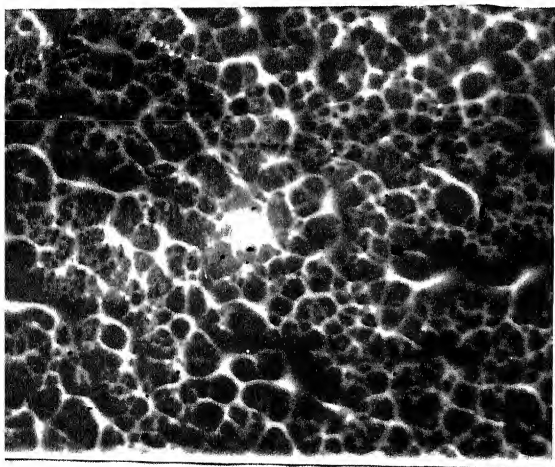


IV.13   20%/1100°C/2h
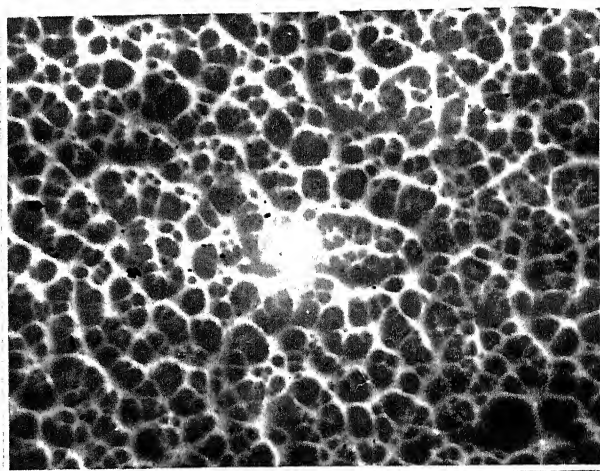


IV.14   30%/1100/2h

Figs. IV.10-14 Microstructures of liquid phase sintered
          BaTiO$_3$ samples with different glass contents.
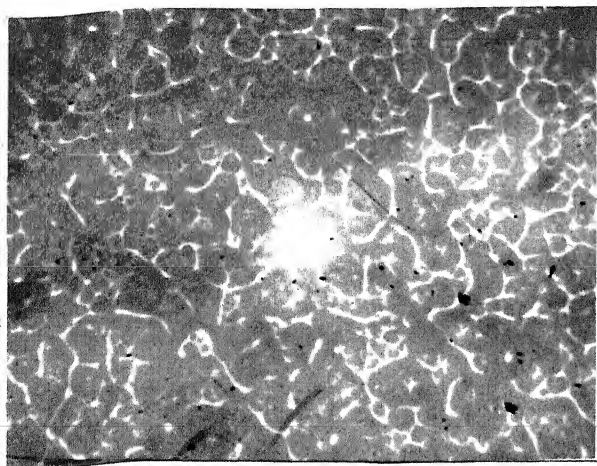
IV.15   10%/1000°C / 10 min.
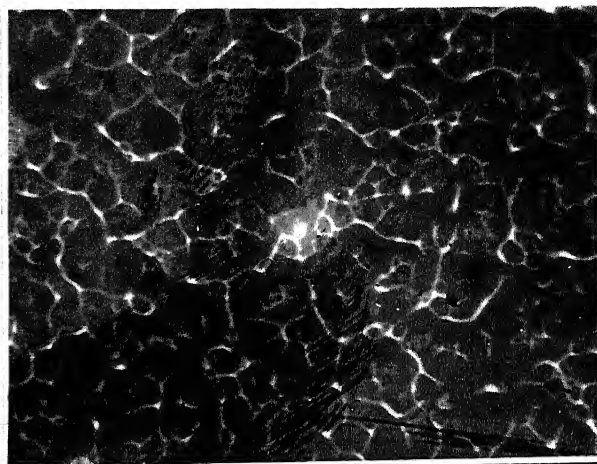


IV.16:   10%/1000°C/ 1/2h.
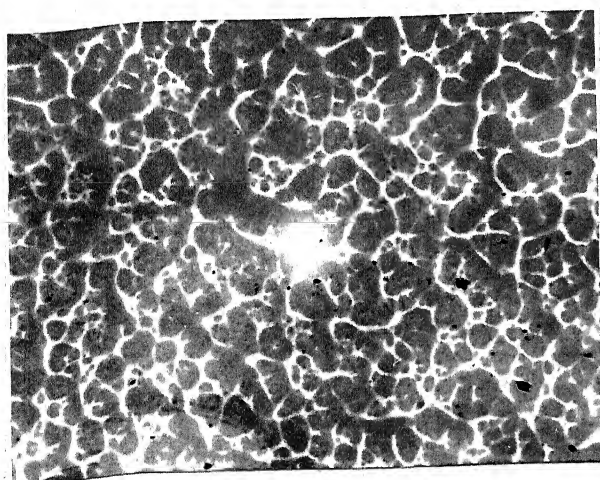


IV.17   :   10%/1000°C/ 1h.
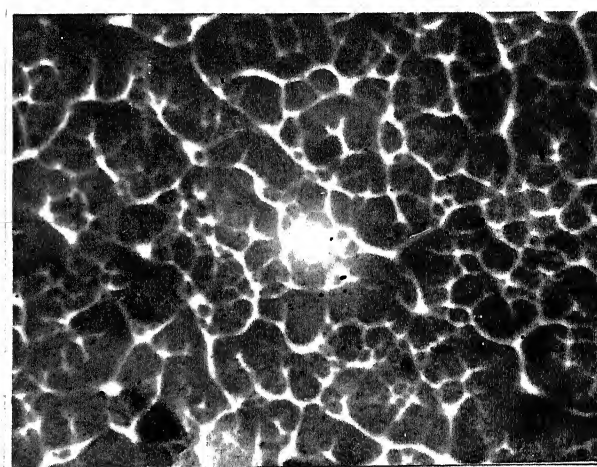


IV. 18 : 10%/1000°C/ 2h.

Figs. 15-18: Microstructures of liquid phase sintered
           BaTiO$_3$ samples with 10% glass addition
           sintered at 1000°C for different times.

(×150)
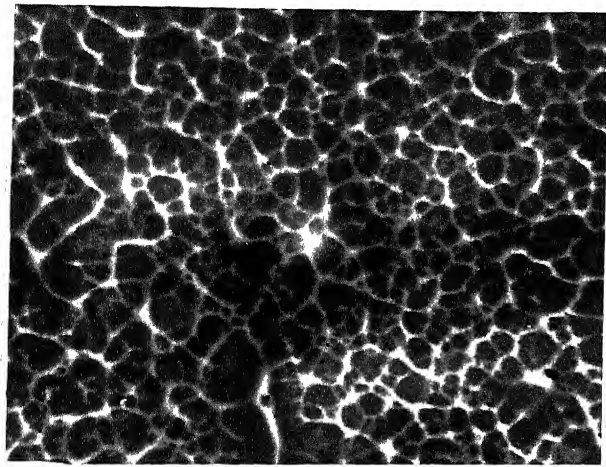
IV.19: 10%/1100°C/ 10 min.
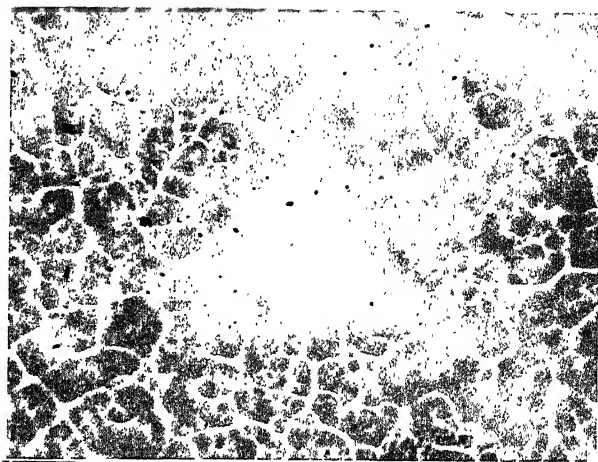


IV. 20:   10%/1100°C/ 1/2h.
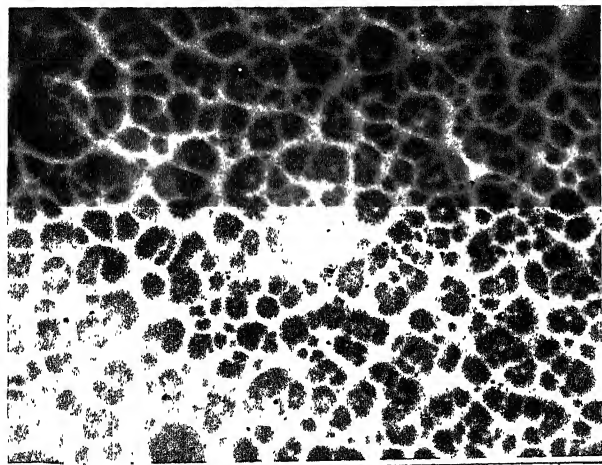


IV.21:   10%/1100°C/ 1h.
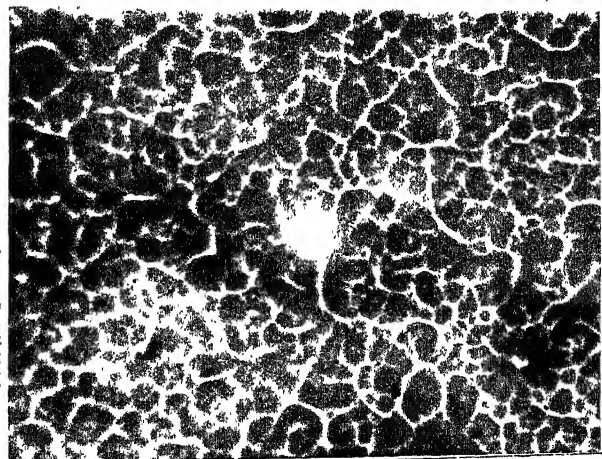


IV. 22:   10%/1100°C/2 h.

Figures 19-22: Microstructures of liquid phase sintered
BaTiO$_3$ samples with 10% glass addition
sintered at 1100°C for different times.

(×150)

for this purpose were carried out on 150-250 grains in each case . These results are given in Table IV.6

Table IV.6 Variation of grain size and grain boundary Thickness with sintering temperature and time.

| Sintering Time (h) | Sintering Temperature °C | | | |
| | 1000 | | 1100 | |
| | Grain size /u | Boundary layer thickness /u | Grain Size /u | Boundary layer thickness /u |
| --- | --- | --- | --- | --- |
| 1/6 | 13 | 3 | 19 | 7 |
| 1/2 | 16 | 5 | 24 | 7 |
| 1 | 19 | 7 | 24 | 9 |
| 2 | 20 | 6 | 21 | 10 |

This table shows that the grain size is increasing with increasing sintering time from 1/6 to 2 h at a particular temperature and also for the corresponding times the grain size was more at 1100°C than at 1000°C . The grain boundary thickness is also increasing correspondingly with sintering time and temperature. The grain size range has also been found to be rather narrow. This is to be expected since in

the liquid phase sintering process during solution and reprecipitation stage smallest grains will get dissolve and reprecipitate on larger grains.

Through thermal analysis ( Section IV.2) and X-ray diffraction studies it is confirmed that the bismuth borate glass reacts with barium titanate at about 725°C forming $Ba\ Bi_4\ Ti_4 O_{15}$ and that the amount of $Ba\ Bi_4 Ti_4\ O_{15}$ reaches a maximum at 900°C and afterwords it is decomposing with increasing temperature from 900°C to 1000°C. The Kinetics of these reactions were discussed in detail in section IV.5 and sintering models in section IV.6. The sintering model presented clearly suggests that the grain size as well as the thickness of the glass layer increases as the temperature is raised from 1000 to 1100°C keeping sintering time constant, and also these perameters increase with the sintering temperature. The observed microstructural changes therefore are in conformation with the proposed sintering models.

IV.5.  <u>X-ray diffraction studies:</u>

The sequence of reactions taking place during liquid
phase sintering of Ba Ti $O_3$ mixed with bismuth borate glass
was studied by X-ray diffraction techniques using (i) amount
of glass added (ii) sintering temperature and (iii) sintering
time as parameters. In general the X.ray diffraction petterns
were taken on sintered pellets, except in special cases
where the sintered pellet was crushed into powder before
taking an X-ray diffraction pattern. Thus, unless other
wise mentioned, all the X-ray diffraction data presented here
were obtained on sintered discs.

The X-ray diffraction patterns of sintered discs
of Ba Ti $O_3$ containing 0,2,10,20,and 30 wt. pct bismuth
borate glass is shown in Table IV.7. All the discs were sintered
at 1200°C for 2 hrs. These patterns showed Ba Ti $O_3$ is the
predominant phase. With no noticeable shift in the lattice
perameters. It indicates that no solid solutions were
formed with Ba Ti $O_3$ during liquid phase sintering. In
addition there were some extra reflections observed whose
intensity seem to increase with increasing glass constant.
It may be mentioned that the glass tended to  visibly
ooze out to the lower side of the disc during sintering at a
high temperature such as 1200°C particularly in the case of
samples containing larger additions of glass. In order to
study this more closely the two sides of a disc containing

## TABLE IV.7

X-ray diffraction data of liquid phase sintered $BaTiO_3$

| wt.% of glass | | | | | | | | | | $BaTiO_3$ (Ref. 9) | |
|---|---|---|---|---|---|---|---|---|---|---|---|
| 0 | | 2 | | 10 | | 20 | | 30 | | | |
| d | $I/I_o$ | d | $I/I_o$ | d | $I/I_o$ | d | $I/I_o$ | d | $I/I_o$ | d | $I/I_o$ |
| 3.97 | MS | 4.01 | MS | 4.18 | MS | 4.04 | MS | 4.03 | MS | 4.058 | 20 |
| | | | | | | | | | | 4.022 | 50 |
| 3.13* | VW | 3.15* | VW | 3.13* | VW | 3.13 | VW | – | – | – | – |
| | | | | 2.97 | VVW | 2.99 | MS | 2.97 | MS | | |
| 2.82 | VVS | 2.85 | VVS | 2.83 | VVS | 2.84 | VVS | 2.84 | VVS | 2.84 | 100 |
| | | | | 2.74 | VVW | 2.76 | VVW | 2.76 | MS | | |
| 2.31 | S | 2.32 | S | 2.32 | S | 2.32 | S | 2.32 | S | 2.315 | 60 |
| 2.01 | MS | 2.02 | MS | 2.00 | VS | 2.01 | VS | 2.00 | VS | 2.018 | 55 |
| 1.99 | VS | 2.02 | VS | | | | | | | 1.998 | 80 |
| | | | | | | 1.94 | VW | | | | |
| 1.82 | W | 1.79 | W | 1.79 | W | 1.80 | W | 1.79 | W | 1.804 | 15 |
| | | | | | | | | 1.76 | VVW | 1.791 | 15 |
| 1.63 | VS | 1.64 | VS | 1.63 | VS | 1.64 | VS | 1.64 | VS | 1.642 | 60 |
| | | | | | | | | | | 1.634 | 80 |
| | | | | | | | | | | 1.419 | 50 |

\* These values corresponds to $Ba_2TiO_4$ phase.

30% glass sintered at 1200°C for 2 hrs. was subjected to
X-ray diffraction and these results were included in
Table IV.8. It may be noticed that there is a distinct
difference in the location of some of the reflections on
the two sides, but more importantly a substantial difference
in intensity of certain lines was observed.  The extra lines
observed  on the glassy side of the disc compare very well
with those of $Bi_4.Ti_3 O_{12}$[18] though some serious enhancement
of the intensity of some of the reflections was observed
for certain reflections on the glassy side of the disc.
Recalling that $Bi_4 Ti_3 O_{12}$ has a layer type structure with
a morphology like to that of mica it is not surprising to
observe that some of the (ool) type lines exhibit
anamolously large intensities characterstic of strong
preferred orientation.  In order to unambigiously identity
the second phase in these materials and also to over-come
the problems due to preferred orientation, the discs were
ground to minus 325 mesh powder and an X-ray diffraction
pattern was again obtained .  These results are presented
in Table IV.8 Here again $Ba Ti O_3$  continues to be the
predominant phase as can be expected.  The coexisting
second phase can now clearly be identified as $Ba Bi_4 Ti_4 O_{15}$[19]
The intensity of the $Ba Bi_4 Ti_4 O_{15}$ lines appear  to be
increasing with increasing glass addition.  It must be
pointed out that the powdered sample of the disc with 30%

30% glass sample

| Side 1 d | Side 1 $I/I_0$ | Side 2 (glassy) d | Side 2 $I/I_0$ | Powder d | Powder $I/I_0$ | $BaTiO_3$ d | $I/I_0$ | hkl | $BaBi_4Ti_4O_{15}$ d | $I/I_0$ | hkl | $Bi_4Ti_3O_{12}$ d | $I/I_0$ | hkl |
|---|---|---|---|---|---|---|---|---|---|---|---|---|---|---|
| | | | | | | | | | 4.20 | 20 | 0.0.10 | 4.09 | 15 | 008 |
| 4.03 | MS | 4.14 | VS | | | 4.058 | 20 | 001 | | | | | | |
| | | 4.00 | VW | 4.03 | W | 4.022 | 50 | 100 | 3.87 | 70 | 101 | 3.80 | 20 | 11ī |
| | | | | 3.36 | W | | | | | | | 3.30 | 4 | 115 |
| 2.97 | MS | 2.97 | VVW | 2.97 | S | | | | 2.98 | 100 | 109 | 2.96 | 100 | 117 |
| | | 2.83 | VS | 2.84 | VVS | 2.84 | 100 | 101 / 110 | | | | | | |
| 2.76 | MS | 2.74 | W | 2.74 | MS | | | | 2.74 | 70 | 110 | 2.72 | 20 | 200 |
| | | 2.56 | MS | 2.41 | VVW | | | | | | | 2.70 | 20 | 020 |
| | | 2.30 | VVS | 2.32 | S | | | | 2.33 | 60 | 0.0.18 | 2.34 | 20 | 0.0.14 |
| 2.32 | S | 2.26 | MS | 2.29 | MS | 2.315 | 60 | 111 | 2.29 | 80 | 1.1.10 | | | |
| | | | | | | | | | 2.10 | 20 | 0.0.20 | 2.25 | 10 | 0.28 |
| | | | | | | | | | 2.07 | 20 | 1.0.17 | | | |
| 2.00 | VS | 1.99 | S | 2.00 | S | 2.018 | 55 | 002 | 1.934 | 70 | 2 0 0 | | | |
| | | | | | | 1.998 | 80 | 200 | | | | | | |
| | | 1.92 | W | 1.94 | W | | | | 1.910 | 30 | 1.0.19 | 1.92 | 10 | 0.2.12 |
| | | 1.91 | W | | | | | | 1.890 | 20 | 1.1.16 | 1.90 | 8 | 1.1.15 |
| | | | | | | | | | 1.812 | 10 | 2 0 8 | | | |
| 1.79 | W | 1.79 | VW | 1.82 | VVW | 1.804 | 15 | 102 | 1.773 | 70 | 1.1.18 | 1.770 | 20 | 0.2.14 |
| 1.76 | VVW | 1.76 | VVW | 1.80 | W | 1.791 | 15 | 201 | | | 1.0.21 | | | |
| | | | | 1.77 | W | | | | | | | | | |
| 1.64 | VS | 1.64 | VS | 1.64 | VS | 1.642 | 60 | 112 | 1.619 | 80 | 2.0.14 | 1.605 | 15 | 1 3 7 |
| | | 1.63 | S | 1.62 | MS | 1.634 | 80 | 211 | | | 2 1 9 | | | |

(C5)

glass also shows only a mixture of $Ba\,Ti\,O_3$ and $Ba\,Bi_4\,Ti_4O_{15}$ and does not show the presence of $Bi_4Ti_3O_{12}$. This apparent anamoly can be resolved if it is considered that only an exceedingly thin layer of $Bi_4Ti_3O_{12}$ is formed on the glassy side of the disc and its amount in the overall volume of the disc is too small to be detected.

From what has been said above it is clear that the bismuth borate glass reacts with bariumtitanate forming barium bismuth titanate as a distinct phase. The thin layer of $Bi_4\,Ti_3\,O_{12}$ that appears to form on the glassy side of the disc is so small in quantity that it may not be considered any further.

The kinetics of formation of $Ba\,Bi_4\,Ti_4\,O_{15}$ as a function of time and temperature of sintering was studied in the case of samples with 10% glass. These samples were sintered at 1000, 1050, 1100, and 1150°C for 1/6, 1/2, 1 and 2 hrs. Varying amounts of $Ba\,Bi_4Ti_4\,O_{15}$ was detected in nearly all the sintering experiments. In order to quantify the amount of $Ba\,Bi_4\,Ti_4\,O_{15}$ formed under these conditions the ratio of the intensity of ( 109 ) reflection of $Ba\,Bi_4\,Ti_4\,O_{15}$ ( which is the strongest reflection for this material), to that of the (210) reflection of the $Ba\,Ti\,O_3$ was computed for different sintering temperatures and times. These results are plotted in Fig. IV.23 as a function of sintering temperature

for fixed time as well as a function of sintering time for fixed temperature. The relative amount of $Ba\ Bi_4\ Ti_4\ O_{15}$ present decreases gradually with increasing temperature for all sintering times or in other words the maximum $Ba\ Bi_4\ Ti_4\ O_{15}$ was observed for the lowest sintering temperature employed namely 1000°C. The relative amount of $Ba\ Bi_4\ Ti_4\ O_{15}$ present also decreases with increasing sintering time at a given temperature, though the decrease at and above 1100°C seems to be rather small. In order to provide further support for what has been said above and also to confirm the interpretation of thermal analysis of $Ba\ Ti\ O_3$ with 20% glass ( Section IV.2) two additional experiments were carried out. In the first experiment one sample of 74% $Bi_2\ O_3$ 26% $B_2O_3$ glass employed in this study was heated by it self at 525°C for 8 h. A second sample was melted in a platinum crucible at approximately 750°C and taken out of the furnace and allowed to cool. X-ray patterns of these two samples given in Table IV.9 were identical and consists of 2 $Bi_2\ O_3 . B_2\ O_3$ and 12 $Bi_2\ O_3 . B_2O_3$[111] with the former in a larger concentration. From this it could be concluded that the crystallization of the bismuth borate glass employed here, takes place at temperatures as low as 525°C and the crystallized phases confirm to the ones expected from the phase diagram for 74% $Bi_2\ O_3$ 26% $B_2O_3$ composition. In the second experiment a mixture of $Ba\ Ti\ O_3$ powder with 20% glass powder was heated at 725, 800, 900,
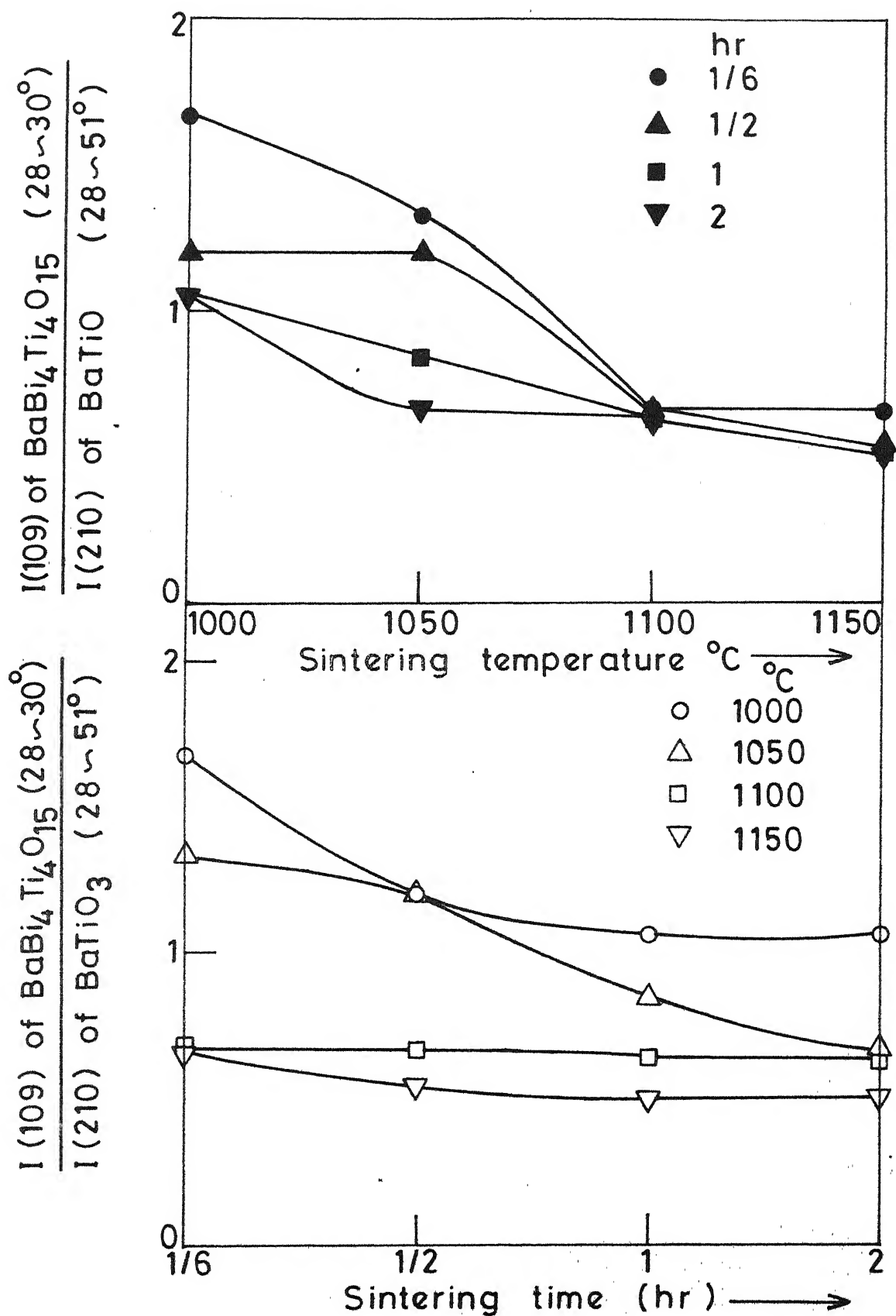
Fig. Ⅳ-23 Formation of BaBi₄Ti₄O₁₅ at various sintering temperatures and times.

Table IV: 9 X-ray diffraction data of the 74% $Bi_2O_3$, 26% $B_2O_3$ glass crystallized at 750°C and 525°C

| Glass Crystallized at 750°C | | 525°C | | $2\ Bi_2O_3 \cdot B_2O_3$ | | $12\ Bi_2O_3\ B_2O_3$ | |
|---|---|---|---|---|---|---|---|
| d | $I/I_o$ | d | $I/I_o$ | d | $I/I_o$ | d | $I/I_o$ |
| 4.28 | 4 | 4.26 | 2 | 4.25 | 5 | | |
| 3.97 | 16 | 3.96 | 10 | 3.98 | 12 | | |
| 3.9 | 20 | 3.89 | 17 | 3.95 | 13 | | |
| | | | | 3.87 | 18 | | |
| 3.6 | 25 | 3.58 | 34 | | | 3.574 | 30 |
| 3.41 | 7 | 3.40 | 10 | 3.39 | 8 | | |
| 3.33 | 20 | | | 3.312 | 20 | | |
| | | | | 3.207 | 7 | | |
| 3.21 | 100 | 3.21 | 100 | | | 3.198 | 100 |
| | | | | 3.173 | 9 | | |
| 3.11 | 70 | | 80 | 3.111 | 63 | | |
| 3.1 | 100 | 3.09 | 100 | 3.101 | 100 | | |
| | | | | 3.089 | 60 | | |
| 2.94 | 60 | 2.94 | 65 | 3.075 | 45 | | |
| | | 2.93 | 30 | 3.045 | 24 | 2.918 | 28 |
| 2.85 | 9 | 2.86 | 10 | 2.842 | 11 | | |
| 2.79 | 4 | 2.79 | 4 | 2.805 | 5 | | |
| | | | | 2.774 | 6 | | |
| 2.72 | 79 | | | 2.748 | 5 | 2.702 | 75 |
| 2.52 | 6 | 2.53 | 6 | 2.52 | 22 | | |
| 2.49 | 7 | 2.50 | 7 | 2.489 | 11 | | |
| 2.17 | 9 | 2.16 | 18 | | | 2.157 | 17 |
| 2.06 | 9 | 2.07 | 10 | 1.976 | 9 | | |
| 1.98 | 12 | 1.98 | 27 | 1.972 | 11 | | |
| 1.93 | 20 | 1.93 | 14 | 1.929 | 14 | | |
| | | 1.87 | 14 | 1.87 | 11 | | |
| 1.85 | 30 | 1.85 | 6 | 1.866 | 10 | | |
| | | 1.82 | 11 | 1.838 | 20 | | |
| 1.74 | 39 | 1.74 | 45 | | | 1.735 | 34 |
| 1.69 | 20 | 1.69 | 20 | | | 1.686 | 16 |
| 1.65 | 30 | 1.65 | 25 | | | 1.641 | 24 |

1000 and 1100°C for 15 min. The same mixture was also heated at 725°C for 2 h. A powder X-ray pattern was obtained of all these materials. These results were given in table IV.10.It can be seen that the sample heated at 725°C for 15 min. shows $Ba\,Ti\,O_3$ and a second phase, which was identified as $12\,Bi_2O_3 \cdot B_2O_3$ which apparently crystallized from the bismuth borate glass added to $Ba\,Ti\,O_3$. However the sample heated at 725°C for a longer period namely 2h shows a mixture of $Ba\,Ti\,O_3$, $Ba\,Bi_4\,Ti_4\,O_{15}$ and $12\,Bi_2\,O_3 \cdot B_2O_3$ phases. This means that given sufficient time the glass reacts with $Ba\,Ti\,O_3$ to form $Ba\,Bi_4Ti_4\,O_{15}$ at as low a temperature as 725°C. On the other hand the same sample heated to 800°C for 15 min. does not contain $12\,Bi_2\,O_3 \cdot B_2\,O_3$ but shows $Ba\,Ti\,O_3$ as the predominant phase with $Ba\,Bi_4\,Ti_4\,O_{15}$ as a minor phase. The relative amount of $Ba\,Bi_4\,Ti_4\,O_{15}$ formed appears to attain a maximum at 900°C and its amount appears to decrease at 1000°C and even more so at 1100°C.

The decreasing amount of $Ba\,Bi_4Ti_4O_{15}$ as the sintering temperature is increased from 900 to 1000 to 1100°C is in line with the results discussed earlier on discs with 10% glass sintered between 1000 and 1100°C for periods varying from 10 min. to 2 h. The important results of the X-ray diffraction study of the liquid phase sintering process of $Ba\,Ti\,O_3$ in the presence of $Bi_2\,O_3 \cdot B_2O_3$
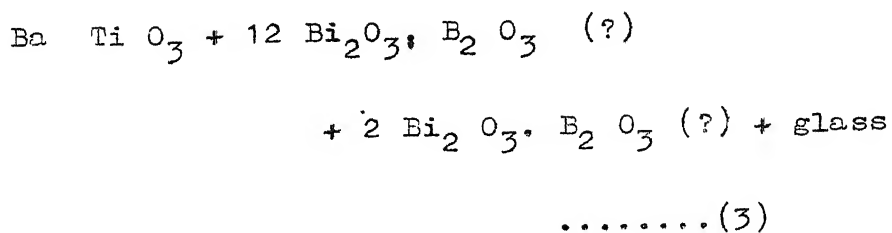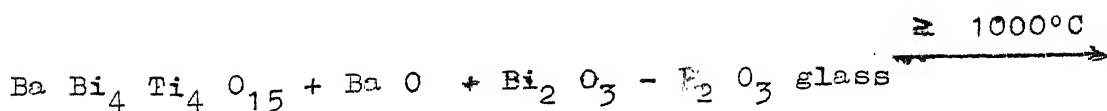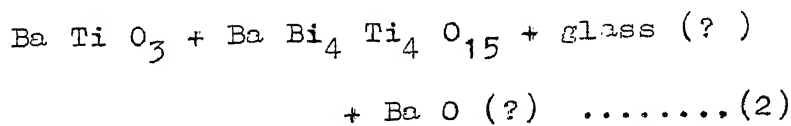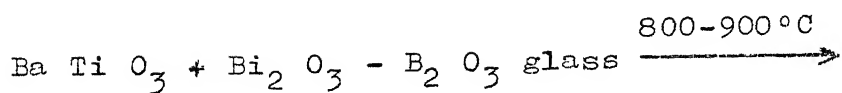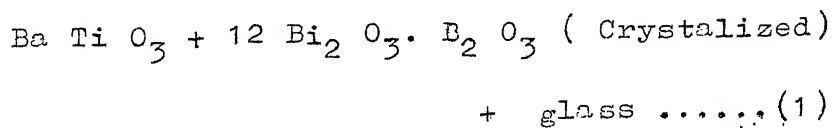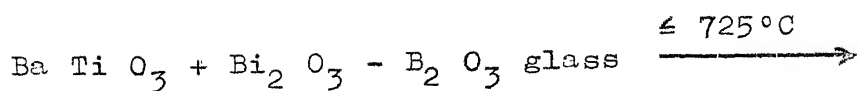
Table IV.10 X-ray Diffraction data of mixture of BaTiO₃ and 20% glass mixture heated to different temperatures.

| Temperature °C | | | | | | | | | | | | | | | | | | | | |
|---|---|---|---|---|---|---|---|---|---|---|---|---|---|---|---|---|---|---|---|---|
| 15 min. | | 725 2h | | 800 15 min | | 900 15 min | | 1000 15 min | | 1100 15 min | | $BaTiO_3$ | | $BaBi_4Ti_4O_{15}$ | | $12Bi_2O_3 \cdot B_2O_3$ | |
| d | $I/I_o$ | d | $I/I_o$ | d | $I/I_o$ | d | $I/I_o$ | d | $I/I_o$ | d | $I/I_o$ | d | $I/I_o$ | d | $I/I_o$ | d | $I/I_o$ |
| 4.02 | 20 | 4.01 | 20 | 4.02 | 20 | 4.01 | 20 | 4.02 | 20 | 4.01 | 20 | 4.058 | 20 | | | | |
| | | | | | | | | | | | | 4.022 | 50 | | | | |
| 3.6 | 3 | | | | | | | | | | | | | 3.87 | 70 | 3.574 | 30 |
| 3.22 | 13 | 3.22 | 5 | | | | | | | | | | | | | 3.198 | 100 |
| 2.93 | 4 | 2.97 | 10 | 2.98 | 10 | 2.98 | 11 | 2.98 | 5 | 2.97 | 2 | | | 2.98 | 100 | 2.918 | 28 |
| 2.84 | 100 | 2.84 | 100 | 2.84 | 100 | 2.84 | 100 | 2.84 | 100 | 2.84 | 100 | 2.84 | 100 | | | | |
| 2.72 | 9 | 2.73 | 5 | 2.74 | 5 | 2.74 | 5 | 2.73 | 2 | | | | | 2.74 | 70 | 2.702 | 75 |
| 2.32 | 40 | 2.31 | 40 | 2.32 | 40 | 2.32 | 40 | 2.32 | 40 | 2.32 | 40 | 2.315 | 60 | 2.33 | 60 | | |
| | | | | | | | | | | | | | | 2.29 | 80 | | |
| | | | | | | | | | | | | | | 2.10 | 20 | | |
| | | | | | | | | | | | | | | 2.07 | 20 | | |
| 2.00 | 30 | 2.00 | 30 | 2.00 | 30 | 2.00 | 30 | 2.00 | 30 | 2.00 | 30 | 2.018 | 55 | | | | |
| | | | | | | | | | | | | 1.998 | 80 | | | | |
| | | 1.93 | 2 | 1.94 | 2 | 1.94 | 2 | | | | | | | 1.934 | 70 | | |
| | | | | | | | | | | | | | | 1.910 | 30 | | |
| | | | | | | | | | | | | | | 1.890 | 20 | | |
| 1.79 | 10 | 1.79 | 10 | 1.79 | 10 | 1.79 | 10 | 1.79 | 10 | 1.79 | 10 | 1.804 | 15 | | | | |
| | | | | | | | | | | | | 1.791 | 15 | 1.773 | 70 | | |
| 1.74 | 5 | 1.74 | 2 | | | | | | | | | | | | | 1.735 | 34 |
| 1.69 | 3 | | | | | | | | | | | | | | | 1.686 | 16 |
| 1.64 | 35 | 1.64 | 35 | 1.64 | 35 | 1.64 | 35 | 1.64 | 35 | 1.64 | 35 | 1.642 | 60 | | | 1.641 | 24 |
| | | | | | | | | | | | | 1.634 | 80 | | | | |

(71)

glass may be summarised on follows. At temperatures as low as 725°C or even lower, bismuth borate glass tends to crystallize into $12 Bi_2 O_3 . B_2 O_3$. At about 800°C the bismuth borate glass reacts with $Ba Ti O_3$ forming $Ba Bi_4 Ti_4 O_{15}$. At this stage the crystallized $12 Bi_2 O_3 . B_2 O_3$ was no longer detected. It appears to have melted since the liquidus temperature corresponding to this composition was given as 743°C (11). The amount of $Ba Bi_4 Ti_4 O_{15}$ formed increases upto 900°C and decreases at higher temperatures. This decrease in the relative amount of $Ba Bi_4 Ti_4 O_{15}$ is interpreted as a decomposition of $Ba Bi_4 Ti_4 O_{15}$ into $Ba Ti O_3$ and some bismuth rich phase. The bismuth oxide released by the decomposition of $Ba Bi_4 Ti_4 O_{15}$ may combine with $B_2 O_3$ present to form additional glass, or alternately it may combine with $B_2 O_3$ to form crystalline bismuth borate glasses. Some of the weak reflections observed at temperatures where a fair amount of decomposition of $Ba Bi_4 Ti_4 O_{15}$ has proceeded may be accounted for by the strongest reflections of $12 Bi_2 O_3 . B_2 O_3$ and $2 Bi_2 O_3 . B_2 O_3$. It may be recalled that the composition of the glass chosen for this study falls in between these two compounds in the phase diagrams ( 11 ).

The sequence of reactions taking place during the liquid phase sintering of $Ba Ti O_3$ in the presence of busmuth borate glass ( 76 mole % $Bi_2 O_3$, 24 mole % $B_2 O_3$)

may tentatively be proposed as follows.

$$Ba\ Ti\ O_3 + Bi_2\ O_3 - B_2\ O_3\ glass \xrightarrow{\leq 725°C}$$

$$Ba\ Ti\ O_3 + 12\ Bi_2\ O_3 \cdot B_2\ O_3\ (Crystalized)$$

$$+\ glass\ \ldots\ldots (1)$$

$$Ba\ Ti\ O_3 + Bi_2\ O_3 - B_2\ O_3\ glass \xrightarrow{800-900°C}$$

$$Ba\ Ti\ O_3 + Ba\ Bi_4\ Ti_4\ O_{15} + glass\ (?\ )$$

$$+\ Ba\ O\ (?)\ \ldots\ldots (2)$$

$$Ba\ Bi_4\ Ti_4\ O_{15} + Ba\ O\ +\ Bi_2\ O_3 - B_2\ O_3\ glass \xrightarrow{\geq 1000°C}$$

$$Ba\ Ti\ O_3 + 12\ Bi_2 O_3 \cdot B_2\ O_3\ (?)$$

$$+\ 2\ Bi_2\ O_3 \cdot B_2\ O_3\ (?) + glass$$

$$\ldots\ldots (3)$$

IV. 6  Densification Mechanisms:

In liquid phase sintering process there are th:
stages of densification corresponding to three mechanisms
during sintering:    1)  particle rearrangement (2) Solution
precipitation (3) Coalescence.    (20)

In the first stage liquid phase is formed, the
pores are filled, and the solid particles are rearranged,
resulting in close packing.  In the second stage the fine
particles go into solution, followed by reprecipitation
on the large particles.  In the third stage the substance
is slowly consolidated as the result of the solid particles
growing together in accordance with the rules of solid-phase
sintering.  The result is that a rigid skeleton is formed
in the body undergoing sintering.  The predominance of one
mechanism  or another depends on the nature of the phases
and the amount of  liquid present.  Fig. IV 24 shows a
hypothetical densification curve for these three stages of
liquid phase sintering.  An important condition for the
occurrence of solution and precipitation  as well as the
regrouping  process; is  the penetration of the liquid
between the grains.  The extent to which the liquid enters
the joints between the particles depends on the dihedral
angle formed by the liquid phase at the boundary with the
grains of the solid phase ( Fig. IV. 25).
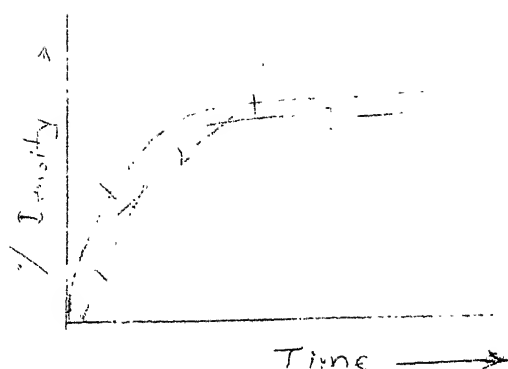
Fig. IV. 24    Hypothetical densification curve for
               liquid phase sintering.
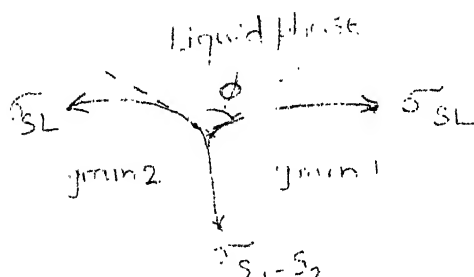


Fig. IV. 25    Dihedral angle formed by the liquid
               phase at the grain boundary.

$$\sigma_{S_1 - S_2} = 2\sigma_{SL} \cos \phi/2$$

$$\text{or } \cos \phi/2 = \sigma_{S_1 - S_2}/2\sigma_{SL}$$

when $\phi$ is zero or near zero penetration of the liquid phase
between the grain faces occurs spreading the liquid over the
surface of the grains.

Particle rearrangement:   On initial formation of the liquid
phase on melting, capillary pressure will tend to rearrange
the  solid  particles in such a way as to give maximum pack-
ing and a minimum resultant pore surface.   The process
occurs very rapidly and is the principal reason for
densification.   With a sufficient quantity of liquid phase

the theoretical density can be attained as the result of th

rearranging process alone. According to Kingery's

calculations (21) , if the solid phase particles are

spherical then the minimum quantity of liquid phase.

required for complete densification is 35 Vol%. The

degree of densification decreases at smaller quantities.

In this case, other sintering processes are necessary for

complete densification.

2. Solution and precipitation:

As mentioned earlier a limited solubility of

solid in the liquid phase is necessary for this mechanism

to occur. This stage leads to densification but at a

slower rate than in the first stage.

According to Prince-Smittells-William (22)

theory during solution-precipitation stage smaller

particles will go into solution and precipitate on larger

particles there by leading to densification. The solu-

bility of a substance increases with decreasing radius of

curvature of the particles. For spherical surfaces

$$\ln \frac{C}{C_D} = \frac{2\,\sigma_{S-L}\,V_0}{r R T}$$

where $C/C_0$ is the ratio of the solubility of fine parti-
cles with a radius $r$ and large particles with a radius
$r \rightarrow \infty$ (solubility of a substance with plane interfaces).

$\sigma_{S-L}$ is the specific free surface energy at the solid-
liquid interface, $V_0$ is the molor volume, R is the gas
constant, and T is absolute temperature.

Thus, the fine particles are gradually reduced
in size during sintering and dissolve in the liquid phase,
while at the same time, due to the lower solubility of the
large particles, an excess of the substance in solution is
reprecipitated on the large particles, there by still
further increasing their size. The growth of the large
particles continues until all the fine particles disappear
and the structure becomes relatively uniform. In systems
in which the solution and precipitation mechanisms is
dominant the amount of liquid phase also affects the grain
growth.

3. Coalescence process:

It is to be expected that during the sintering
process a certain number of grains will be oriented such
that the grain boundary energy is smaller than twice the
solid-liquid interface energy ( $\sigma_{S_1-S_2} < 2\,\sigma_{S-L}$ )

and consequently, liquid will not penetrate completely between the grains. In this case, along a line between grain centers the material will all be solid and in order for densification to take place, material must be transferred with in the solid phase. Consequently, rapid densification corresponding to liquid phase processes are stopped, and densification rate should decrease to that observed for solid particles under similar conditions.

Liquid phase sintering results in the formation of characteristic structures consisting of evenly distributed grains of solid phase in a matrix of the crystallized liquid phase. Particles of different shape may be formed. If the surface tension at the interface between different crystallographic planes of the solid particles and the liquid phase is approximately identical then the particles have rounded shapes. If, however, the surface tension at the interface differs substantially for different crystallographic planes, then grains of prismatic shape are formed. In the systems forming spherical particles considerable grain growth occurs during sintering. While the grain growth is less in systems forming prismatic grains, a higher density is attained with comparatively small amounts of liquid phase.

In general it can be said that (1) an appreciable amount of liquid (2) a limited solubility of the solid (3) complete wetting are the necessary requirements for complete densification.

In the present work, the usability of the bismuth borate glass as an additive for the liquid phase sintering of $Ba\ Ti\ O_3$ can be seen from the following observations:

(1)        X-ray diffraction studies of the liquid phase sintered samples, showed that the glass reacts with $Ba\ Ti\ O_3$ forming $Ba\ Bi_4\ Ti_4\ O_{15}$ indicating a limited solubility of the solid in the liquid phase.

(ii)        Microstructural observation of these samples shows complete wetting of $Ba\ Ti\ O_3$ grains with glass.

In the present work sintering process was studied by volume shrinkage measurements during sintering, supplemented by weight loss measurements, Thermal analysis, density measurements, Microstructural observation and grain size measurements and X-ray diffraction studies.

Volume shrinkage measurements were made on 10% and 20% glass samples sintered at different temperatures and times. These results are plotted in Fig. IV. 26 and 27.

Fig. IV. 26 shows volume shrinkage for the samples with 10% glass addition sintered at different temperatures and times. From this figure it can be observed that at 1100 and 1150°C most of the densification is taking place with in the first 10 min. and afterwords there is very little increase in density with increasing sintering time from 10 min. to 2h. At 1050°C, also it can be observed that most of the densification is taking place with in first 10 min. but here there is gradual increase in density with sintering times from 10min. to 2h, whereas at 1000°C such a sharp rise in density was not observed. Here the density is increasing gradually with increasing sintering time.

As described previously there are three stages in liquid phase sintering (i) Particle rearrangement (ii) solution precipation and (iii) coalescence. These three stages can be clearly observed in the densification curve at 1050°C. The large densification observed during the initial stages ( first 10 min.) must be due to the particle rearrangement process by liquid flow. The increase in densification with increase in sintering time from 10 min. to 1h can be attributed to the solution and precipitation stage. After 1h the little increase in densification with increase in sintering time indicates that the third stage i.e. coalescence process is acting between 1 and2h.
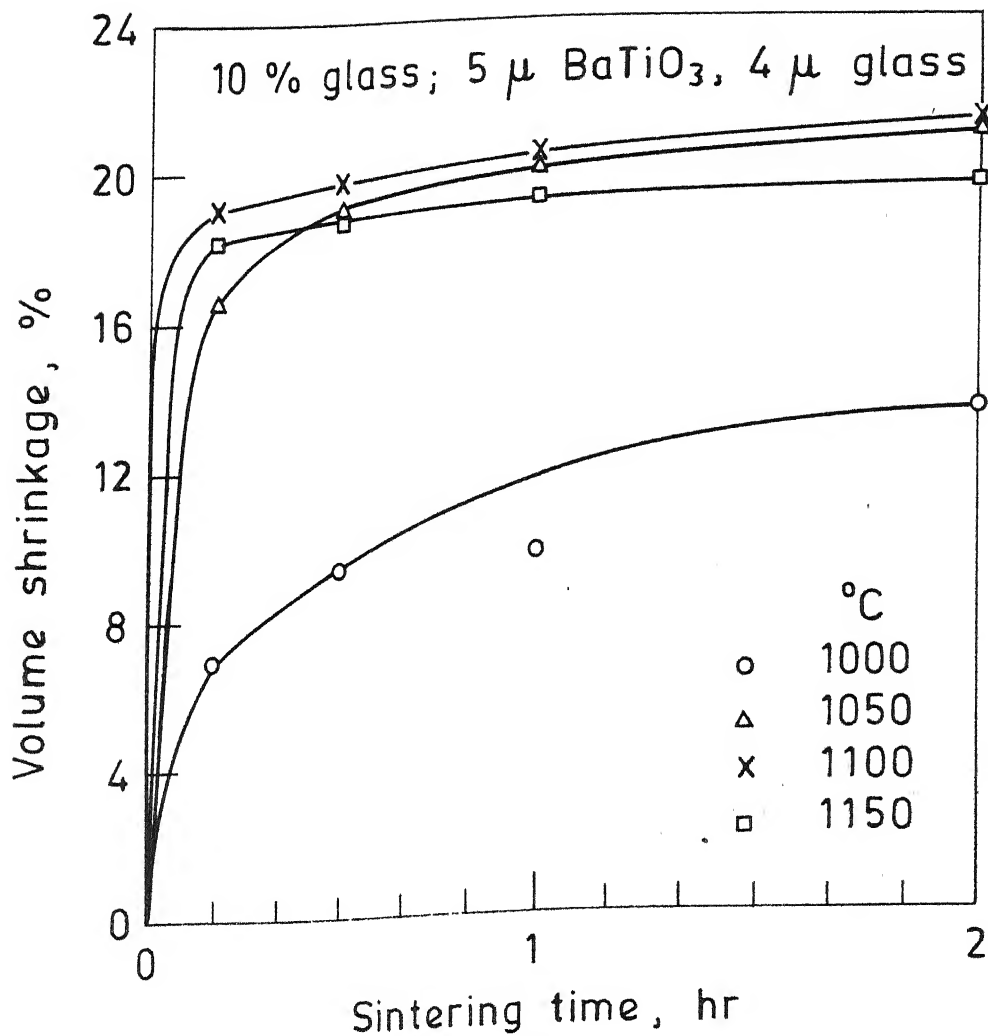
Fig. IV-26- Volume shrinkage vs sintering time for BaTiO₃ with 10 % glass addition at different sintering temperatures.

The absence of the sharp increase in densification in the initial stages at 1000°C indicates that the particle rearrangement stage is not prominent here. It may be due to the higher viscosity of the glass at this temperature. X-ray diffraction studies on Ba Ti $O_3$ and glass mixture indicates that the glass is reacting with Ba Ti $O_3$ forming Ba $Bi_4$ $Ti_4$ $O_{15}$ at as low a temperature as 725°C. It indicates the solution of Ba Ti $O_3$ in the liquid phase. So the gradual increase in densification observed at 1000°C may be due to the solution and precipitation process.

Again at 1100 and 1150°C the viscosity of the glass must be sufficiently low, facilitating particle rearrangement process as can be seen in the figure.

Because of this easy flow of the liquid at these temperatures most of the densification is taking place by particle rearrangement process and solution and precipitation stage is not so prominent, though this must also be present to some extent.

Volume shrinkage plots for 20% and 10% glass samples sintered at 1000 and 1100°C for 1/6, 1/2, 1 and 2h. are compared in Fig. IV.27. The volume shrinkage curves with 20% glass also shows similar trend as with 10% glass
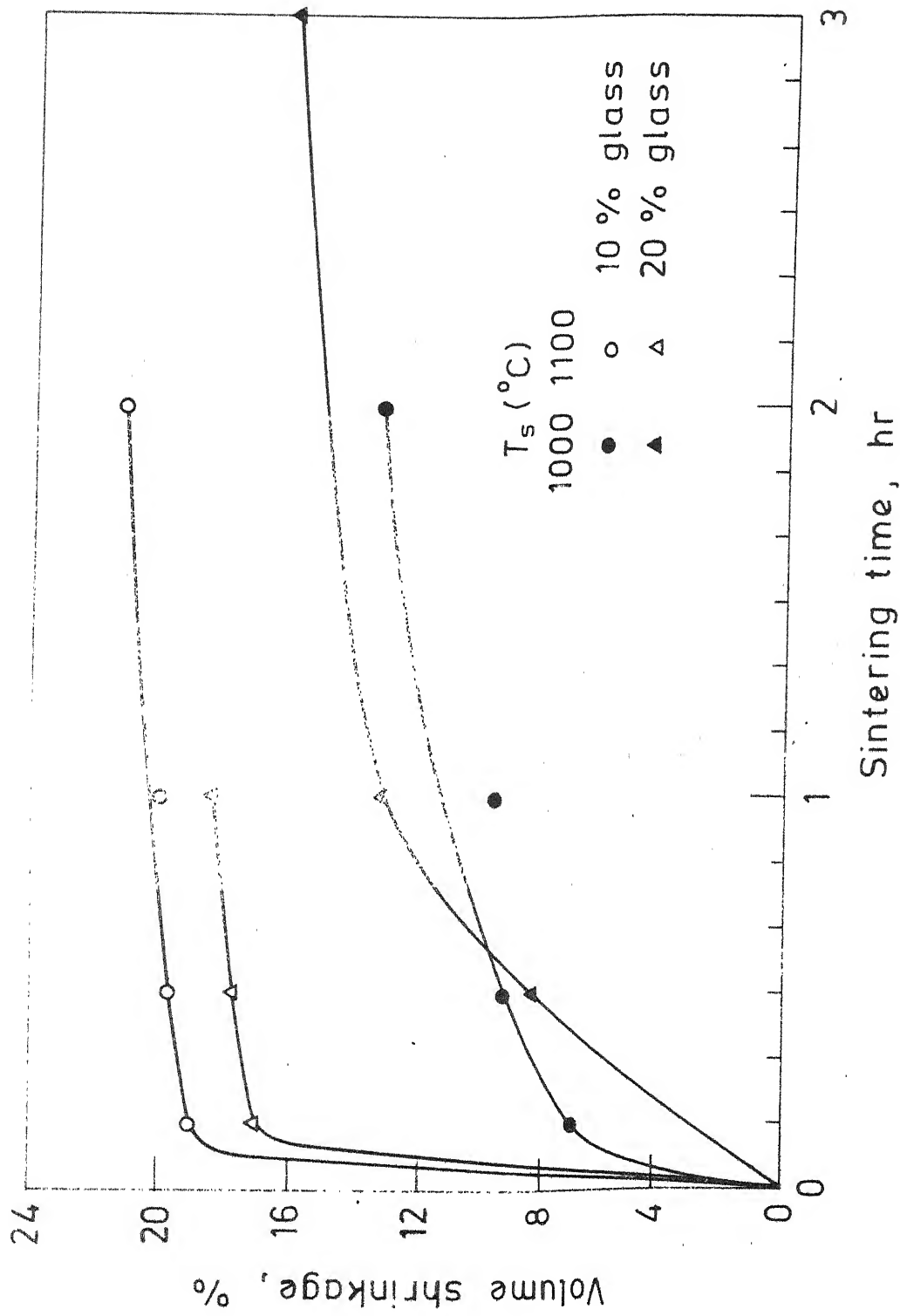
Fig. IV-27- Volume shrinkage vs sintering time for BaTiO₃ with 10 % and 20 % glass addition at 1000 and 1100 °C.

indicating that the same mechanisms are applicable here also. It can be observed from this figure that at 1000°C the densification is slightly more with 20% glass addition than with 10% glass. It was mentioned earlier that at 1000°C the major mechanism causing densification is solution and precipitation process, rather than particle rearrangement process. So it can be expected that the densification will be more with higher glass addition as the solution of the solid will increase with increasing liquid phase. This figure also shows that at 1100°C the densification was more with 10% glass addition than with 20% glass addition. At this temperature most of the densification is taking by particle rearrangement process because of the easy flow of liquid. Actually the viscocity this temperature must be too low as it is observed that some of the glass is oozing out from the pellet, particularly with higher glass additions like 20 and 30%. This may be reason for these 20% samples showing lower volume shrinkage than 10% samples at 1100°C.

Microstructural observation of the liquid phase sintered sample shows that the glass is distributing uniformly around the grains indicating complete wetting of the grains. Grain size measurements made on the 10% glass sample sintered t 1000 and 1100°C for 1/6, 1/2, 1 and 2h shows that at 1000°C there is a considerable grain

growth from 1/6 to 2h ( 13/um to 20/um ), where as at
1100°C the grain growth from 1/6 to 2h was less (19/um
to 21/um). Considering the initial particle size of
Ba Ti O$_3$ used ( 13/um ), it can be observed that at 1100°c
also there is a considerable grain growth taking place
with in the first 10min. It indicates that at 1100°C
even though particle rearrangement stage is predominant
due to the easy flow of the liquid, solution precipita-
tion stage is also acting at this temperature, where as
at 1000°C it can clearly be observed that the major
mechanism causing densification is solution and precipi-
tation process.

IV.7      <u>Dielectric Measurements:</u>

<u>IV. 7.1</u>     Temperature dependence of dielectric
            properties.

        Dielectric properties ( dielectric constant and
dissipation factor ) were measured as a function of tempera-
ture for the liquid phase sintered Ba Ti O$_3$ samples to
observe i) the effect of glass addition and ii) the effect
of sintering temperature and time.

        All the dielectric constant values reported were
corrected for porosity using the relation given by Rushman
and Strivens ( 23 )

$$K = \bar{\bar{K}} \frac{2 + V}{2(1-V)}$$

where      V  =  Volume fraction of pores.

           $\bar{\bar{K}}$  =  Dielectric constant measured with porosity.

           K  =  Dielectric constant corrected for porosity.

i)   <u>Effect of glass addition:</u>

        Figs. IV 28 and 29 show the effect of glass addition
on dielectric properties.  Fig. IV.28 shows the dielectric
constant as a function of temperature for the samples with
0.4, 2, 10, 20 and 30 wt pct glass addition.  All these
samples were sintered at 1100°C for 1h. except the 30%
sample which was sintered for 2h.  It can be observed from
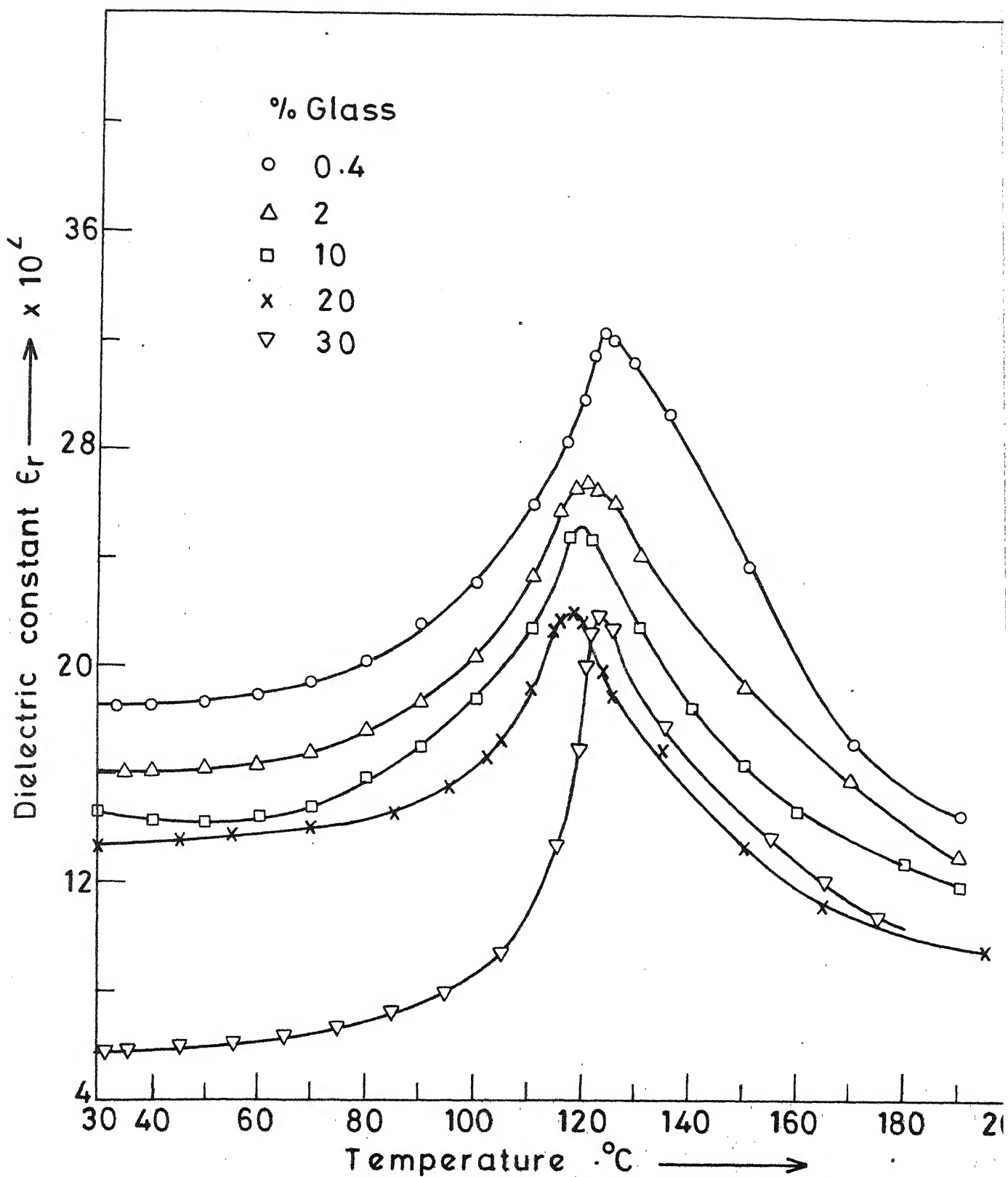this figure that the curie temperature was almost constant

Fig. IV -28 Temperature dependence of dielectric consto
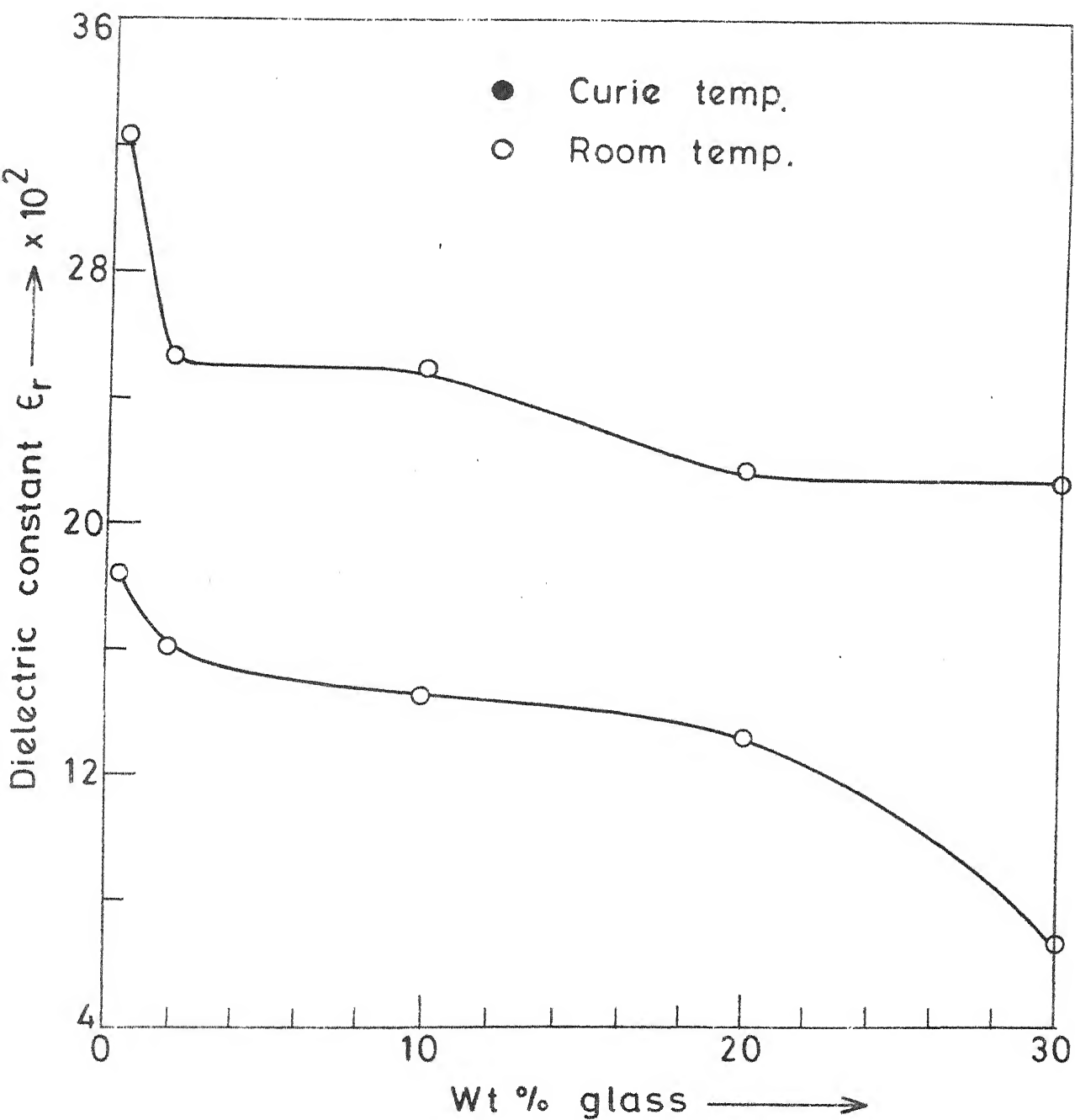for the samples with different glass additi

Fig. IV-29 Variation of dielectric constant with glass addition.

at 120°C for all these samples within the experimental
error ( ± 2°C). This indicates that there is no change in
the basic Ba Ti $O_3$ structure due to liquid phase sintering
with bismuth borate glass. This was also confirmed through
X-ray diffraction studies, which show no shift of X-ray
diffraction reflections. The dielectric constant at room
temperature for 0.4, 2, 10 and 20% glass samples (1800-1300)
are comparable with that of Ba Ti $O_3$ (1500-2000) but the
peak value is reduced from 6000-10000 for pure Ba Ti $O_3$ to
2000 - 3000 for liquid phase sintered Ba Ti $O_3$ samples. It
can also be observed from this figure that the dielectric
constant is decreasing with increasing glass content. These
data are plotted separately in Fig. IV.29, which shows the
variation of room temperature dielectric constant and
maximum dielectric constant with glass content. This figure
shows that the dielectric constant decreases with increasing
glass content from 0.4 to 30%. This decrease is gradual
from 0.4 to 10%, and there is very little decrease in
dielectric constant with increase in glass content from 10-20%
and afterwords it is decreasing very steeply between 20
and 30% glass ( to about 570).

Since the bismuth borate glass employed in liquid
phase sintering has very low dielectric constant ($\sim$50)
(as given in section III 1.3) compared to that of Ba Ti $O_3$
it is expected that the dielectric constant should decrease
considerably with increasing glass content. However a large

decrease in the room temperature dielectric constant was
not observed till 20% glass.  Through  X-ray diffraction
studies it is confirmed that the glass reacts with $Ba\ Ti\ O_3$
at about 725°C forming $Ba\ Bi_4\ Ti_4\ O_{15}$ which is also a
ferroelectric material with a dielectric constant of
($\epsilon_{25}$ — 150  and  $\epsilon_{max}$ — 1650) (24).  It is also observed
through X - ray diffraction studied that the formation of
$Ba\ Bi_4\ Ti_4\ O_{15}$ continues till 900°C and afterwords it is
decomposing forming a glassy phase and 12 $Bi_2O_3$. $B_2\ O_3$.
Microstructure observation of the liquid phase sintered
samples with 0.4 - 30% glass showed that a glass is dis-
tributed uniformly around each grain as a coating over the
grain and also the amount of glassy phase increases with
increasing glass content.  Grain growth was also observed
with increasing glass content.  So we can consider the
whole sintered body as a composite consisting of $Ba\ Ti\ O_3$
grains uniformly coated with layers of $Ba\ Bi_4\ Ti_4O_{15}$  and
$Bi_2\ O_3$ . $B_2\ O_3$ glass giving it a 3-0 connectivity (25) .
That is, the boundary layers are connected to each other in
3- dimensions and the $Ba\ Ti\ O_3$ grains are separated from
each other by these  boundary layers.  So the dielectric
constant of this composite will depend on the volume
fraction of the second phase(s) and also on its dielectric
constant.

<u>Three important results emerged from this study:</u>

i)     With-in the experimental error the Curie temperature
remains constant at 120°C irrespective of the amount
of the glass added. varying from 0.4 to 30 wt pct.
This clearly indicates that none of the constituents
of the glass entered the Ba Ti O$_3$ lattice. This is
in confirmitility with the X-.ray diffraction results.

ii)    The room temperature dielectric constant decreases
with increasing amount of glass. In order to
account for it one may consider the present materials
as two phase mixtures of Ba Ti O$_3$ with a room
temperature dielectric constant of 2000 and bismuth
borate glass with a room temperature dielectric
constant of about 50  . The dielectric constant of
the composite could be computed assuming series and
parallel arrangement of the two phase or by
logarithermic mixing rule. The concepts have been
recently reviewed by Payne and Cross ( 26 ) who give
the following formulae for these three mixing rules:

a)   parallel mixing: $\overline{K} = V_1 K_1 + V_2 K_2$

b)   series Mixing : $\dfrac{1}{\overline{K}} = \dfrac{V_1}{K_1} + \dfrac{V_2}{K_2}$

c)   Logarithmic mixing: $\log \overline{K} = \sum_i V_i \log K_i$

where $\overline{K}$ is the average dielectric constant, $V_1$ and $V_2$
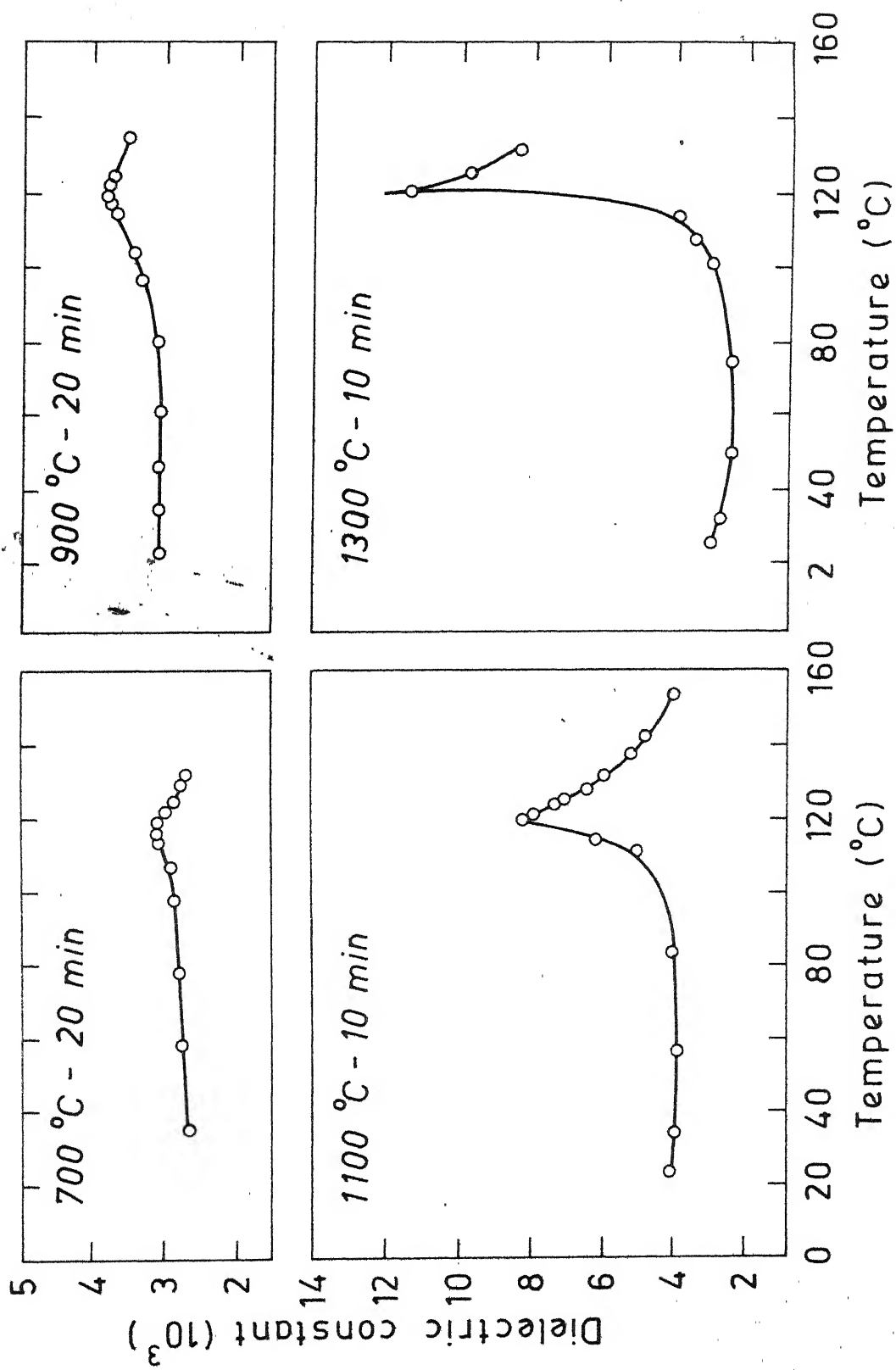are the two volume frachions such that $V_1 + V_2 = 1$ and

Fig. IV 3o.

similar to the above data obtained on reheating of hot
pressed Ba Ti O₃ ceramic. This may be due to the fact that
the sintering temperatures employed in the present study are
mostly 1000 to 1100°C. The reason for this behaviour may
be the fact that the grain size does not increase from its
initial value ( 13 μm) even by a factor of 2 under the
sintering conditions employed in the present study. On the
other hand in conventional sintering of Ba Ti O₃ ceramics
considerable grain growth takes place which leads to a
prominent dielectric peak at the curie temperature. This
line of reasoning is supported by the observation that a
higher sintering temperature or a longer sintering time
invariably lead to a higher dielectric constant at the
curie temperature than the values corresponding to a lower
temperature or shorter sintering time.

Table IV.11 Comparison of Observed dielectric constants and calculated values using mixed rules.

| Wt% glass | Vol% Glass | Vol% BaTiO$_3$ | Dielectric Constant (K) | | | |
|---|---|---|---|---|---|---|
| | | | Experi-mental | Logari-th mic mixing | Parallel mixing. | Series Mixing. |
| 0 | 0 | 0 | 2000 | 2000 | 2000 | 2000 |
| 0.4 | 0.3 | 99.7 | 1848 | 1925 | 1994 | 1800 |
| 2 | 1.5 | 98.5 | 1611 | 1850 | 1970 | 1286 |
| 10 | 7.67 | 92.33 | 1453 | 1475 | 1851 | 521 |
| 20 | 15.75 | 84.25 | 1325 | 1100 | 1693 | 293 |
| 30 | 24.27 | 75.73 | 571 | 820 | 1527 | 200 |

IV.7.1.2    Effect of sintering temperature and time:

Figs.IV. 31-25 show the effect of sintering temperature and time on dielectric properties. These results are briefly summerised in Table IV.12/Fig. IV.31 shows the dielectric properties of the samples with 20% glass sintered at 1000°C for 1/2, 1 and 3 h. This figure shows that the dielectric constant values are slightly more for the samples sintered for 3 h, while they are very close for the samples sintered for 1/2 and 1h. The dielectric losses for all these samples are less than 3% till 120°C and after-wards they increase sharply upto 7% at 180°C. Fig. IV.32 shows
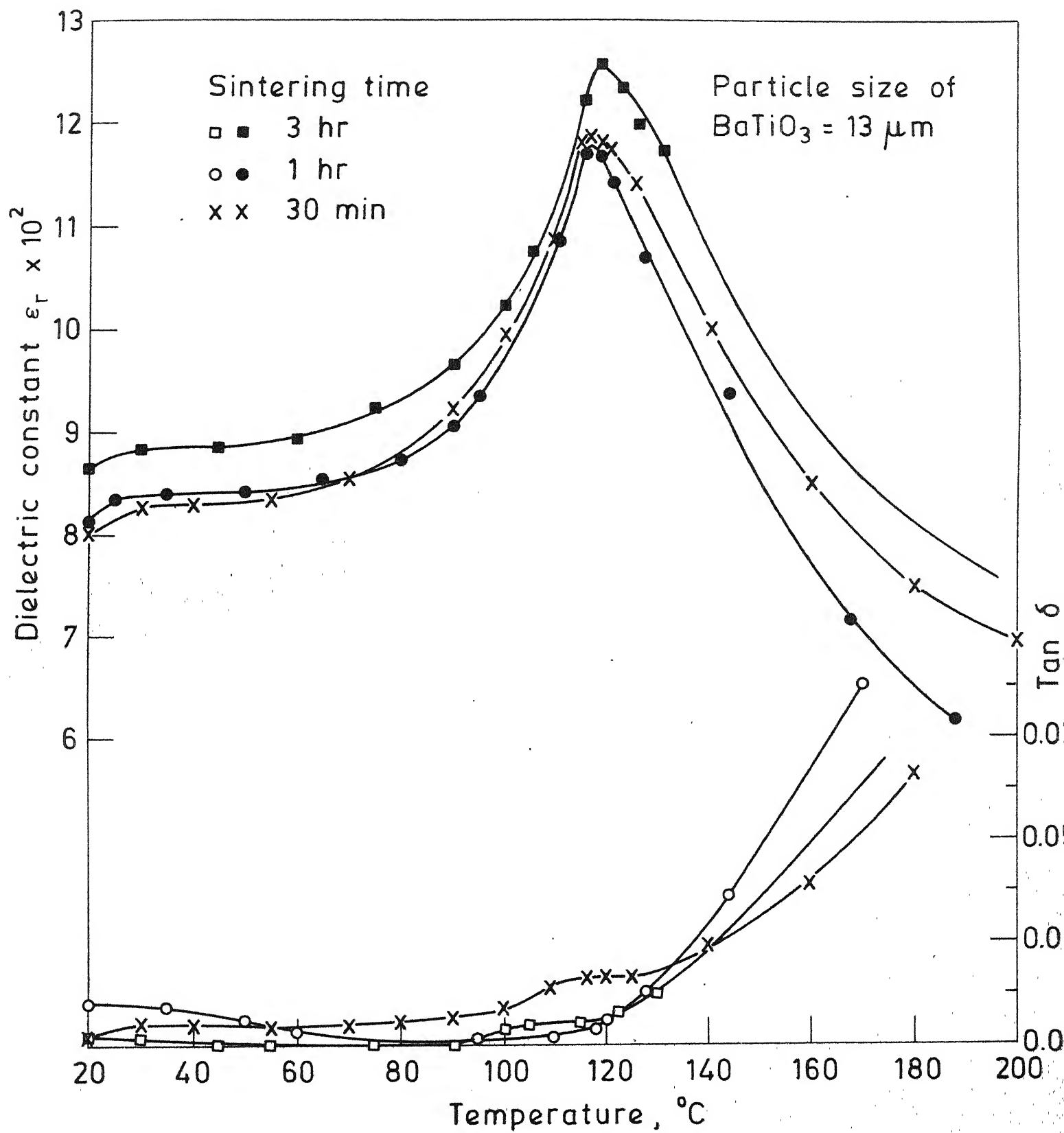
Fig. IV 31 - Relative dielectric constant vs temperature for the samples with 20 % glass addition sintered at 1000 for different times.

Fig. IV-32 - Relative dielectric constant vs temperature for th
samples with 20 % glass addition sintered at 1100
for different times.

Fig. IV 33 - Relative dielectric constant vs temperature for the samples with 10 % glass addition sintered at 1000 °C for different times.
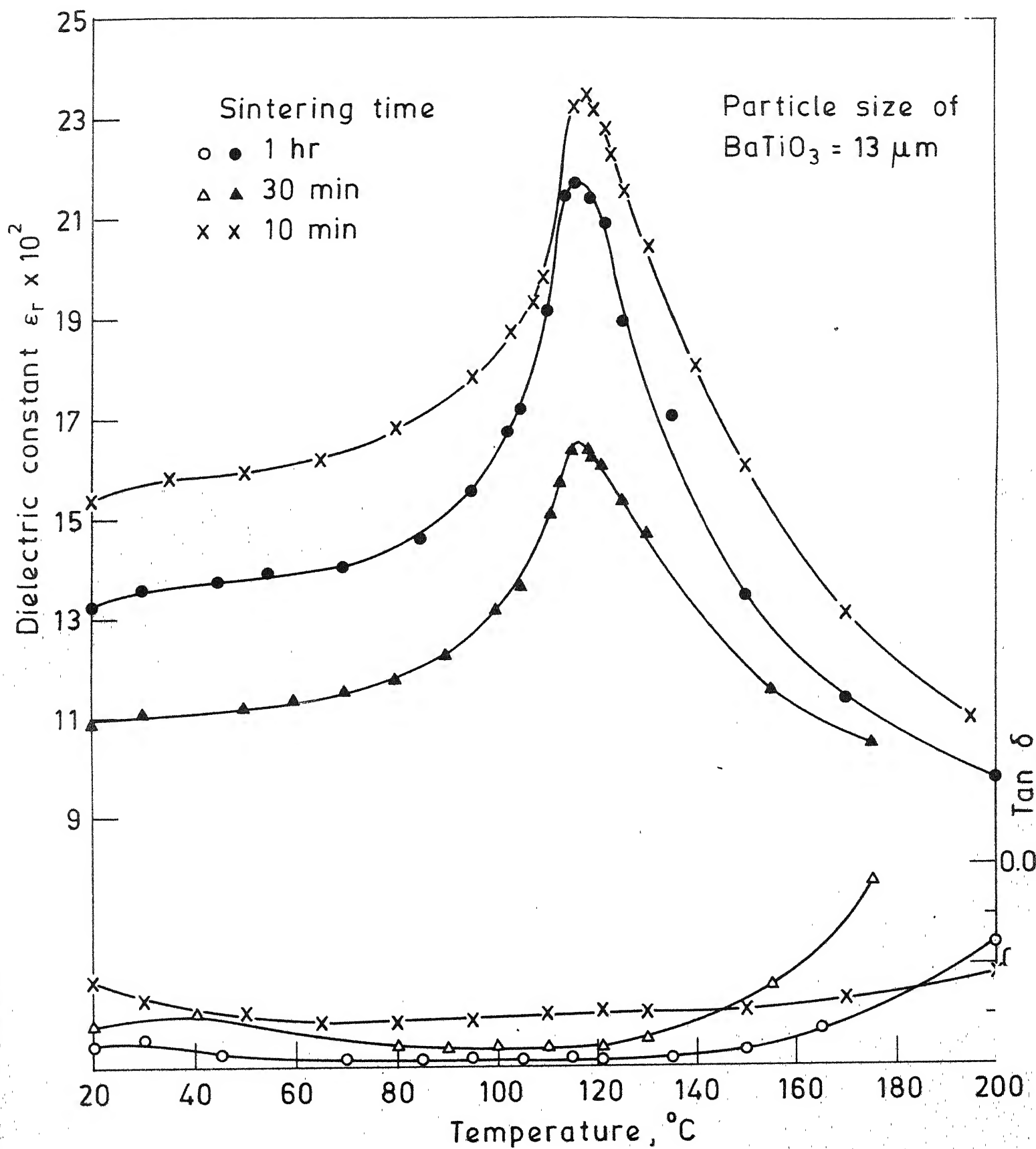
Fig. IV-34 - Relative dielectric constant vs temperature for the samples with 10 % glass addition sintered at 1100 °C for different times.
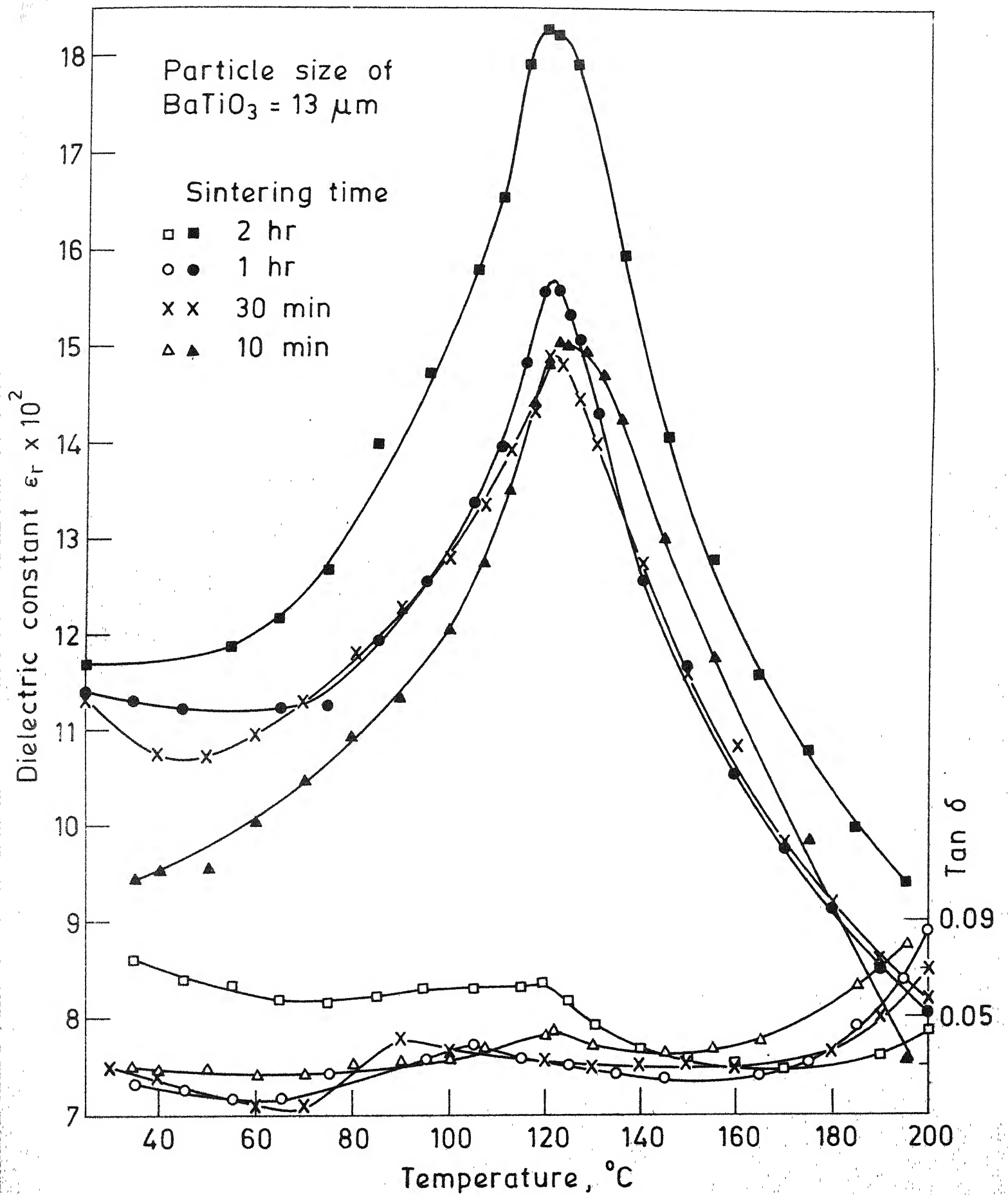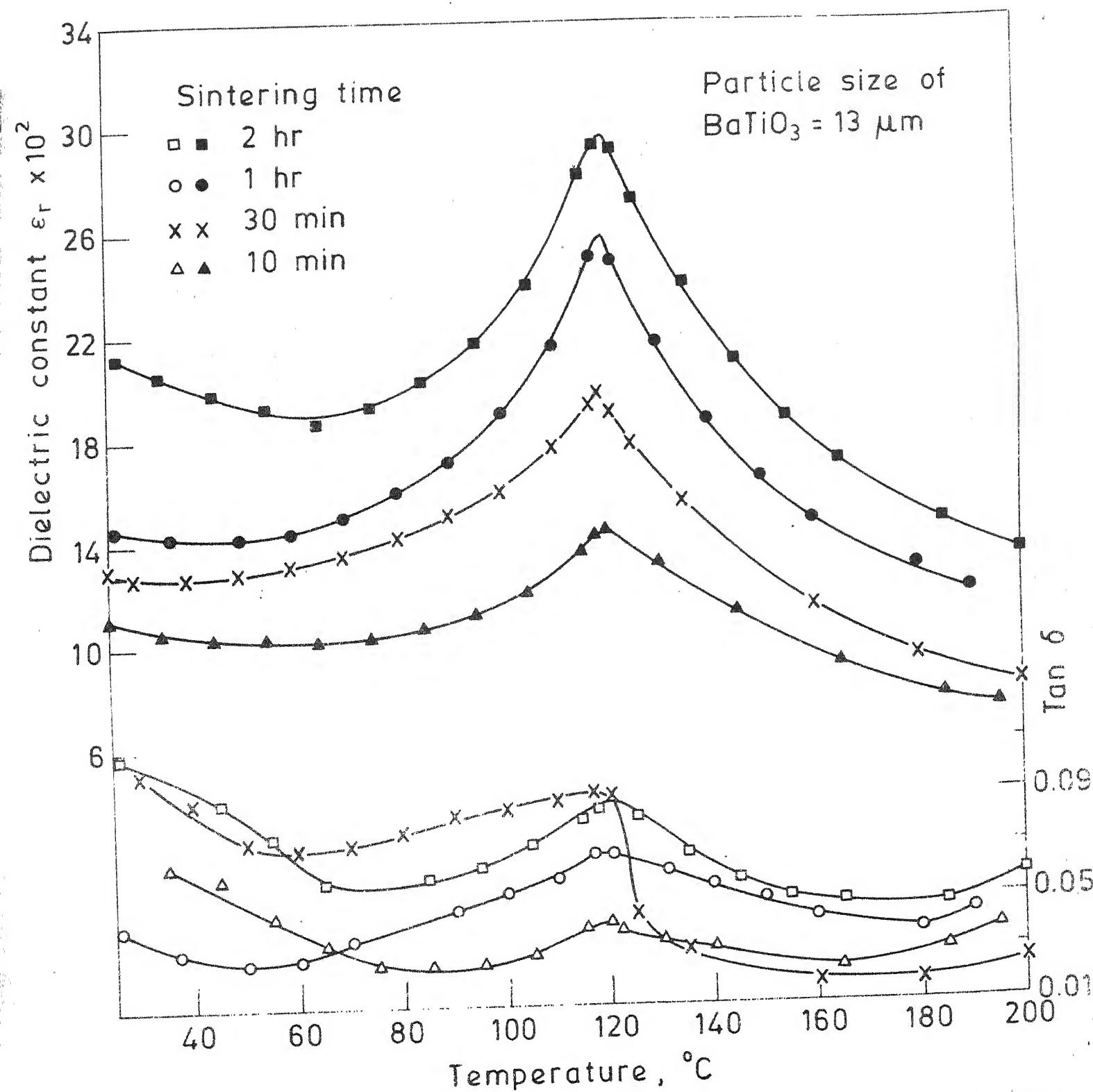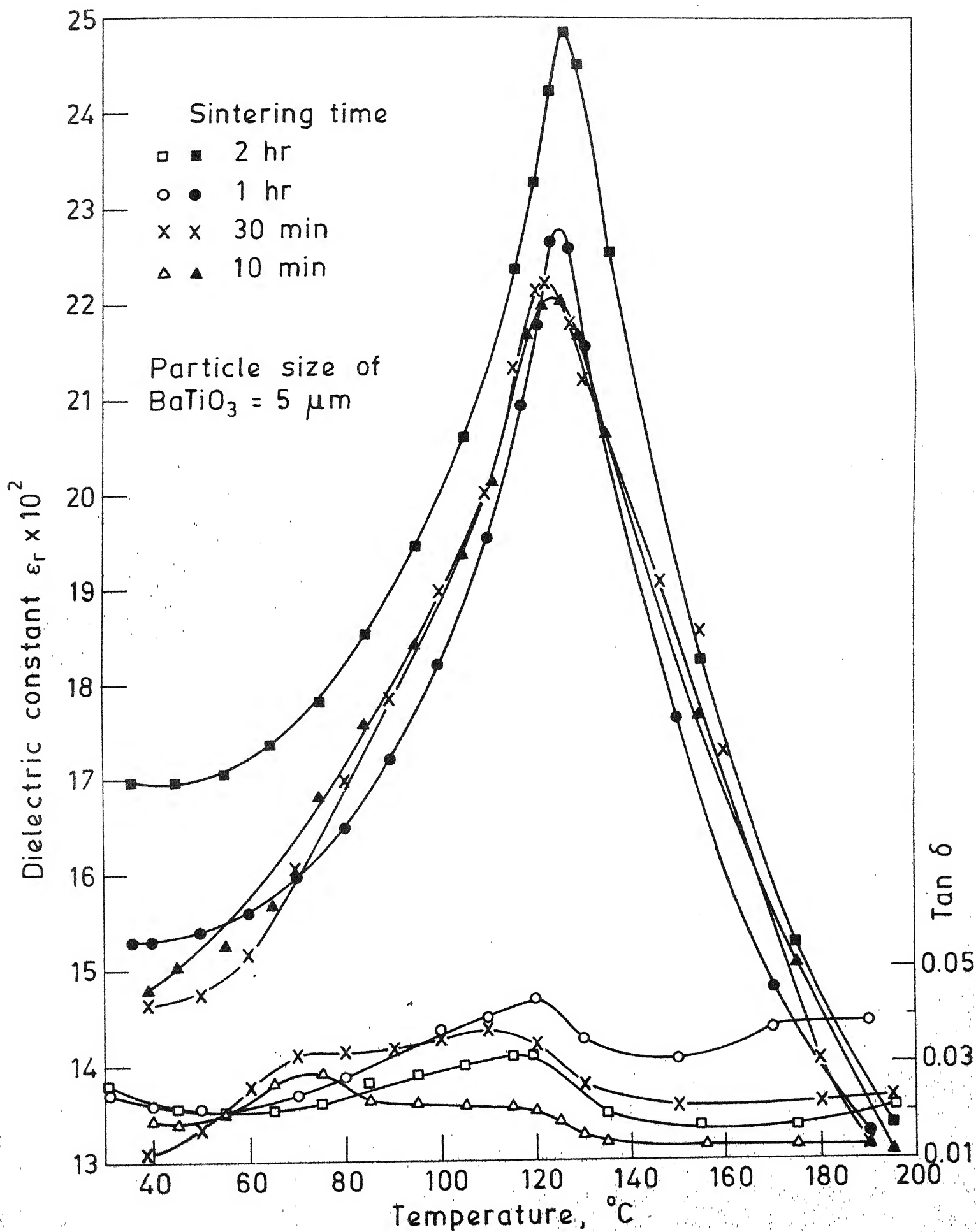
Fig. IV 35 - Relative dielectric constant vs temperature for the samples with 10 % glass addition sintered at 1050 °C for different times.

Table IV.12:    Variation of dielectric constant with glass
addition, sintering temperature and time.

| Sample | Sintering Temp. °C | Sintering Time | | Density g/cc | | $\epsilon_r$ at RT | $\epsilon_r$ max |
|---|---|---|---|---|---|---|---|
| BaTiO$_3$ with 20% glass addition 13 $\mu$m BaTiO$_3$ 17 $\mu$m glass | 1000 | 1/2 | h | 4.66 | (77.4) | 801 | 1192 |
| | | 1 | h | 5.02 | (83.4) | 812 | 1168 |
| | | 3 | h | 5.16 | (85.7) | 867 | 1253 |
| | 1100 | 10min. | | 5.10 | (84.7) | 1119 | 1634 |
| | | 1/2 | h | 5.15 | (85.5) | 1539 | 2332 |
| | | 1 | h | 5.18 | (86.0) | 1325 | 2165 |
| BaTiO$_3$ with 10% glass addition 13 $\mu$m BaTiO$_3$ 17 $\mu$m glass | 1000 | 10 min | | 4.78 | (79.4) | 942 | 1508 |
| | | 1/2 | h | 4.87 | (80.9) | 1132 | 1462 |
| | | 1 | h | 5.03 | (83.6) | 1136 | 1558 |
| | | 2 | h | 5.26 | (87.4) | 1168 | 1827 |
| | 1100 | 10 min | | 5.06 | (84.1) | 1113 | 1414 |
| | | 1/2 | h | 5.24 | (87.0) | 1300 | 1942 |
| | | 1 | h | 5.25 | (87.2) | 1453 | 2495 |
| | | 2 | h | 5.27 | (87.5) | 2119 | 2914 |
| BaTiO$_3$ with 10% glass addition 5 $\mu$m BaTiO$_3$ 4 $\mu$m glass | 1050 | 10 min | | 5.20 | (86.4) | 1479 | 2204 |
| | | 1/2 | h | 5.32 | (88.4) | 1439 | 2219 |
| | | 1 | h | 5.40 | (89.7) | 1529 | 2264 |
| | | 2 | h | 5.37 | (89.2) | 1699 | 2459 |

the dielectric properties of the 20% samples sintered at 1100°C for 1/6, 1/2 and 1h. This figure shows that the dielectric constant values are more for the samples sintered for 10 min. and 1h. and least for the samples sintered for 1/2 h. Here also it can be observed that the dielectric losses for all the samples were less than 3% till 120°C and afterwords they are increasing sharply upto 9% and 7% for 1/2 and 1h. samples. The losses were minimum (4%) at 180°C for 10 min. sample.

Fig.IV.33&34 shows the dielecttic properties of the samples with 10% glass sintered at 1000 and 1100°C for 1/6, 1/2, 1 and 2h. In both the cases it can be observed that the dielectric constant is increasing with increasing sintering time from 1/6 to 2h. at a particular sintering temperature. It can also be observed that the dielectric losses are more for the samples sintered at 2h than at 1/6. At both the temperatures the maximum losses till 200°C are less than 9%.

For all the samples discussed above the initial particle size of Ba Ti $O_3$ and glass are nearly 13 and 17 $\mu$m respectively. Fig. IV $_{35}$ shows the dielectric properties of the samples with 10% glass sintered at 1050°C for 1/6, 1/2, 1 and 2h. Here the particle size of Ba Ti $O_3$ and glass are 5 $\mu$m and 4 $\mu$m respectively. These samples also show that the dielectric constant is increasing with increasing sintering time, though the values are very close for 10 min.

1/2h and 1h sintered samples. It can also be observed that the dielectric constant values for these samples are more, compared to those values for the samples containing coarser $Ba\ Ti\ O_3$ sintered at 1000 and 1100°C ( Table IV.12 )

It was mentioned earlier that this liquid phase sintered body can be considered as a composite consisting of $Ba\ Ti\ O_3$ grains coated uniformly with $Ba\ Bi_4\ Ti_4\ O_{15}$ and a glassy phase giving it a 3-0 connectivity. Through the X-ray diffraction studies ( section IV.4) it is observed that the $Ba\ Bi.Ti_4O_{15}$ is decomposing at higher temperatures there by reducing its amount as the temperature increases from 1000 - 1100°C, and also at a particular temperature the amount of $Ba\ Bi_4\ Ti_4\ O_{15}$ is decreasing with increasing sintering time    Fig. IV.23.Microstructures  of the 10% glass samples sintered at 1000 and 1100°C also showed, that the amount of glass portion around the grain boundries is increasing with increasing sintering temperature and also at a particular sintering temperature it is increasing with sintering time.  The grain size was also found to be increasing with sintering temperature and time . This may be due to the decomposition of $Ba\ Bi_4\ Ti_4\ O_{15}$ forming glass and $Ba\ Ti\ O_3$, there by increasing the volume fraction of $Ba\ Ti\ O_3$. So at a particular temperature with increasing sintering time the volume fraction of $Ba\ Ti\ O_3$ and the amount of glass around the grain is increasing. This

increase in the volume of $Ba\ Ti\ O_3$ may be the reason for the samples showing more dielectric constant at higher sintering times. The same reasoning also can be applied for higher dielectric constants at 1100°C than at 1000°C. The trend observed in the dielectric losses, that is increasing losses with increasing sintering time may be due to the increase in the amount of glassy phase around the grains. As seen from Table II the resistivity of the bismuth borate glass employed in liquid phase sintering decreases with increasing temperature from 130-230°C by nearly three orders of magnitude. That is, the conductivity of these glasses is increasing at higher temperatures causing more dielectric losses. Hirayama and Subbarao(12) give the dissipation factor for this glass as 0.01 at 130°C increasing to 0.14 at 230°C. So the increase in dielectric losses at higher temperatures for the liquid phase sintered samples can be accounted for by the increase in dielectric loss of the glass with temperature.

So from these measurements of $\epsilon_r$ and $\tan \delta$ with sintering temperature and time, it can be said that the interaction between the glass and $Ba\ Ti\ O_3$ at the temperatures ( 1000 - 1100°C) and the degree to which the reaction can proceed may be partially responsible for the attainment of various levels of electrical characteristics. To detect the presence of ferroelectric $Ba\ Bi_4\ Ti_4\ O_{15}$ in

the liquid phase sintered samples, temperature dependence of dielectric properties were measured upto 420°C since Ba Bi$_4$ Ti$_4$ O$_{15}$ has a curie point at 395°C (24). These measurements were done on two 20% samples sintered at 1000°C for 1h and 3 h. These results are shown in Fig. IV.36 It shows a little peak at about 395°C for these two samples. Since the dielectric losses are increasing very high (60-70%) at these temperatures, measurements become difficult and clear indication of Ba Bi$_4$ Ti$_4$ O$_{15}$ peak could not be identified. But these measurements show the presence of Ba Bi$_4$ Ti$_4$ O$_{15}$ which supports the X-ray diffraction results.

IV.₂.2. Voltage dependence of dielectric properties:

Dielectric constant and tan $\delta$ were measured on a 10% glass sample sintered at 1050°C for 2h. with increasing and decreasing D.C. bias. Measurements were made upto 100V/mil ( 40 KV/cm) and no break-down was observed. These results are plotted in Fig. IV.37 and 38 Fig. IV 37 shows the percent change in permittivity with increasing and decreasing d.c. bias. This Figure shows 29% decrease in permittivity at 100V/mil.

In Fig. IV.38 change in permittivity with D.C. bias is compared for liquid phase sintered Ba Ti O$_3$ of the present sudy with that of Ba Ti O$_3$ (28) and glass bonded Ba Ti O$_3$ (1 ) . The figure show a similar behaviour for all these samples, but the decrease in permittivity at
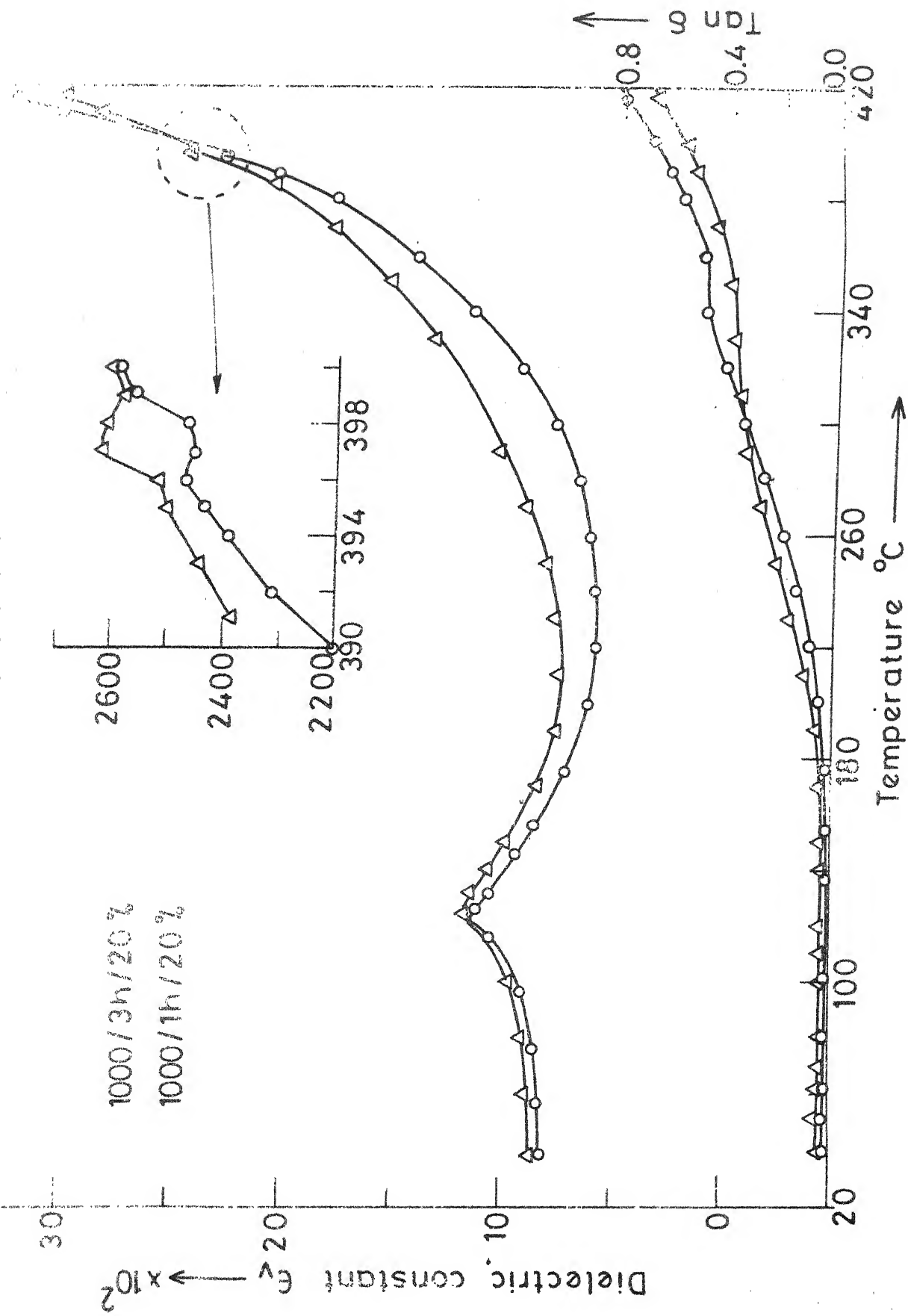
Fig. $\overline{IV}$-36 Relative dielectric constant vs temperature for the samples with 20% glass addition sintered at 1000°C for different times.

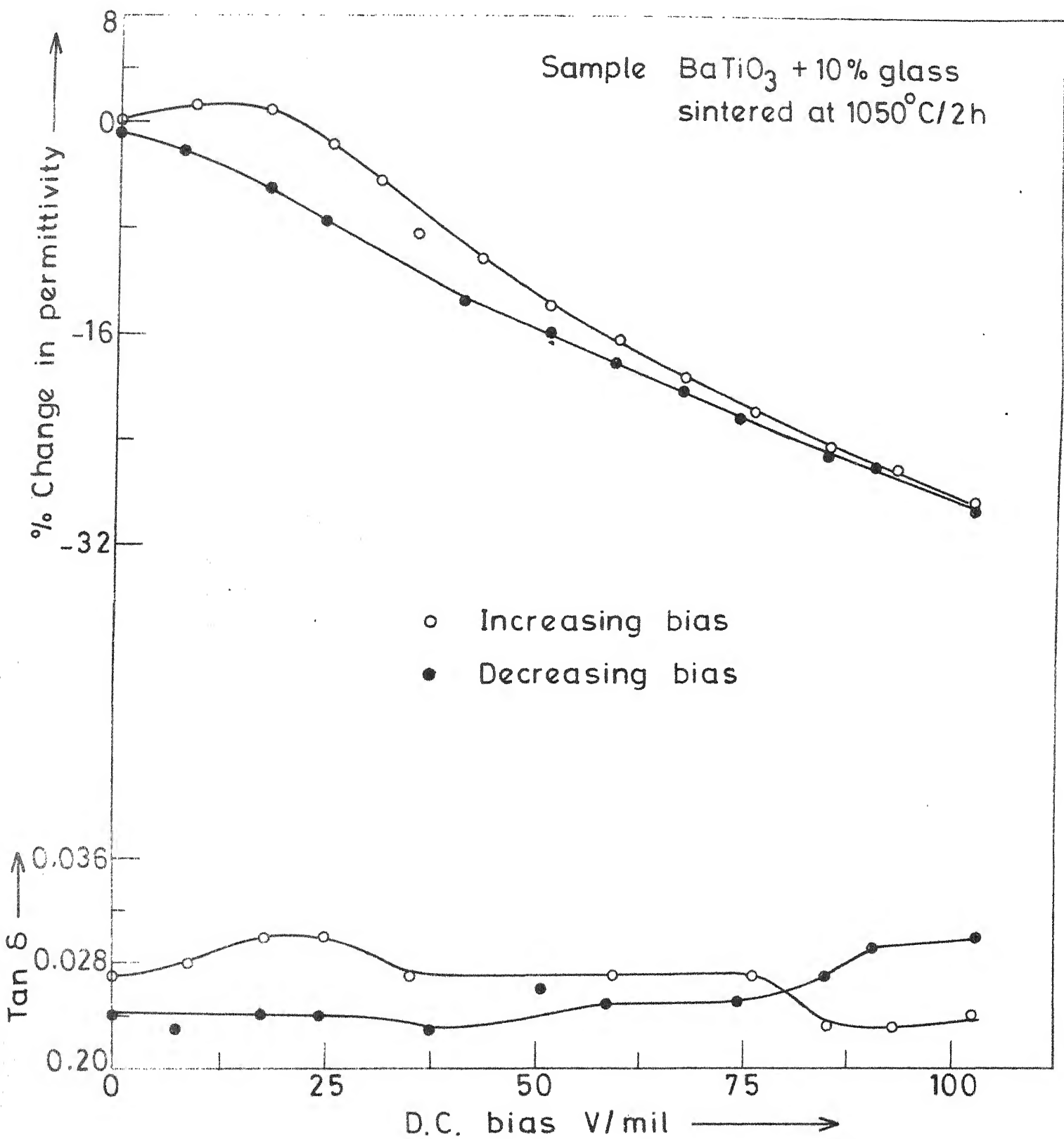Fig. $\overline{IV}$ -37 Percent change in permittivity and dissipation factor with D.C. bias.
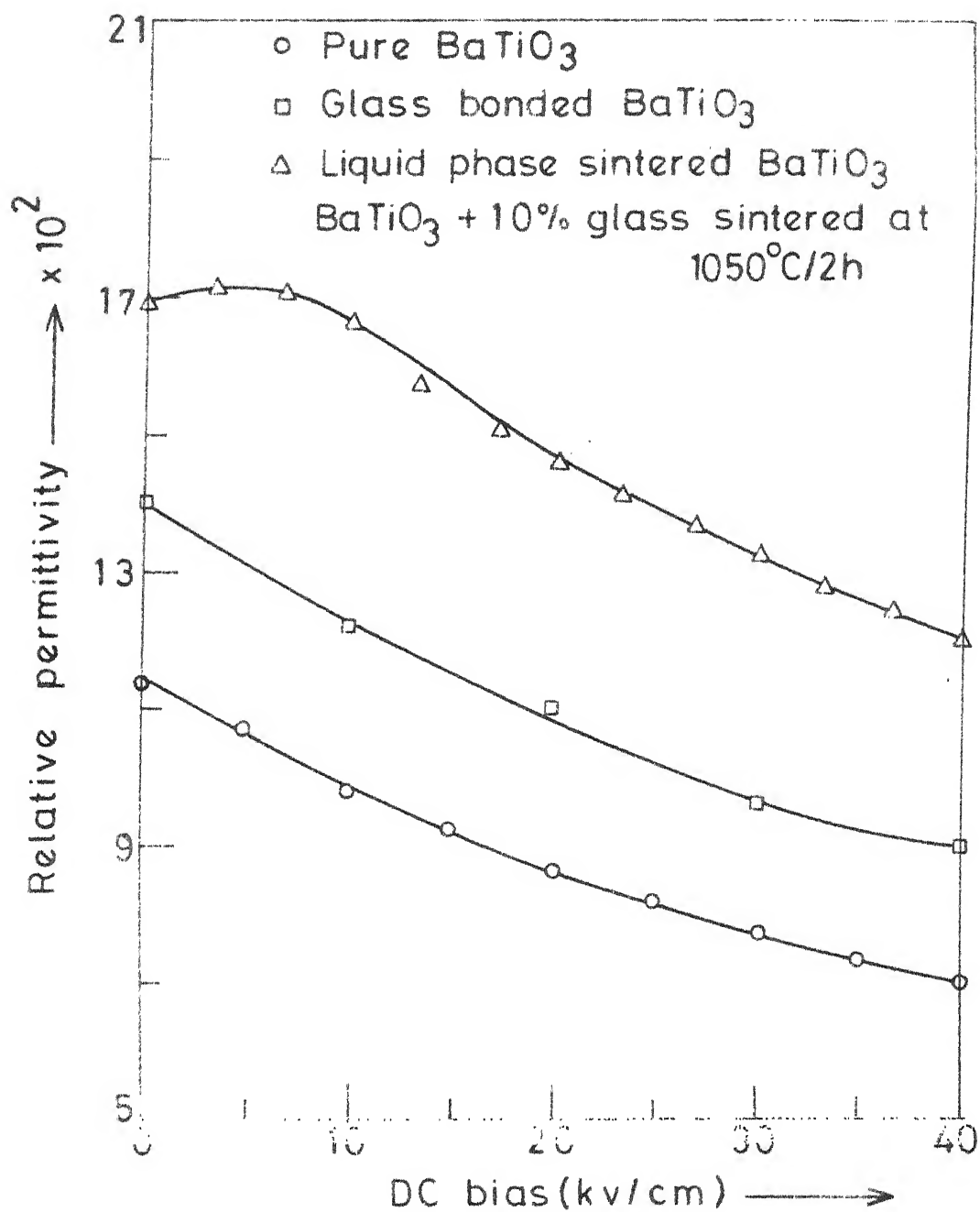
Fig. IV -38 Comparison of permittivity vs D.C. bias for different BaTiO$_3$ samples.

100 V/mil was 29% for liquid phase sintered Ba Ti $O_3$ and 36% for Ba Ti $O_3$. The glass bonded Ba Ti $O_3$ is in between these two.

IV.7.3   Frequency dependence of dielectric properties:

Dielectric constant and tan $\delta$ were measured with respect to frequency on a 10% sample sintered at 1050°C/1h. These measurements were made at two temperatures namely room temperature (37°C) and 80°C and are shown in Fig. IV.39 This figure shows a dispersion at about 300 Hz at room temperature and this dispersion frequency was shifting to 1 KHz at 80°C. Very large change in the dissipation factor was observed with increasing frequency, for example it is changing from 0.3 at 100 Hz to 0.00038 at 100 KHz.
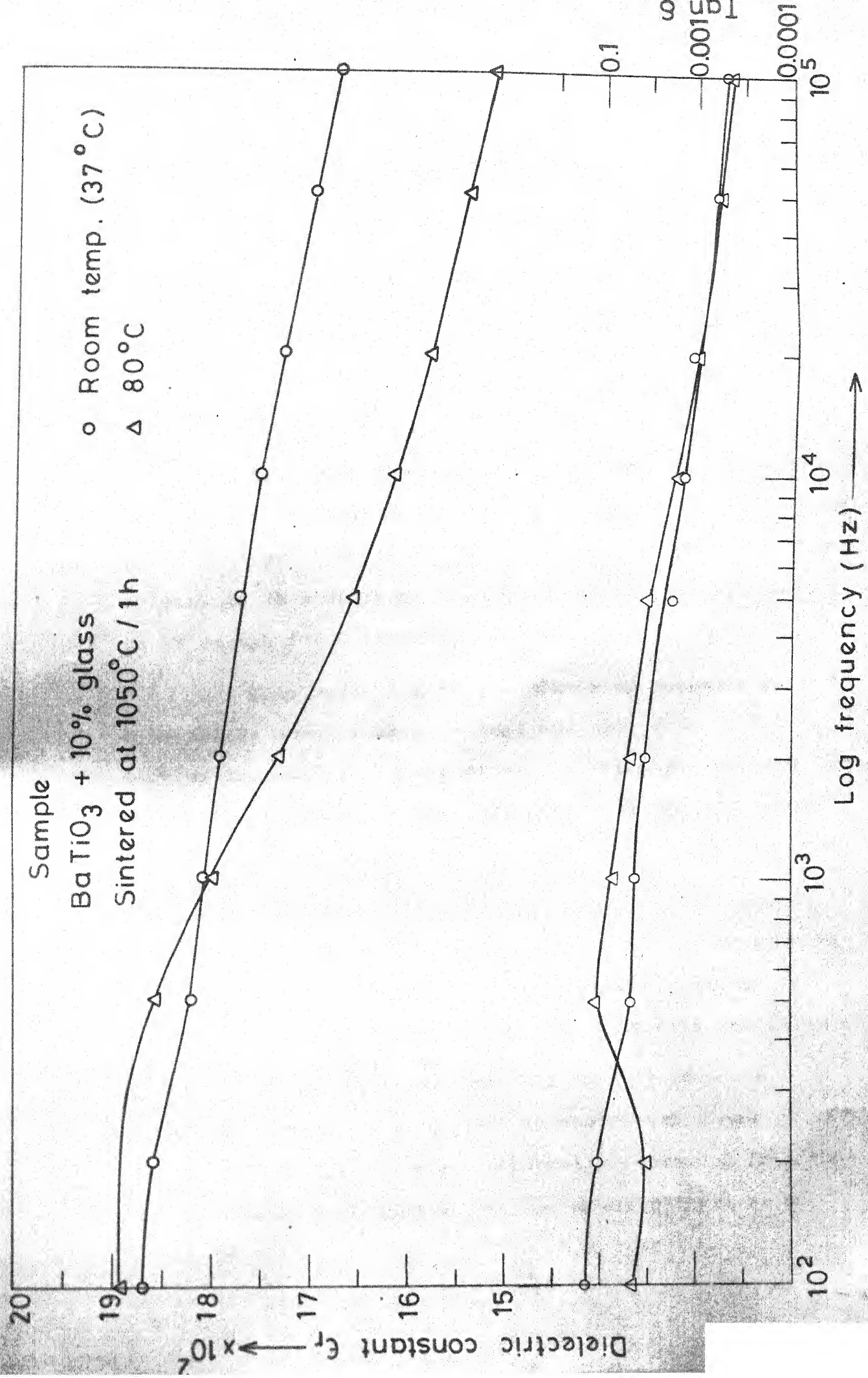
Fig. IV-39 Frequency dependence of dielectric constant for liquid phase sintered BaTiO₃.

# V. CONCLUSIONS AND RECOMMENDATIONS

Sintering temperature of $Ba\ Ti\ O_3$ has been reduced from the usual 1350°C to 1050°C by liquid phase sintering of $Ba\ Ti\ O_3$ using a bismuth borate glass upto 10 to 20 wt percent.

Sintering time also has been reduced considerably without effecting the densification. A total heating cycle of approximately 6h consisting of 2h 30min. heating, 10 min. to 2h soaking and finally a 2h cooling are found to be enough for sintering.

This reduction in the sintering temperature and time brings about energy savings and also reduces the cost of the multilayer capacitors by replacing the costlier Pd and Pt electrodes with a relatively cheaper 70 Ag-30Pd alloy.

Both particle rearrangement and solution precipitation processes are found to be the major mechanisms causing densification, however the predominance of one over the other depends upon the sintering conditions.

Dielectric constants of the liquid phase sintered $Ba\ Ti\ O_3$ samples with 10 and 20 wt% glass ( 1453 and 1325 ) are not considerably decreased from that of pure $Ba\ Ti\ O_3$ ( 1500 - 2000 ). However there is a

marked decrease in peak value from 6000 - 10000 for pure Ba Ti $O_3$ to 2000 - 3000 for liquid phase sintered samples showing a less sensitivity with temperature. Response with d.c. bias of these samples seems to be slightly better than that of pure Ba Ti $O_3$ samples.

From the observations got during this study the following recommendations can be made which are worth considering.

i)    Effect of particle size has been studied in the present work but to a very limited extent. The particle size being an important parameter, the effect of that should be studied further particularly with lower particle sizes of Ba Ti $O_3$.

(ii)  Detailed study on 20% samples should be done similar to that was done on 10% samples, because this glass range was found to be suitable for sinter-ing at 1000 to 1100°C.

(iii)   Frequency response as a function of temperr-ture should be studied thoroughly.

## VI. APPENDIX - A

## CHEMICAL ANALYSIS

Chemical analysis of the glass used for liquid phase sintering, barium titanate and the liquid phase sintered barium titanate are undertaken. In the case of barium titanate, materials ground in an alumina jar with alumina balls to various particle sizes were also analysed to estimate the pick up of impurities during grinding. The procedure for the method for the preparations of the above substances was given in (1).

**VI. 1   Analysis of Glass:**

A weighed quantity of the powdered glass was heated with the minimum quantity of concentrated nitric acid. The solution was diluted, boiled, cooled and made up to a known volume.

**VI. 1.1   Determination of Bismuth:**

Complexometric method was adopted for the determination of $Bi^2$. Reagents used: Pyrocatechol violet. 0.1% solution in water, ammonia solution -0.5 M, EDTA - 0.01 M and pH indicator paper.

A known volume of the glass solution (20-40 mg of Bi) was pipetted out into a clean conical flask. The solution was diluted to about 100-150 ml and 3 to 4 drops of

the indicator solution were added. Dilute ammonia was added in drops until the violet colour changed to blue. The pH was checked with indicator paper to see that it was about 2. This was titrated against 0.01 M. EDTA until the colour changed to yellow.

If the amount of Bi is large an appreciable amount of hydrogen ions is released during the titration. Therefore the pH is checked during the titration either by indicator paper or by observing the colour of the bismuth-indicator complex.

Calculation: 1 ml of 0.01 M. EDTA corresponds to 2.09 mg of Bi. From the value obtained for Bi, the amount of $Bi_2O_3$ was calculated.

## IV. 1.2 Determination of Aluminium:

Aluminium also was analysed complexometrically. Titration procedure was the same as done by Bhargava.[3]

Reagents used: EDTA - 0.01 M, xylenol organge 0.1%, sodium hydroxide solution - 10% and 1%, zinc solution- 0.01 M, ammonium fluoride - 10% and acetate buffer - 136 g of sodium acetate trihydrate is dissolved in about 600ml water. 7 ml of glacial acetic acid is added and diluted to 1.1.

A known volume of the solution was pipetted out in a beaker and treated with excess of EDTA. For pH was

adjusted to 4 using a pH meter by drop-wise addition of 10%
sodium hydroxide solution till the pH reached 2.5 and then
of 1% sodium hydroxide. The solution was diluted with water,
covered, boiled and kept boiling for 10 minutes. The solution
was cooled, added 7 drops of xylenol orange and 15 ml of
acetate buffer. This mixture was titrated with zinc to pink
colour. 10 ml of ammonium fluoride (10%) was added, boiled
gently for 10 minutes, cooled and titrated against zinc.

Calcutation: 1 ml of 0.01 M zinc corresponds to
0.27 mg of Al. From the value obtained for Al, the amount
of $Al_2O_3$ was calculated.

II. 1.3   Determination of Boron:

$B_2O_3$ was found out by difference. Results of
analysis are given in Table 1.

## REFERENCES

1. W.R. Buessem and T.I. Prokopowicz, Ferroelectrics 10, 255 (1976)

2. Metals Hand Book, 8, 255

3. L. Burn and G.H. Maher. J. Mat. Sci. 10, 645 (1963)

4. S.B. Desu, M. Tech. Thesis, I.I.T. Kanpur, 1979.

5. S.B. Desu and E.C. Subbarao, J. Mat. Sci. 15, 2113 (1980)

6. S.B. Desu and E.C. Subbarao in Advances in Ceramics, Vol. 1, Am. Ceramic Soc. (1980) (in press)

7. E.C. Subbarao in proc. Symp. on Sintering and Sintered products, Bombay, 1979.

8. S.M. Park, Ph.D. Thesis, Univ. of Illinois.

9. J.L. Mukherjee and H.S. Ravishankar in proc. Symp. on sintering and sintered products, Bombay, 1979, 281

10. D. Hennings, Ber. Dtsch. Keram. Ges. 55, 359 (1978)

11. E.M. Levin and C.L. Mc Daniel, J. Am. Ceram. Soc. 45, 355, (1962)

12. C. Hirayama and E.C. Subbarao, Phys. Chem. Glasses, 3, 111 (1962)

13. S. Nanamutsu, H. Sugiyama, K. Doi and Y. Kondo
    J. Phys. Soc. Japan 31, 616 (1971 )

14. J.F. Murray, Am. Ceram. Soc. Bull.
    37, 476 (1958)

15. D.E. Rase and Rustam Roy, J. Am. Ceram. Soc.
    38, 102 (1955)

16. F. Kulcsar, J. Amer. Ceram. Soc.
    39, 13 ( 1956 )

17. J.V. Biggers and W.A. Schulze, Am. Ceram. Soc.
    Bull. 51, 620 (1972)

18. A.S.T.M. X-ray diffraction data Card No. 12-213

19. A.S.T.M. X-ray diffraction data Card No. 8-261.

20. V.N. Eremenko, Yu. V. Naidich and I.A. Lawrineko,
    "Liquid Phase Sintering". A special research report
    translated from Russian Consultants bureau.

21. W.D. Kingery, J. Appl. Phy,
    30, 301 (1959)

22. T. Prince, C. Smithells and S. Williams,
    J. Inst. Met. 62, 239 (1938)

23. D.F. Rushman and M.A. Strivens, Trans. Faraday Soc.
    42A, 231 (1946).

24. E.C. Subbarao, Int. J. Phys and Chem. of Solids. 23, 665 (1962 )

25. R.E. Newnhorn, D.P. Skinner and L.E. Cross, Mat. Res. Bull. 13, 525 (1978)

26. D.A. Payne and L.E. Cross " Ceramic Microstructures 1976" Ed. R.M. Fulruth and J. A. Park. Proc. of the Sixth International Materials Symposium. Univ. of California, Berkeley, Aug. 1976.

27. H.C. Graham, N.M. Tallem and K.S. Mazdiyasni. J. Am. Cerm. Soc. 52, 548 (1967)

28. S. Roberts, Phys. Rev. 71, 890 (1947)

ME - 1981 - M - CHO-LIQ